DOE/NV/10845–34
UC–703

WELLHEAD PROTECTION AREA DELINEATION UNDER UNCERTAINTY

by

Elizabeth Jacobson
Roko Andricevic
Thomas Hultin

DISCLAIMER

This report was prepared as an account of work sponsored by an agency of the United States Government. Neither the United States Government nor any agency thereof, nor any of their employees, makes any warranty, express or implied, or assumes any legal liability or responsibility for the accuracy, completeness, or usefulness of any information, apparatus, product, or process disclosed, or represents that its use would not infringe privately owned rights. Reference herein to any specific commercial product, process, or service by trade name, trademark, manufacturer, or otherwise does not necessarily constitute or imply its endorsement, recommendation, or favoring by the United States Government or any agency thereof. The views and opinions of authors expressed herein do not necessarily state or reflect those of the United States Government or any agency thereof.

SEPTEMBER 1994

Publication #45118

MASTER

DISTRIBUTION OF THIS DOCUMENT IS UNLIMITED

DISCLAIMER

Portions of this document may be illegible in electronic image products. Images are produced from the best available original document.

This report was prepared as an account of work sponsored by the United States Government. Neither the United States nor the United States Department of Energy, nor any of their employees, makes any warranty, express or implied, or assumes any legal liability or responsibility for the accuracy, completeness or usefulness of any information, apparatus, product or process disclosed, or represents that its use would not infringe privately owned rights. Reference herein to any specific commercial product, process, or service by trade name, mark, manufacturer, or otherwise, does not necessarily constitute or imply its endorsement, recommendation, or favoring by the United States Government or any agency thereof. The views and opinions of authors expressed herein do not necessarily state or reflect those of the United States Government or any agency thereof.

This report has been reproduced directly from the best available copy.

Available to DOE and DOE contractors from the Office of Scientific and Technical Information, P.O. Box 62, Oak Ridge, TN 37831; prices available from (615) 576–8401.

Available to the public from the National Technical Information Service, U.S. Department of Commerce, 5285 Port Royal Rd., Springfield, VA 22161.

DOE/NV/10845–34
UC–703

WELLHEAD PROTECTION AREA DELINEATION UNDER UNCERTAINTY

by

Elizabeth Jacobson
Roko Andricevic
Thomas Hultin

Water Resources Center
Desert Research Institute
University and Community College System of Nevada

Publication No. 45118

prepared for
Nevada Operations Office
U.S. Department of Energy
Las Vegas, Nevada

September 1994

The work upon which this report is based was supported by the U.S. Department of Energy under Contract #DE–AC08–90NV10845.

CONTENTS

FIGURES i

TABLES iii

EXECUTIVE SUMMARY iv

INTRODUCTION 1

METHODOLOGY FOR WELLHEAD PROTECTION AREA DELINEATION UNDER UNCERTAINTY 3

WELLHEAD PROTECTION DELINEATION FOR THE WATER-SUPPLY WELLS AT THE NEVADA TEST SITE 6

Ultimate Capture Zones 9

Time–Dependent Capture Zones 9

SUMMARY 11

REFERENCES 64

APPENDIX A: MATHEMATICAL DEVELOPMENT OF METHODOLOGY FOR WELLHEAD PROTECTION AREA DELINEATION UNDER UNCERTAINTY 65

FIGURES

1. Schematic of pumping well in a regional flow system; shown in (a) vertical profile and (b) plan view 2

2. Capture zones corresponding to the deterministic (i.e., 0.50 value) curve and two bounding curves corresponding to the reliability levels shown on the curves. 4

3. Schematic of two capture zones for a specified reliability level 5

4. Map of the NTS showing the location of 14 water-supply wells 7

5. NTS water table map 8

6a. Ultimate capture zone for the 50% reliability level for Well Army #1 13

6b. Ultimate capture zones for the 95% reliability level for Well Army #1 14

7a. Ultimate capture zone for the 50% reliability level for Well J–12 15

7b. Ultimate capture zones for the 95% reliability level for Well J–12 16

8a. Ultimate capture zone for the 50% reliability level for Well J–13 17

8b. Ultimate capture zones for the 95% reliability level for Well J–13 18

9a. Ultimate capture zone for the 50% reliability level for Well 5B 10

9b. Ultimate capture zones for the 95% reliability level for Well 5B 20

10a. Ultimate capture zone for the 50% reliability level for Well 5C 21
10b. Ultimate capture zones for the 95% reliability level for Well 5C 22
11a. Ultimate capture zone for the 50% reliability level for Well UE–5C 23
11b. Ultimate capture zones for the 95% reliability level for Well UE–5C 24
12a. Ultimate capture zone for the 50% reliability level for Wells 4 and 4A 25
12b. Ultimate capture zones for the 95% reliability level for Wells 4 and 4A 26
13a. Ultimate capture zone for the 50% reliability level for Wells C and C-1 27
13b. Ultimate capture zones for the 95% reliability level for Wells C and C-1 28
14a. Ultimate capture zone for the 50% reliability level for Well UE–16d 29
14b. Ultimate capture zones for the 95% reliability level for Well UE–16d 30
15a. Ultimate capture zone for the 50% reliability level for Well 8 31
15b. Ultimate capture zones for the 95% reliability level for Well 8 32
16a. Ultimate capture zone for the 50% reliability level for Well UE–19c 33
16b. Ultimate capture zones for the 95% reliability level for Well UE–19c 34
17a. Ultimate capture zone for the 50% reliability level for Well U–20 35
17b. Ultimate capture zones for the 95% reliability level for Well U–20 36
18a. Time-dependent capture zones for the 50% reliability level for Well J–13 37
18b. Time-dependent capture zones for the 67% reliability level for Well J–13 38
18c. Time-dependent capture zones for the 95% reliability level for Well J–13 39
19a. Time-dependent capture zones for the 50% reliability level for Well 5B 40
19b. Time-dependent capture zones for the 67% reliability level for Well 5B 41
19c. Time-dependent capture zones for the 95% reliability level for Well 5B 42
20a. Time-dependent capture zones for the 50% reliability level for Well 5C 43
20b. Time-dependent capture zones for the 67% reliability level for Well 5C 44
20c. Time-dependent capture zones for the 95% reliability level for Well 5C 45
21a. Time-dependent capture zones for the 50% reliability level for Well UE–5C 46
21b. Time-dependent capture zones for the 67% reliability level for Well UE–5C 47
21c. Time-dependent capture zones for the 95% reliability level for Well UE–5C 48

22a. Time-dependent capture zones for the 50% reliability level for Wells 4 and 4A 40
22b. Time-dependent capture zones for the 67% reliability level for Wells 4 and 4A 50
22c. Time-dependent capture zones for the 95% reliability level for Wells 4 and 4A 51
23a. Time-dependent capture zones for the 50% reliability level for Well UE–16d 52
23b. Time-dependent capture zones for the 67% reliability level for Well UE–16d 53
23c. Time-dependent capture zones for the 95% reliability level for Well UE–16d 54
24a. Time-dependent capture zones for the 50% reliability level for Well 8 55
24b. Time-dependent capture zones for the 67% reliability level for Well 8 56
24c. Time-dependent capture zones for the 95% reliability level for Well 8 57
25a. Time-dependent capture zones for the 50% reliability level for Well UE–19c 58
25b. Time-dependent capture zones for the 67% reliability level for Well UE–19c 59
25c. Time-dependent capture zones for the 95% reliability level for Well UE–19c 60
26a. Time-dependent capture zones for the 50% reliability level for Well U–20 61
26b. Time-dependent capture zones for the 67% reliability level for Well U–20 62
26c. Time-dependent capture zones for the 95% reliability level for Well U–20 63

LIST OF TABLES

1. Hydraulic Properties and their Statistics for Each Water-Supply Well at the NTS. ... 10
2. Maximum Upgradient Width of Ultimate Capture Zone for Each Water-Supply Well at the NTS. 11

EXECUTIVE SUMMARY

A program to protect groundwater resources used for water supply from all potential threats due to contamination was established in the Amendments to the Safe Drinking Water Act (SDWA). The goal of the State Wellhead Protection (WHP) Program is to "protect wellhead areas within their jurisdiction from contaminants which may have any adverse effect on the health of persons." A major component of WHP is the determination of zones around water–supply wells called Wellhead Protection Areas (WHPAs) within which contaminant source assessment and management should be addressed. WHPAs are defined in the SDWA as "the surface and subsurface area surrounding a water well or wellfield, supplying a public water system, through which contaminants are reasonably likely to move toward and reach such water well or wellfield." A total of 14 water–supply wells are currently being used at the Nevada Test Site (NTS). Eleven of the wells are used for potable water supplies and the remaining three wells are used for construction purposes only. The purpose of this study as conducted by the Desert Research Institute (DRI) for the Department of Energy, Nevada Operations Office (DOE/NV), is to estimate WHPAs for each water–supply well at the NTS. Due to the limited information about the hydraulic properties needed for estimating the WHPAs, an approach that considered the uncertainty in the estimates of the hydraulic properties was developed and implemented.

The delineation of WHPAs as suggested by the U.S. Environmental Protection Agency is based on a steady-state analytic solution of a groundwater flow system that consists of a pumping well in a homogeneous aquifer with a regional gradient. The zone of influence (ZOI) corresponds to the drawdown curve and is related to the hydraulics of the system, not necessarily actual contaminant movement. The zone of capture represents the WHPA for the flow system and varies depending on the time period of desired well protection. The ultimate capture zone, also called the zone of contribution (ZOC), assumes infinite time available for travel of a contaminant and is terminated upgradient at the groundwater divide for the flow system. The time-dependent capture zone, also called the zone of transport (ZOT), is determined based on the distance a contaminant can travel in the selected time period. Both ultimate and time-dependent capture zones that considered uncertainties in the estimates of the hydraulic properties were developed for the water-supply wells at the NTS.

In this report, the focus is on the parameter uncertainty, the uncertainty in the modeling of capture zones coming primarily from the uncertainty in the magnitude and direction of the regional flow. At this stage, the spatial variability of the regional flow is not considered, only the uncertainty of the parameters used to form the analytical model of the capture zone. In general, the magnitude of the mean regional flow is not measured, but rather estimated indirectly using a form of Darcy's law, $q = TJ$, where T is the aquifer transmissivity and J is the hydraulic head gradient. Since these parameters are estimated from the scarce field data, they are subject to an estimation error which produces the total uncertainty in the regional flow estimate. The approach uses the uncertainties in T and J to estimate the corresponding uncertainty in the q which, in turn, produces the uncertainty in the capture zone. The magnitude of the regional flow and its direction are treated separately. Ultimate capture zones are generated for the 50 percent and 95 percent reliability levels where the reliability level corresponds to a level of confidence. The meaning of the 95 percent capture zone corresponds to the statement that there is a 95 percent level of confidence that the size of that specific

capture zone is large enough to encompass the entire capture zone for that well. The capture zone for the 50 percent reliability level corresponds to the deterministic capture zone based on the mean values of the hydraulic properties. The width of the capture zone is influenced by the uncertainty in the magnitude of the regional flow. The uncertainty in the flow direction produces two capture zones for each reliability level. For example, the two capture zones for the 67 percent reliability level are generated by calculating the q value that represents one standard deviation from its mean value, using this q value to determine the shape of the capture zone and then rotating that capture zone from the mean regional flow direction to the two angles that represent the plus and minus one standard deviation from the mean angle. The outer envelope of these two capture zones is the 67 percent reliability level capture zone. This envelope represents the total capture zone given the uncertainties in q and angle α at a certain reliability level. Time-dependent capture zones were generated for the 50 percent, 67 percent and 95 percent reliability level for the width of the capture zone.

Ultimate and time-dependent capture zones were generated based on the best available information on the hydraulic properties, pumping rates, and well construction. Information on the hydraulic properties needed for calculating the capture zones was obtained from reports. The hydraulic head gradient, both magnitude and direction, for each well is based on the water table map generated by Boughton (1986).

Ultimate capture zones were estimated for the water-supply wells. The ultimate capture zones were not extended to the groundwater divide because information on the location of a divide is unavailable. Only a finite length of the ultimate capture zone was shown to demonstrate the general shape of the capture zones. For water-supply wells J-12, J-13,UE-5C, combined 4 and 4A, combined C and C-1, and 8, the ultimate capture zones are very narrow. These narrow ultimate capture zones are produced primarily by the comparatively larger estimated value for regional flow relative to a low pumping rate.

Time-dependent capture zones were estimated for the water-supply wells. The time-dependent capture zones are long and narrow for wells J-12, J-13, UE-5C, combined 4 and 4A, combined C and C-1, and 8. This shape for these capture zones is again due to the comparatively larger regional flow relative to a low pumping rate, as was seen for the ultimate capture zones. Wells 5B, UE-16d, and U-20 have time-dependent capture zones similar to the expected shapes. The time-dependent capture zones for wells 5C and UE-19c are close to circular in shape. The circular shape for a time-dependent zone is due to very low regional flow compared to the pumping rate of the well.

Due to the lack of studies conducted at the NTS regarding the quantification of subsurface heterogeneity of the basic aquifer properties (e.g., hydraulic conductivity, porosity) and the resulting transport characteristics for mobile radionuclides, several simplifying assumptions are employed. These are:

1. homogeneity and isotropy of hydraulic properties (e.g., hydraulic conductivity, porosity);
2. conservative and advective transport only;
3. uniform hydraulic head gradient and pumping rates; and
4. steady-state flow conditions.

While assumptions 3 and 4 are less likely to significantly alter the estimated capture zones, assumptions 1 and 2 are known to be violated for the complex hydrogeological settings at the NTS.

At the present time, no information is available such that conditions 1 and 2 do not have to be assumed; therefore, this study employed the uncertainty in the mean flow magnitude and direction to indirectly account for the present lack of knowledge regarding the subsurface heterogeneity structure and other important transport properties. Information from additional studies aimed at quantifying the subsurface heterogeneity (at various scales) at the NTS is necessary to describe the groundwater flow and radionuclide transport processes with some confidence.

INTRODUCTION

A program to protect groundwater resources used for water supply from all potential threats due to contamination was established in the 1986 Amendments to the Safe Drinking Water Act (SDWA). The goal of the State Wellhead Protection (WHP) Program is to "protect wellhead areas within their jurisdiction from contaminants which may have any adverse effect on the health of persons." A major component of WHP is the determination of zones around water-supply wells called Wellhead Protection Areas (WHPAs) within which contaminant source assessment and management should be addressed. WHPAs are defined in the SDWA as "the surface and subsurface area surrounding a water well or wellfield, supplying a public water system, through which contaminants are reasonably likely to move toward and reach such water well or wellfield." A total of 14 water-supply wells are currently being used at the Nevada Test Site (NTS). Eleven of the wells are used for potable water supplies and the remaining three wells are used for construction purposes only. The purpose of this study as conducted by the Desert Research Institute (DRI) for the Department of Energy, Nevada Operations Office (DOE/NV), is to estimate WHPAs for each water-supply well at the NTS. Due to the limited information about the hydraulic properties needed for estimating the WHPAs, an approach that considered the uncertainty in the estimates of the hydraulic properties was developed and implemented.

The delineation of WHPAs as suggested by the U.S. Environmental Protection Agency (EPA) is based on a steady-state analytic solution of a groundwater flow system that consists of a pumping well in a homogeneous aquifer with a regional gradient, schematically shown in Figure 1. The zone of influence (ZOI) corresponds to the drawdown curve shown in Figure 1a and is related to the hydraulics of the system, not necessarily actual contaminant movement. The zone of capture represents the WHPA for the flow system and varies depending on the time period of desired well protection. The ultimate capture zone, also called the zone of contribution (ZOC), assumes infinite time available for travel of a contaminant and is terminated upgradient at the groundwater divide for the flow system. The time-dependent capture zone, also called the zone of transport (ZOT), is determined based on the distance a contaminant can travel in the selected time period. Both ultimate and time-dependent capture zones that considered uncertainties in the estimates of the hydraulic properties were developed for the water-supply wells at the NTS.

The ultimate capture zone, as shown in Figure 1b, is obtained by solution of the following equations:

$$\left(\frac{y}{x}\right) = \tan\left[\frac{+ 2\pi q\theta}{Q}\right] \; y > 0 \quad ; \quad \left(\frac{y}{x}\right) = - \tan\left[\frac{+ 2\pi q\theta}{Q}\right] \; y < 0 \qquad (1)$$

where Q is the well pumping rate, $q = TJ$, T is transmissivity of the aquifer, J is the regional hydraulic head gradient, $\theta = (-x \sin \alpha + y \cos \alpha)$ and α is the angle between the x–axis and the direction of uniform regional flow. The derivation of equation (1) is found in Appendix A. As x becomes large, the width of the ultimate capture zone approaches the finite limits

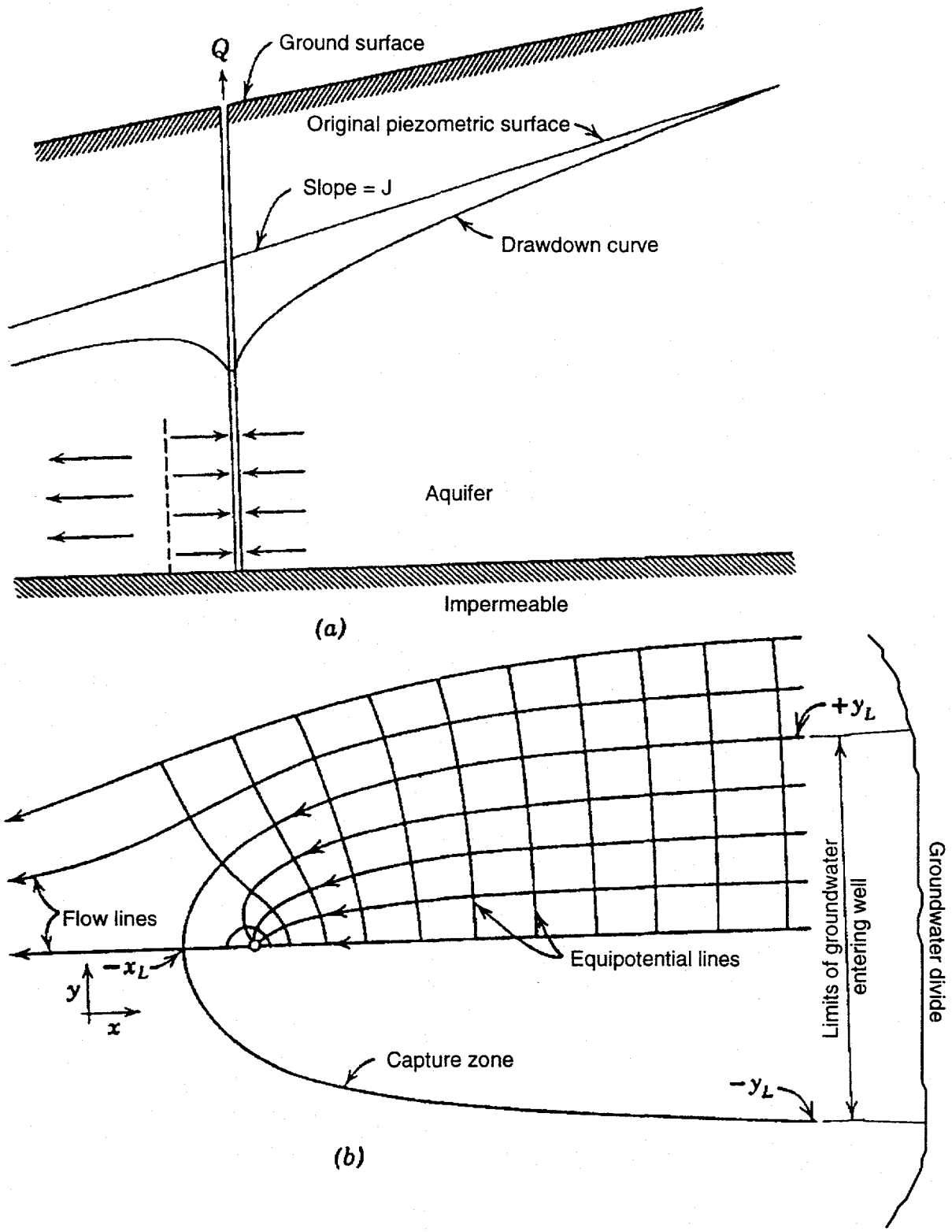

Figure 1. Schematic of pumping well in a regional flow system; shown in (a) vertical profile and (b) plan view (after Todd, 1980).

$$y_L = \pm \frac{Q}{2TJ} \tag{2}$$

as shown in Figure 1b. The boundary of the capture zone extends downstream to a stagnation point, x_L, where

$$x_L = -\frac{Q}{2\pi TJ} \tag{3}$$

as indicated in Figure 1b.

The ultimate capture zone can be obtained from equation (1) given information on the well pumping rate, transmissivity of the aquifer, regional hydraulic head gradient and direction of the uniform regional flow. However, calculation of the time-dependent capture zone also requires information on the porosity of the aquifer, n, and the aquifer thickness, b, which is usually assumed to be the thickness of the screened interval of the well if the actual aquifer thickness is unknown. To calculate a time-dependent capture zone, the flow pattern shown in Figure 1b is used and particles are moved along the flowlines a distance determined from the time of travel and the velocity. The velocity components in the x and y direction are

$$v_x = -\frac{T}{bn}\frac{\partial H}{\partial x} \quad \text{and} \quad v_y = -\frac{T}{bn}\frac{\partial H}{\partial y} \tag{4}$$

where H is the hydraulic head for the flow system. Both the ultimate and time-dependent capture zones are based on the set of parameters that are assumed to be perfectly known. A deterministic solution is based on these representative values for the various model parameters. They usually represent a mean or average value of the system. Since perfect knowledge in model parameters is seldom the case, the influence of the uncertainty becomes a major factor.

There are numerous sources of uncertainty which can influence the formation of capture zones around a pumping well. These uncertainties can range from the conceptual modeling uncertainty, uncertainty in the selected form of a mathematical model, and parameter uncertainty. It is important to identify what is the most important source of uncertainty for a particular case. In this report, the focus is on parameter uncertainty, the uncertainty in the modeling of capture zones coming primarily from the uncertainty in the magnitude and direction of the regional flow. At this stage, the spatial variability of the regional flow is not considered, only the uncertainty of the parameters used to form the analytical model of the capture zone. In addition, the model uncertainty in representing the complex groundwater flow patterns found at the NTS by the simplified analytical model is not addressed and may be a significant component in the total uncertainty in the capture zones.

METHODOLOGY FOR WELLHEAD PROTECTION AREA DELINEATION UNDER UNCERTAINTY

The ability to determine the capture zones conditioned on the uncertainty in the mean regional flow is a first step in delineating the WHPA. In general, the mean flow is not measured, but rather

estimated indirectly using a form of Darcy's law, $q = TJ$, where T is the aquifer transmissivity and J is the hydraulic head gradient. These parameters are estimated from the scarce field data, thus they are subject to an estimation error which produces the total uncertainty in the regional flow estimate, q. If both T and J are lognormally distributed, then so is q (Benjamin and Cornell, 1970). The mean and variance of q is estimated based on the means and variances of T and J. The uncertainty in q causes variations in the capture zone as shown in Figure 2. The mean capture zone as indicated by the 0.50 curve in Figure 2 is the deterministic capture zone based on the mean q value. Capture zones that represent various reliability levels can be determined based on the appropriate uncertainty in the q value for the given reliability level. For example, the 0.67 and the 0.33 percent reliability level capture zones shown in Figure 2 represent the curves generated by the q values obtained from subtracting and adding, respectively, one standard deviation to the mean q value. The larger q value yields a narrower capture zone upgradient (the 0.33 reliability level curve), whereas the smaller q value produces a wider capture zone upgradient (the 0.67 reliability level curve). The 67 percent reliability level capture zone means there is a 67 percent reliability that the capture zone is large enough to include the true capture zone given the uncertainty in the mean flow q.

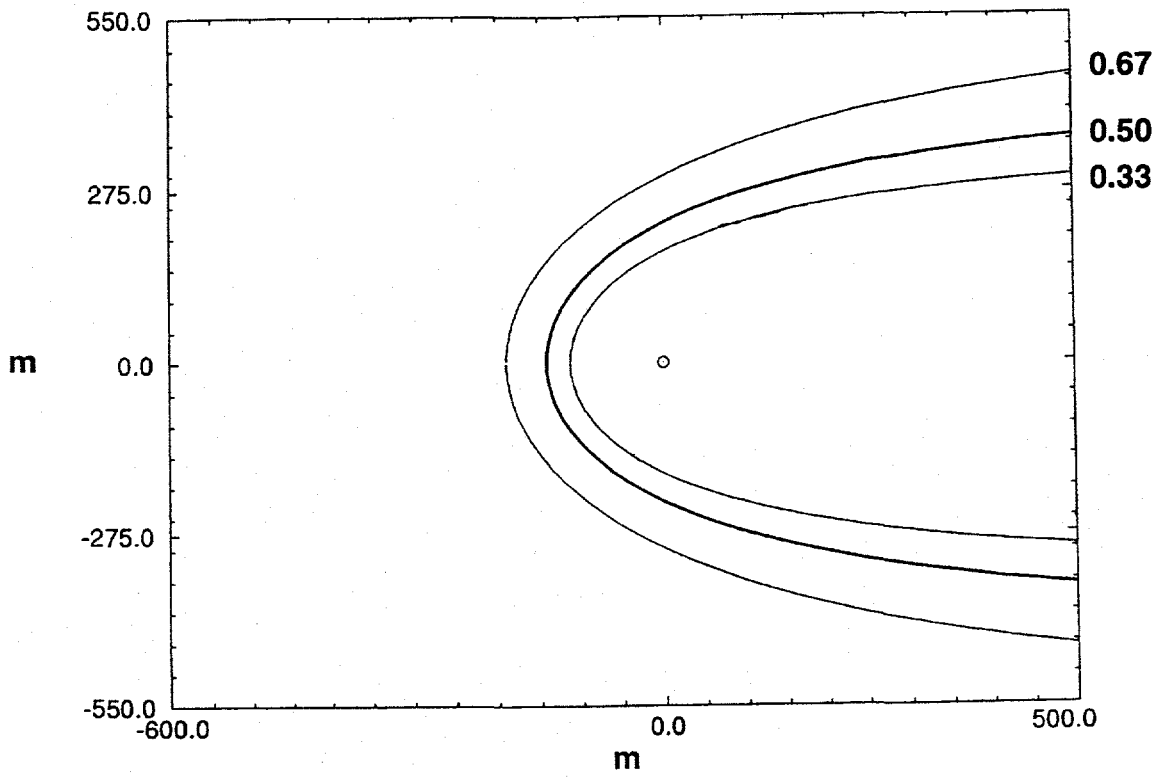

Figure 2. Capture zones corresponding to the deterministic (i.e., 0.50 value) curve and two bounding curves corresponding to the reliability levels shown on the curves.

The uncertainty in the capture zone caused by the uncertainty in the angle α can be estimated in the same manner based on the reliability level. Assuming α is normally distributed, the 67 percent reliability level will correspond to two angles that are equal to the mean α plus and minus one standard deviation of the angle. The two capture zones for the 67 percent reliability level are generated by calculating the q value that represents one standard deviation from its mean value, using this q value to determine the shape of the capture zone and then rotating that capture zone from the mean regional flow direction to the two angles that represent the plus and minus one standard deviation from the mean angle. The outer envelope of these two capture zones is the 67 percent reliability level capture zone. This envelope represents the total capture zone given the uncertainties in q and angle a at a certain reliability level. A schematic of two capture zones and the outer envelope is shown in Figure 3. The 95 percent reliability level corresponds to two standard deviations in uncertainty of q and a, whereas the 67 percent reliability level corresponds to one standard deviation in uncertainty.

A detailed mathematical derivation of the methodology for wellhead protection area delineation under uncertainty is given in Appendix A.

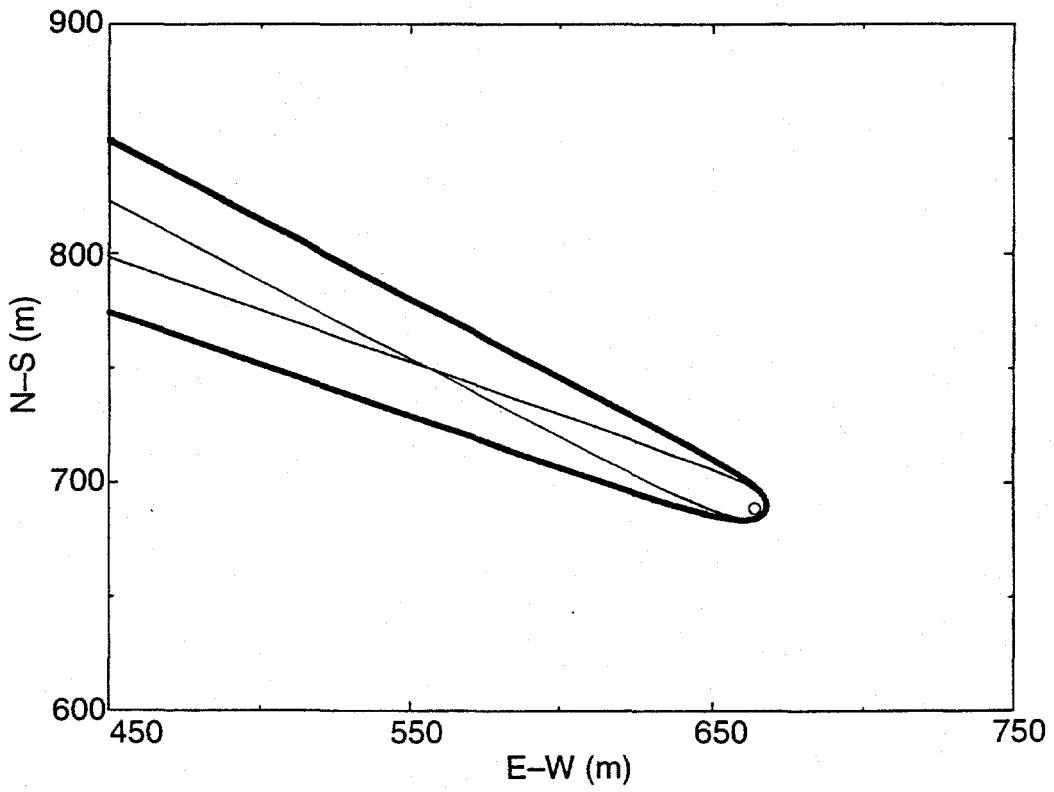

Figure 3. Schematic of two capture zones for a specified reliability level. Heavy line indicates outer envelope for the two curves.

WELLHEAD PROTECTION DELINEATION UNDER UNCERTAINTY FOR THE WATER-SUPPLY WELLS AT THE NEVADA TEST SITE

A total of 14 water-supply wells are currently being used at the NTS and their locations are shown in Figure 4. Coordinates for these wells, along with well construction details, were taken from the Raytheon Services Nevada (1991) "Red Book." The gradients and direction of groundwater flow for all 14 wells were determined by using the NTS water table map prepared by Boughton (1986), as shown in Figure 5. This water table map is based on computer-generated contours of hydraulic heads and is only one possible representation of the hydraulic heads because of the sparse head data available for use in the contouring. As additional hydraulic head data from new wells are collected, the hydraulic head map for the NTS can be modified and any changes to head gradients and directions of groundwater flow can be used to generate new capture zones where appropriate. Pumping rates for all of the wells, with the exception of water well 4A for which there are no data yet, were obtained from David Wood (U.S. Geological Survey, personal communication).

Wells C and C-1 were combined and treated as one well since they are only 30 meters apart, as were wells 4 and 4A, which are 360 meters apart and each pair has identical means and standard deviations in T, J and α. In these two cases, the total pumping rate for the combined well was the sum of the pumping rates for the two wells and the total thickness was the sum of the thicknesses for the two wells.

Capture zones were generated for each of the supply wells using equation (1) with the appropriate statistics on regional flow. Estimates of the mean and variance for transmissivity and the magnitude of the regional gradient were needed to obtain the mean and variance for the q parameter. In general, limited information about the hydraulic properties is available for the various wells at the NTS and statistical information is unavailable. Thus, the statistical information for transmissivity was based on the best judgement of the authors concerning the possible ranges in values of transmissivity for a given area. In general, the range in transmissivity was assumed to be one order of magnitude and the statistics were developed to reproduce this range. The statistical information for the regional gradient was obtained from the NTS water table map prepared by Boughton (1986). The estimates of the means and variances for the regional gradient at each well were obtained by having several individuals estimate the regional gradient using the water table map. The range in their results was used to estimate the mean of variance of the regional gradient for each well. The mean angle of the regional gradient was estimated based on a similar procedure with the variance in the angle taken as 15 degrees at each well to allow for the larger uncertainty in the flow direction expected because of the limited hydraulic head data used to obtain the NTS water table map. Once mean values and standard deviations were derived for the log of transmissivity and the log of hydraulic head gradient, the mean of log q and its associated variance σ^2_{lnq} are calculated from the equations presented in Appendix A. The correlation coefficient between the $ln\ T$ and $ln\ J$ terms for the regional flow was assumed to be –0.8 because for a given regional flow, T is inversely proportional to J.

The information on hydraulic properties and their statistics, pumping rates and well construction used to generate the capture zones for each well is given in Table 1. The transmissivity

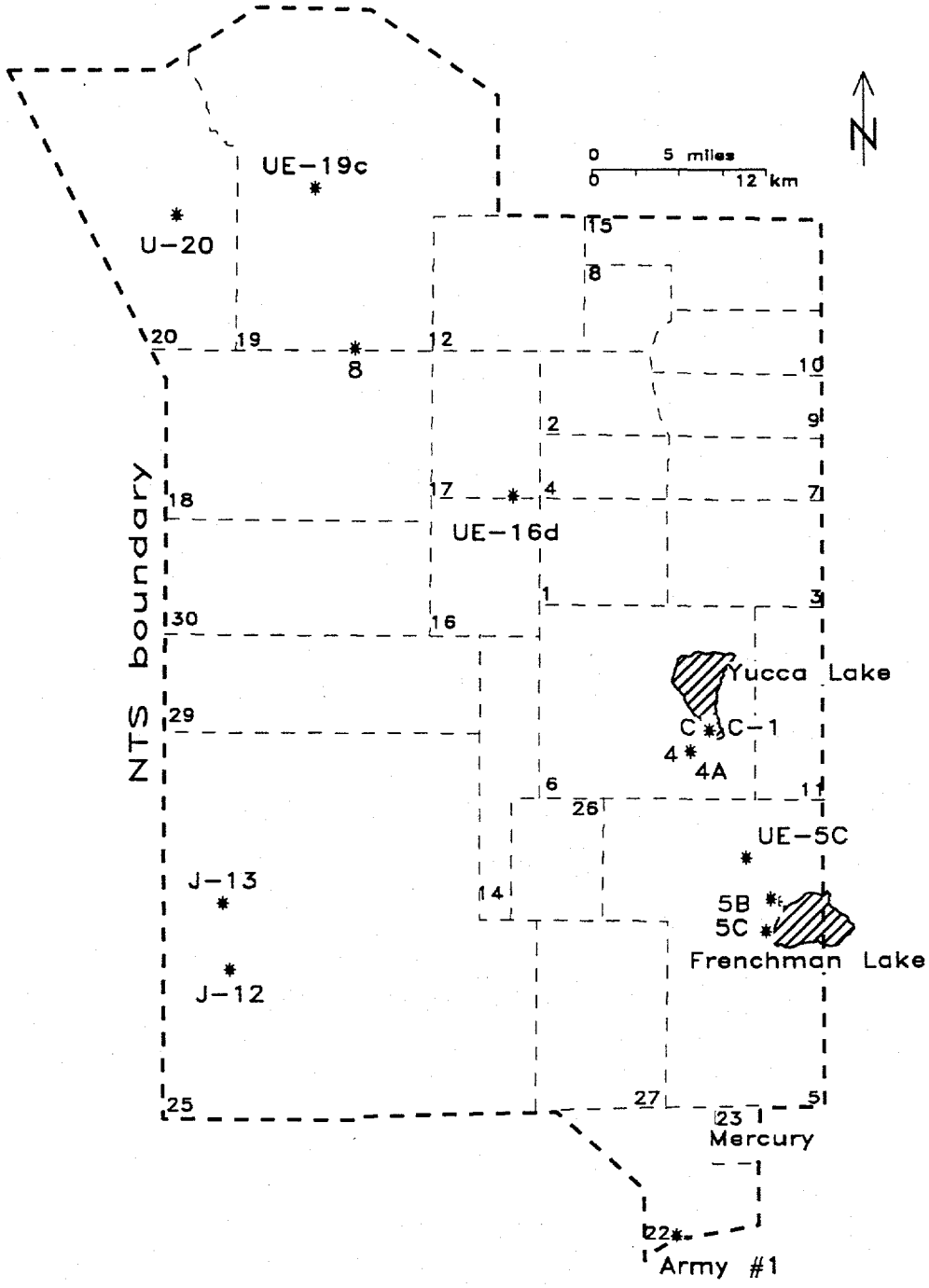

Figure 4. Map of the NTS showing the location of 14 water-supply wells.

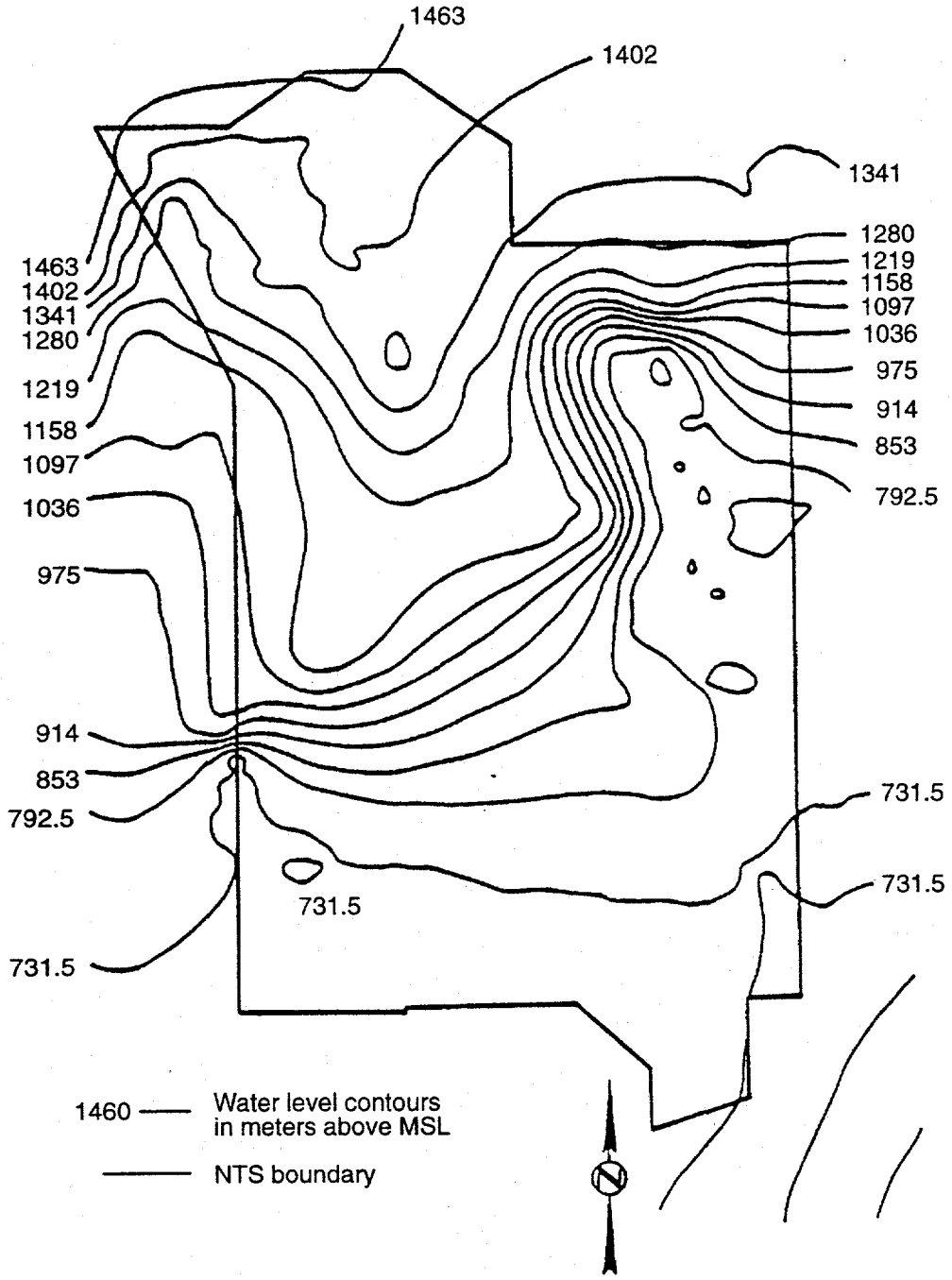

Figure 5. NTS water table map (after Boughton, 1986).

estimates were obtained from Winograd and Thordarson (1975), Raytheon Services Nevada (1990), and Blankennagel and Weir (1973). The well location and construction information was compiled from Raytheon Services Nevada (1991) and Arteaga et al. (1991). The thicknesses were based on the open or screened interval of the wells because no information was available about the actual intervals supplying the water to the wells. The porosity values for each well were estimated based on interval of completion. A porosity of 0.02 was assumed for the carbonate units, 0.05 for the tuff units, and 0.15 for the alluvium units (Sadler, 1990; Blankennagel and Weir, 1973).

Ultimate Capture Zones

Ultimate capture zones for 50 percent and 95 percent reliability levels were estimated for the water-supply wells and presented on individual maps. The figure number for each water-supply well map is listed in Table 1. The ultimate capture zones shown in the figures have not been extended to the groundwater divide because information on the location of a divide is unavailable. Only a finite length of the ultimate capture zone has been shown in the figures to demonstrate the general shape of the capture zones. For water-supply wells J-12, J-13, UE-5C, combined 4 and 4A, combined C and C-1, and 8, the ultimate capture zones are very narrow, as plotted on the figures. The maximum width of the ultimate capture zone for the 50 percent reliability level as calculated from equation (2) is given in Table 2 for each well. The maximum width for the wells listed above is 57 m or less. These narrow ultimate capture zones are produced primarily by the relatively larger regional flow (q) caused by larger T values together with the J values, but at times combined with a low pumping rate.

The uncertainty on the angle of the regional flow was, in general, smaller for the ultimate capture zone than the values listed in Table 1. The standard deviation of the angle used to generate the 95 percent reliability level capture zone is included in the corresponding figure caption for each well. The smaller uncertainty in angle is based on error in estimating the angle from the water table map of Boughton (1986). The objective in estimating the ultimate capture zone for each well is to observe the effect of the large-scale regional flow as represented by the water table map. The time-dependent capture zones are influenced more by the local-scale flow and may have higher uncertainties in flow direction.

Time-Dependent Capture Zones

Time-dependent capture zones for 50 percent, 67 percent and 95 percent reliability levels were estimated for the water-supply wells. The figure number for each well is listed in Table 1 with the time periods used to generate the curves. Time-dependent capture zones for water-supply wells Army #1, J-12, and combined C and C-1 are not presented because they are very similar to the ultimate capture zones. To represent possible variations in the local-scale flow patterns over time, a larger uncertainty in the flow direction of σ_α equal to 15 degrees was used. This leads to more conservative estimates in the width or spread of the capture zone perpendicular to the mean flow direction. Thus, the time-dependent capture zones represent a certain reliability level, such as 67 percent or 95 percent, in the width of the capture zone. The upgradient length of the time-dependent capture zone is best represented by the deterministic (or 50 percent) capture zone because as the

Table 1. Hydraulic Properties and their Statistics for Each Water-Supply Well at the NTS.

Well	X (east) (m)	Y (north) (m)	Q (m^3/day)	T (m^2/day)	s_T (m^2/day)	J	s_J	a	s_α	n	b (m)	Ultimate Capture Zone Figs.	Time-Dependent Capture Zone Figs.	Time (yrs)
Army 1	208719	204491	1446	1190	585	0.0054	.0009	124	15	.02	76	6a, b	6a, b	10
J–12	177092	223573	130	1323	486	0.0056	.0005	22.5	15	.05	23	7a, b	7a, b	10
J–13	176678	228359	274	934	442	0.0133	.0013	27	15	.05	309	8a, b	18a, b, c	5, 10, 15
5B	214659	227795	596	149	63.8	0.0084	.0008	303.5	15	.15	65	9a, b	19a, b, c	30, 40, 50
5C	215155	226424	634	33.6	14	0.0087	.0009	310.5	15	.15	91	10a, b	20a, b, c	40, 50, 60
UE–5C*	213664	231689	55	1020	489	0.0088	.0013	299.5	15	.15	365	11a, b	21a, b, c	30, 40, 50
4	209672	239268	876	1821	702	0.0182	.0017	237	15	.05	151	12a, b	22a, b, c	3, 4, 5
4A	209367	239070	876	1821	702	0.0182	.0017	237	15	.05	94	12a, b	22a, b, c	3, 4, 5
C	210940	240817	154	6175	2797	0.0175	.0025	241.5	15	.02	22	13a, b	13a, b	1
C–1	210962	240795	314	6175	2797	0.0175	.0025	241.5	15	.02	34	13a, b	13a, b	1
UE–16d	197074	257519	341	47	18.5	0.0097	.0005	301	15	.02	50	14a, b	23a, b, c	5, 10, 15
8	185928	268062	587	2477	996	0.0145	.0025	355	15	.05	293	15a, b	24a, b, c	5, 10, 15
UE–19c*	183193	279502	505	162.5	70.8	0.0031	.0012	357	15	.05	1849	16a, b	25a, b, c	40, 50, 60
U–20*	173459	277545	858	207	74.9	0.011	.001	60	15	.05	233	17a, b	26a, b, c	5, 10, 15

* Water-supply wells used for construction purposes only.

reliability levels increase, the corresponding time-dependent capture zone gets wider and shorter, as can be seen for Well 5B in Figure 19a, b, c. This trade-off between width and length of the capture zone is caused by requiring the same volume of water to enter the well for a given time period.

Table 2. Maximum Upgradient Width of Ultimate Capture Zone for Each Water-Supply Well at the NTS.

Well	Q (m^3/day)	q_{50} (m^2/day)	Maximum width ($2y_L$) (m)
Army #1	1446	5.692	254
J–12	130	6.869	18.9
J–13	274	11.179	24.6
5B	596	1.153	517
5C	634	0.267	2374
UE–5C	55	7.965	6.9
4 & 4A	1752	30.723	57
C & C–1	468	97.417	4.8
UE–16d	341	0.428	796
8	587	32.819	17.8
UE–19c	505	0.432	1168
U–20	858	2.132	402

The time-dependent capture zones are long and narrow for wells J-12, J-13, UE-5C, combined 4 and 4A, combined C and C-1, and 8. This shape for these capture zones is again due to the relatively larger regional flow at times combined with lower pumping rates, as was seen for the ultimate capture zones. Wells 5B, UE-16d, and U-20 have time-dependent capture zones similar to the expected shapes (as shown in Figure 1b). The time-dependent capture zones for wells 5C and UE-19c are close to circular in shape. The circular shape for a time-dependent zone is due to very low regional flow compared to the pumping rate of the well.

SUMMARY

Ultimate and time-dependent capture zones were generated based on the best available information on the hydraulic properties, pumping rates, and well construction. Information on the hydraulic properties needed for calculating the capture zones was obtained from reports. The hydraulic head gradient, both magnitude and direction, for each well is based on the water table map generated by Boughton (1986).

Ultimate capture zones were estimated for the water-supply wells. The ultimate capture zones were not extended to the groundwater divide because that information is unavailable. Only a finite length of the ultimate capture zone was shown to demonstrate the general shape of the capture zones.

For water-supply wells J-12, J-13,UE-5C, combined 4 and 4A, combined C and C-1, and 8, the ultimate capture zones are very narrow. These narrow ultimate capture zones are produced primarily by the large estimated value for regional flow relative to a low pumping rate.

Time-dependent capture zones were estimated for the water-supply wells. The time-dependent capture zones are long and narrow for wells J-12, J-13, UE-5C, combined 4 and 4A, combined C and C-1, and 8. This shape for these capture zones is again due to the large regional flow as was seen for the ultimate capture zones. Wells 5B, UE-16d, and U-20 have time-dependent capture zones similar to the expected shapes. The time-dependent capture zones for wells 5C and UE-19c are close to circular in shape. The circular shape for a time-dependent zone is due to very low regional flow compared to the pumping rate of the well.

Due to the lack of studies conducted at the NTS regarding the quantification of subsurface heterogeneity of the basic aquifer properties (e.g., hydraulic conductivity, porosity) and the resulting transport characteristics for mobile radionuclides, several simplifying assumptions are employed. These are:

1. homogeneity and isotropy of hydraulic properties (e.g., hydraulic conductivity, porosity);
2. conservative and advective transport only;
3. uniform hydraulic head gradient and pumping rates; and
4. steady-state flow conditions.

While assumptions 3 and 4 are less likely to significantly alter the estimated capture zones, assumptions 1 and 2 are known to be violated for the complex hydrogeological settings at the NTS. At the present time, no information is available such that conditions 1 and 2 do not have to be assumed; therefore, this study employed the uncertainty in the mean flow magnitude and direction to indirectly account for the present lack of knowledge regarding the subsurface heterogeneity structure and other important transport properties. Information from additional studies aimed at quantifying the subsurface heterogeneity (at various scales) at the NTS is necessary to describe the groundwater flow and radionuclide transport processes with some confidence.

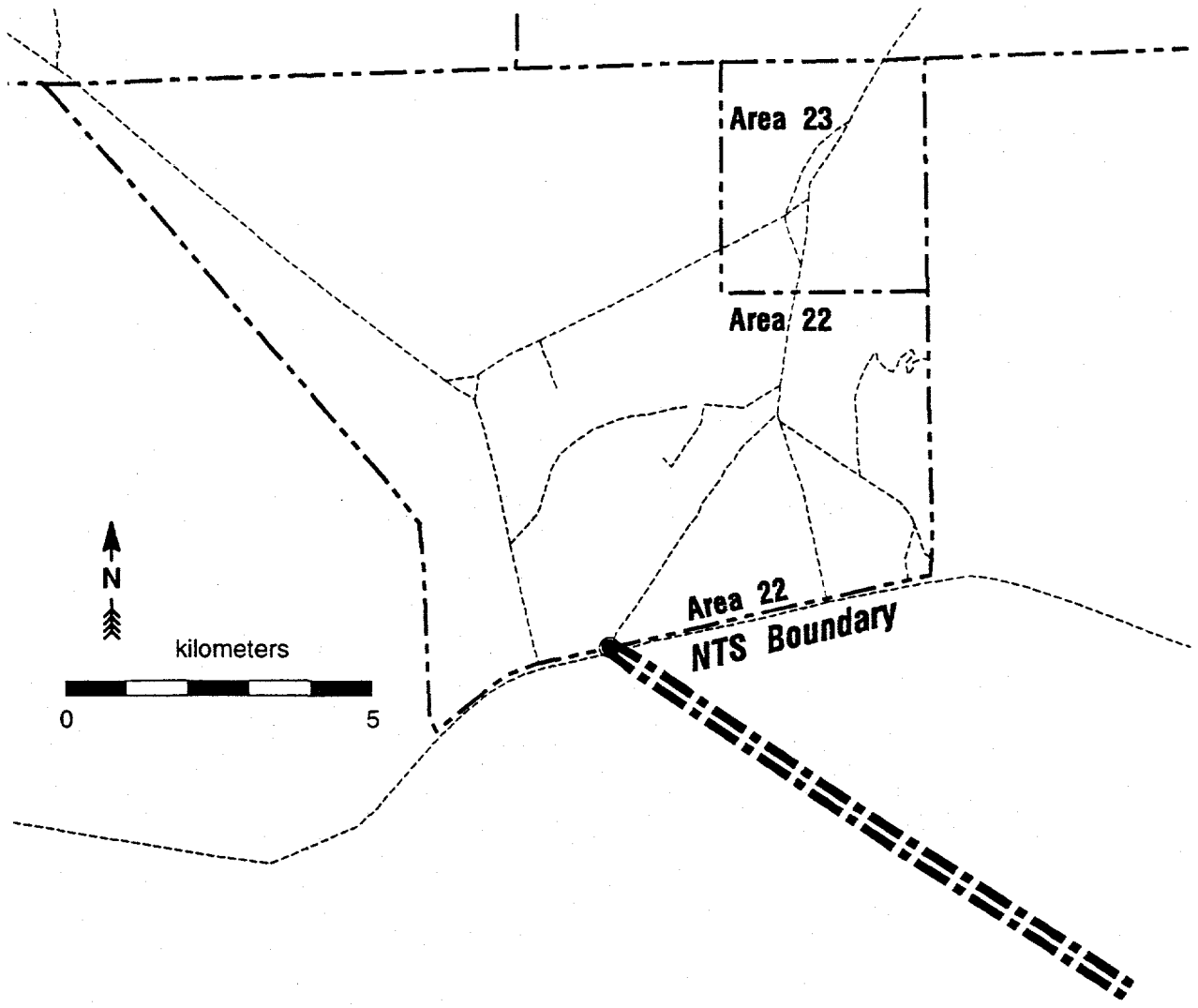

Figure 6a. Ultimate capture zone for the 50% reliability level for Well Army #1. Filled circle indicates a well.

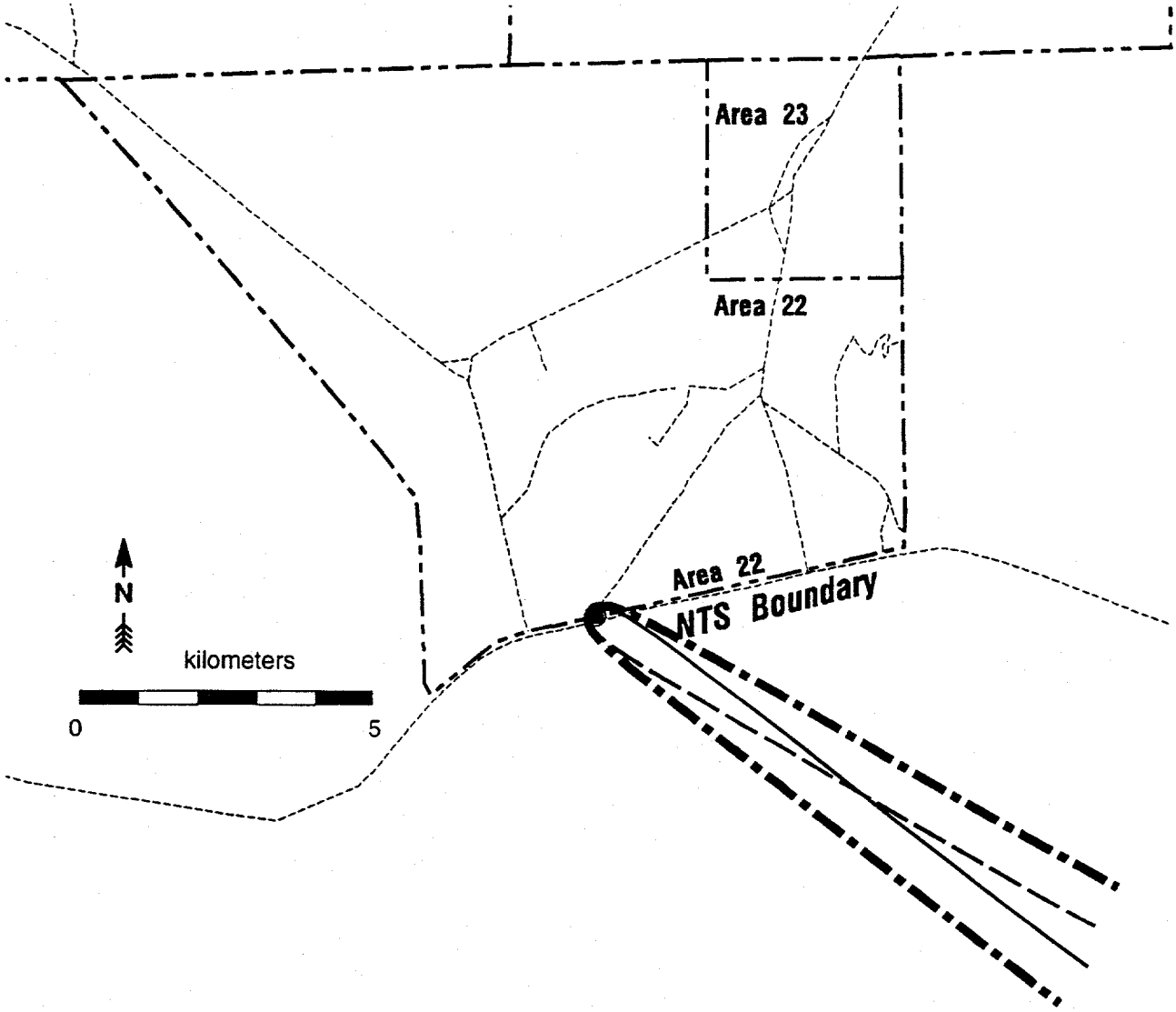

Figure 6b. Ultimate capture zones for the 95% reliability level for Well Army #1. Heavy dashed line is outer envelope for the two curves. Filled circle indicates a well. Standard deviation on the angle is 2°.

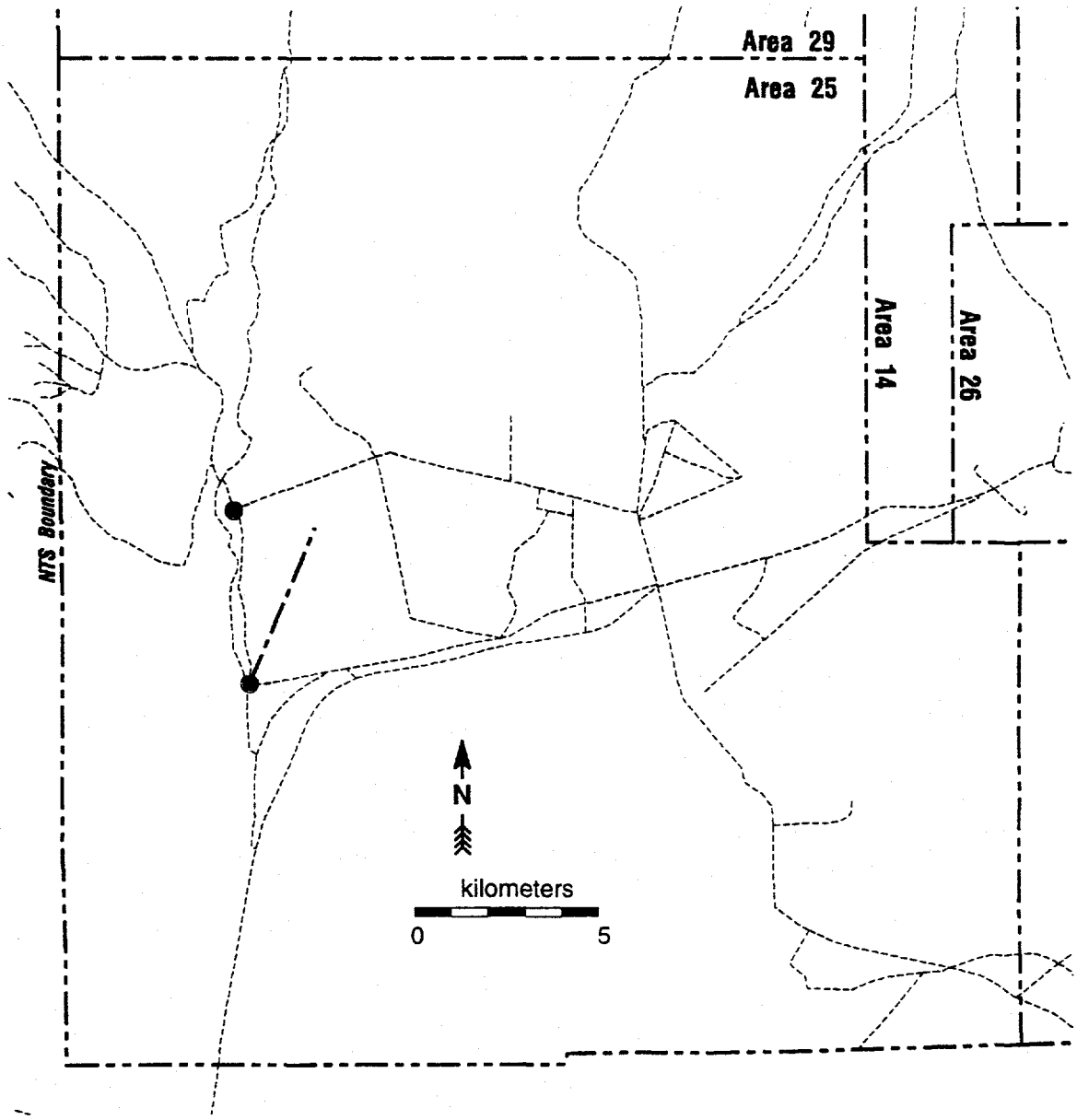

Figure 7a. Ulitmate capture zone for the 50% reliability level for Well J–12. Filled circle indicates a well.

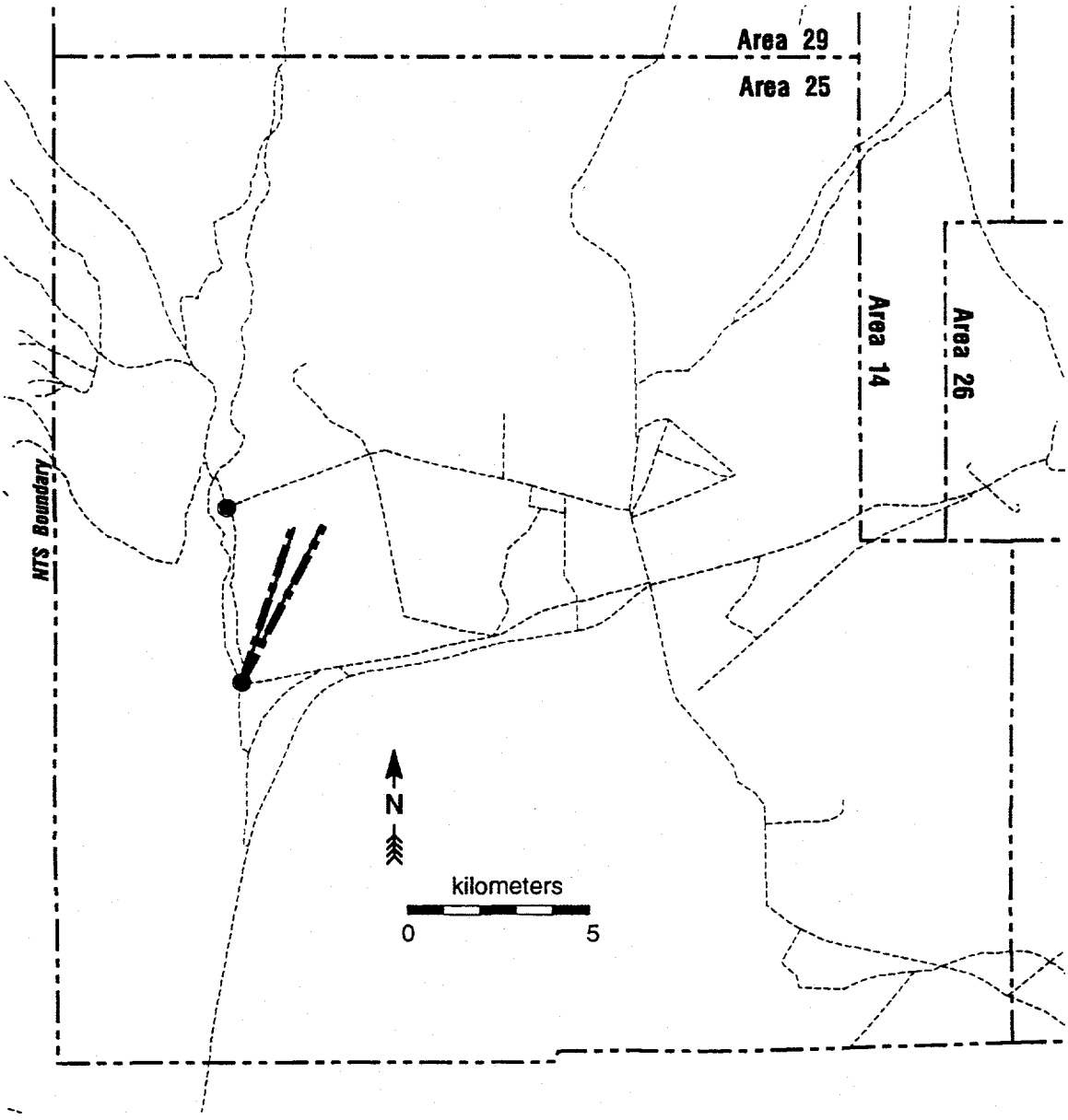

Figure 7b. Ultimate capture zones for the 95% reliability level for Well J–12. Heavy dashed line is outer envelope for the two curves. Filled circle indicates a well. Standard deviation on the angle is 2.2°.

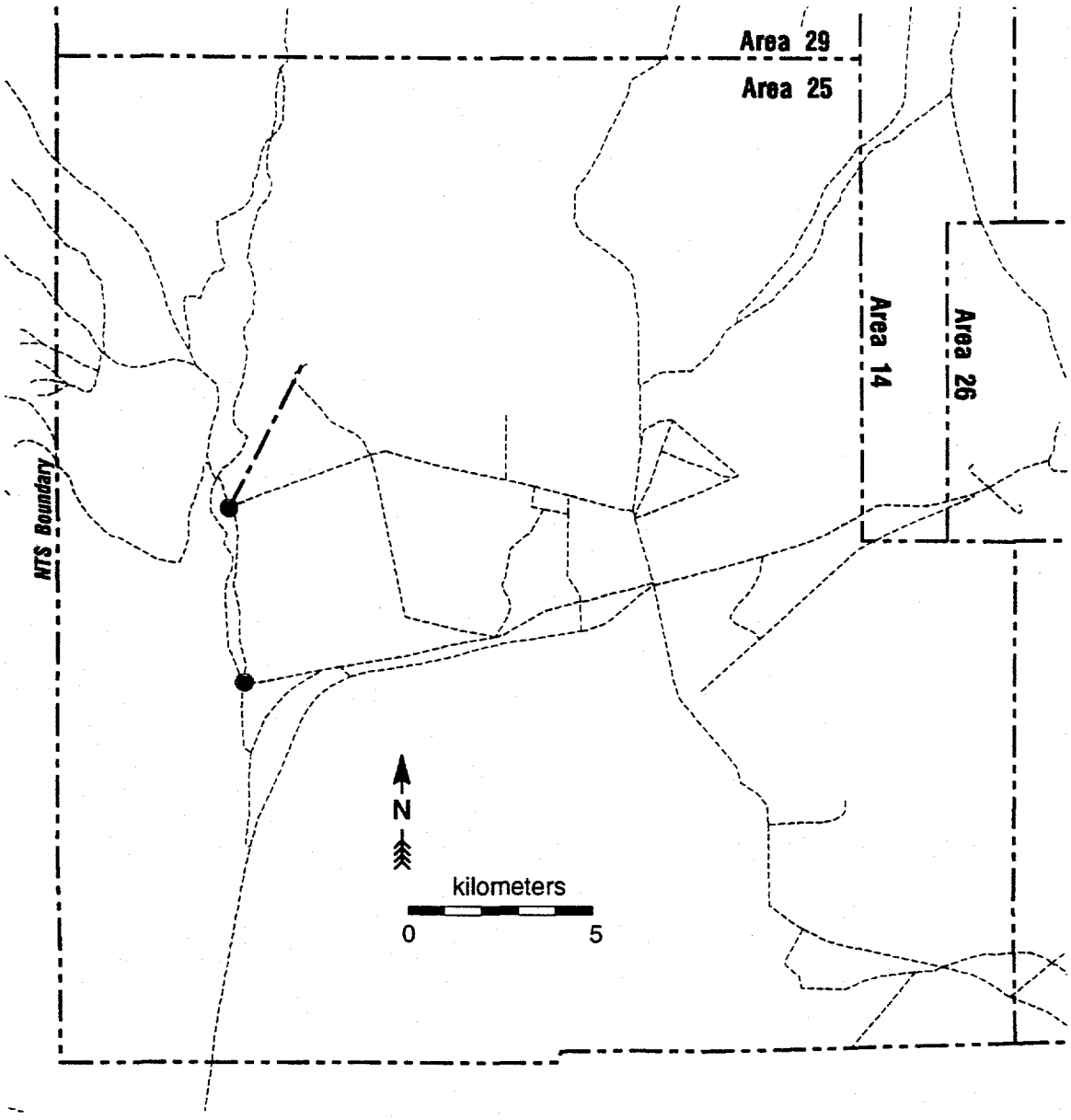

Figure 8a. Ultimate capture zone for the 50% reliability level for Well J–13. Filled circle indicates a well.

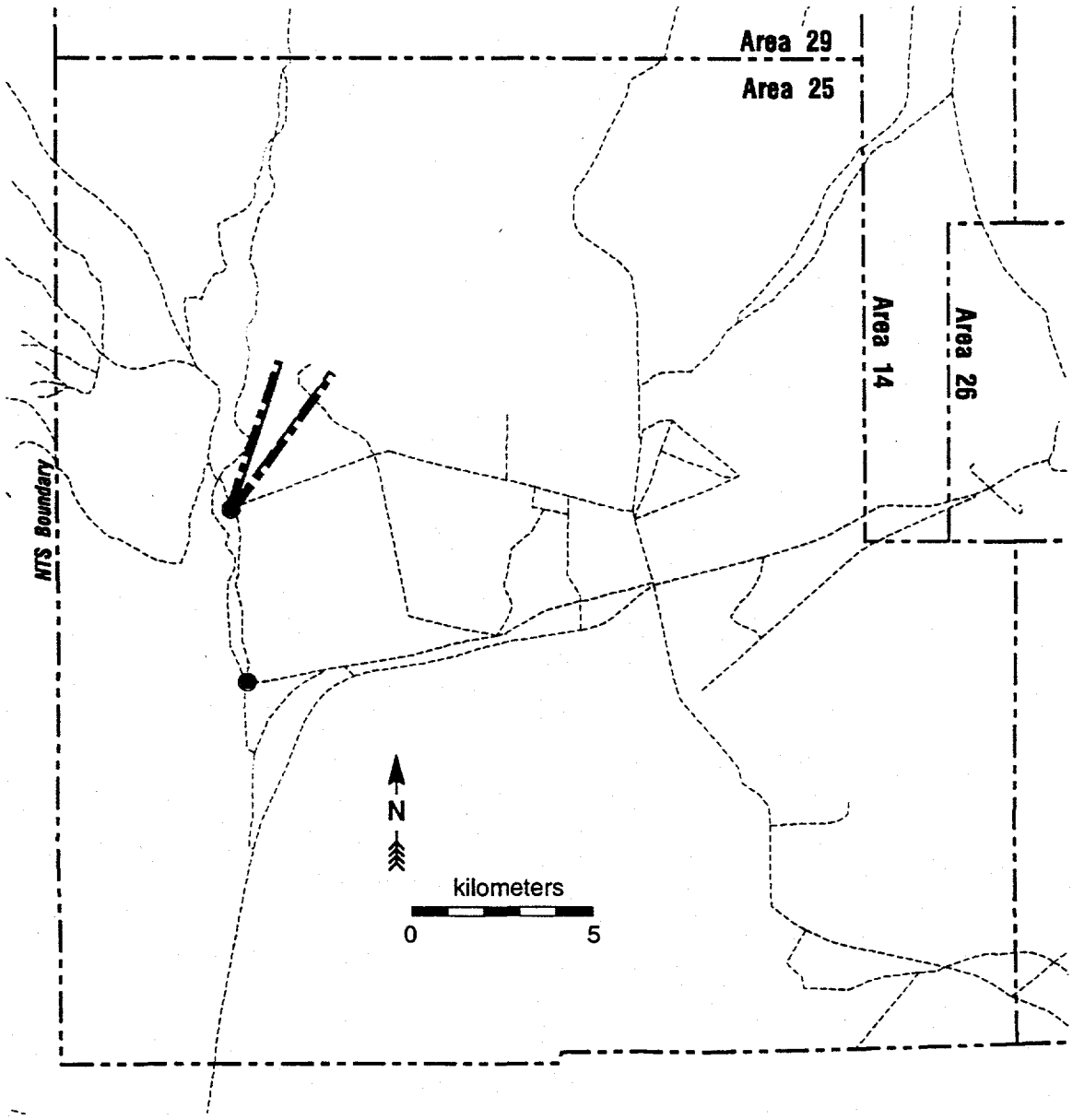

Figure 8b. Ultimate capture zones for the 95% reliability level for Well J–13. Heavy dashed line is outer envelope for the two curves. Filled circle indicates a well. Standard deviation on the angle is 4.7°.

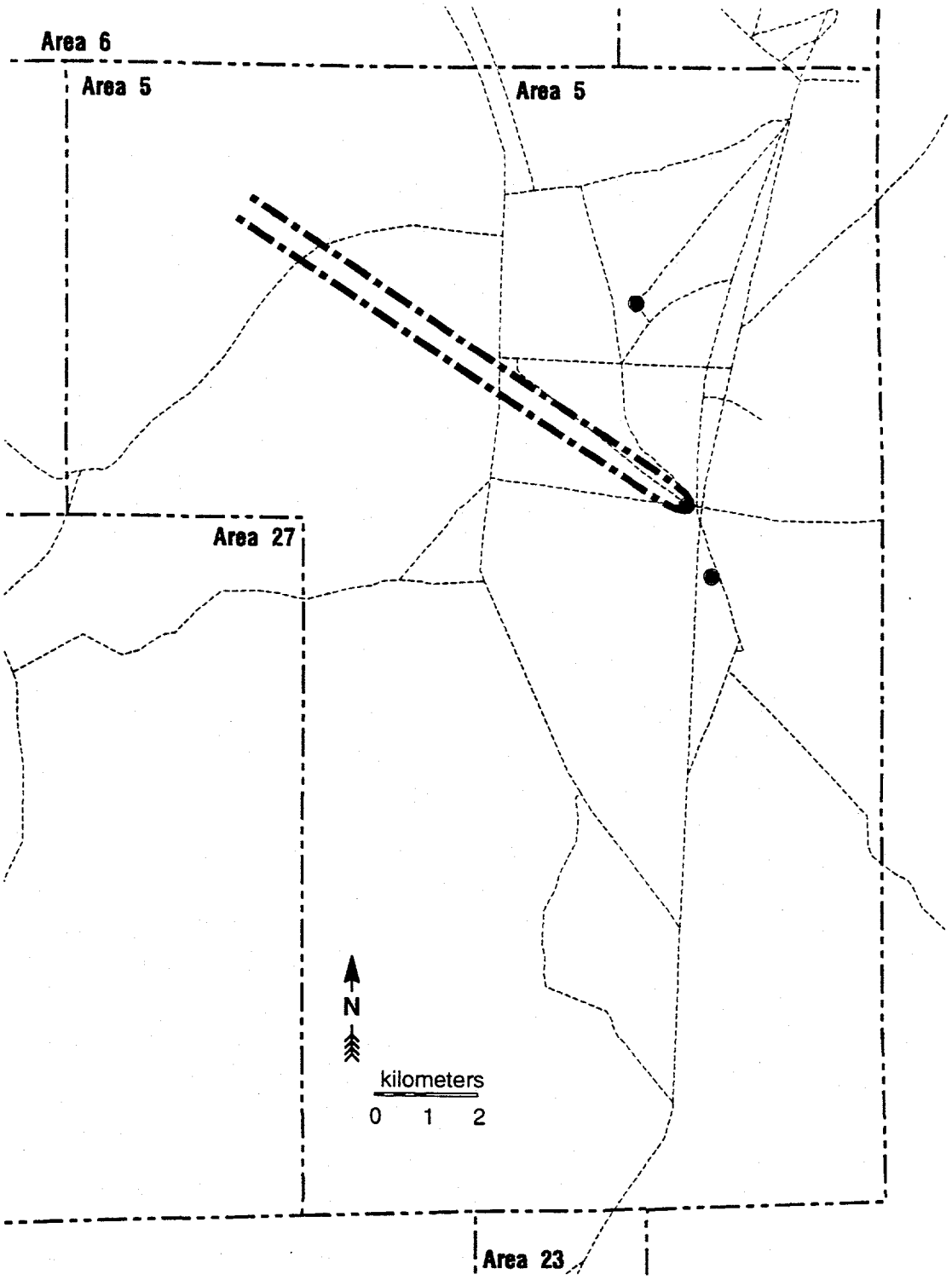

Figure 9a. Ultimate capture zone for the 50% reliability level for Well 5B. Filled circle indicates a well.

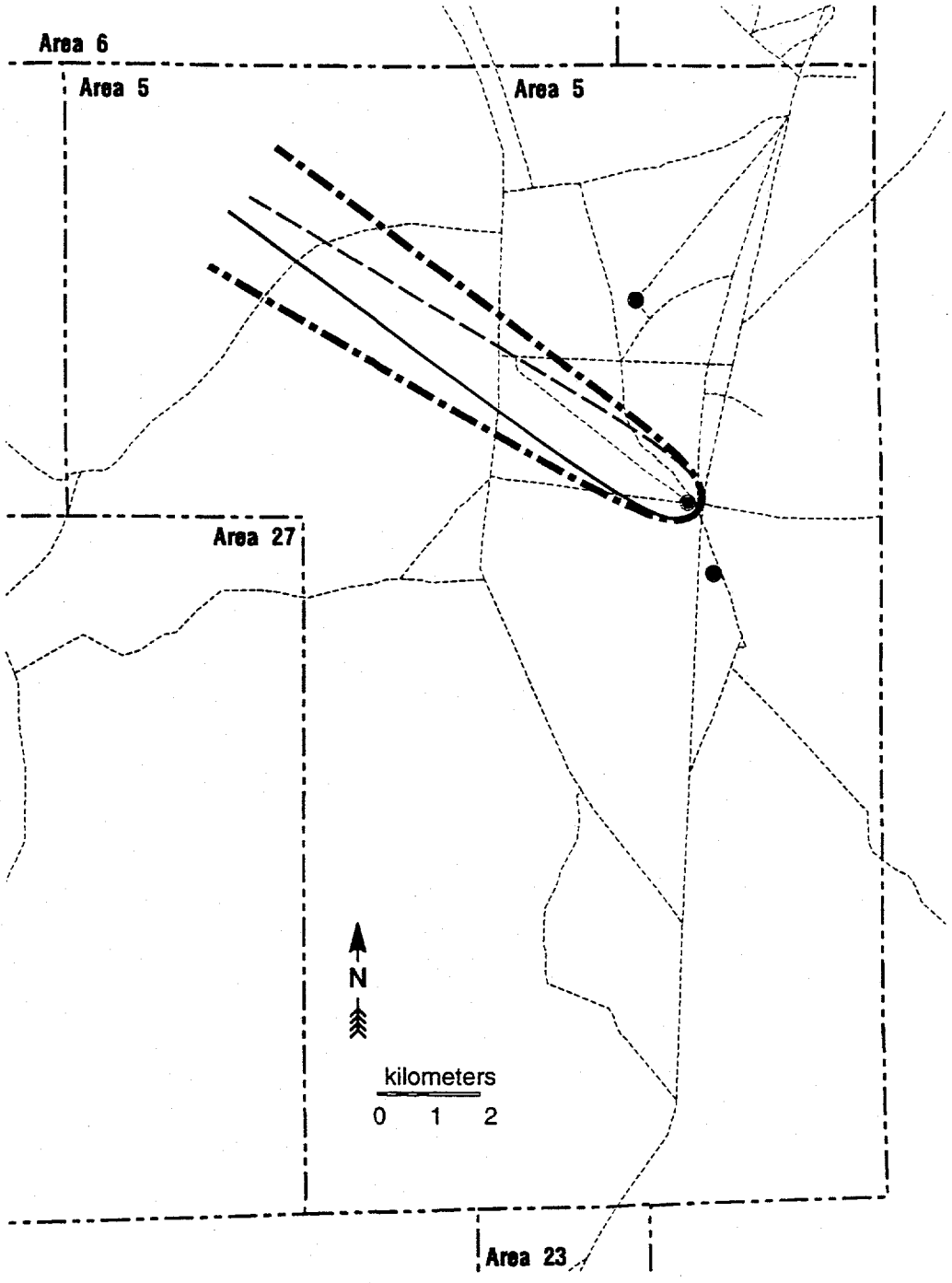

Figure 9b. Ultimate capture zones for the 95% reliability level for Well 5B. Heavy dashed line is outer envelope for the two curves. Filled circle indicates a well. Standard deviation on the angle is 1.5°.

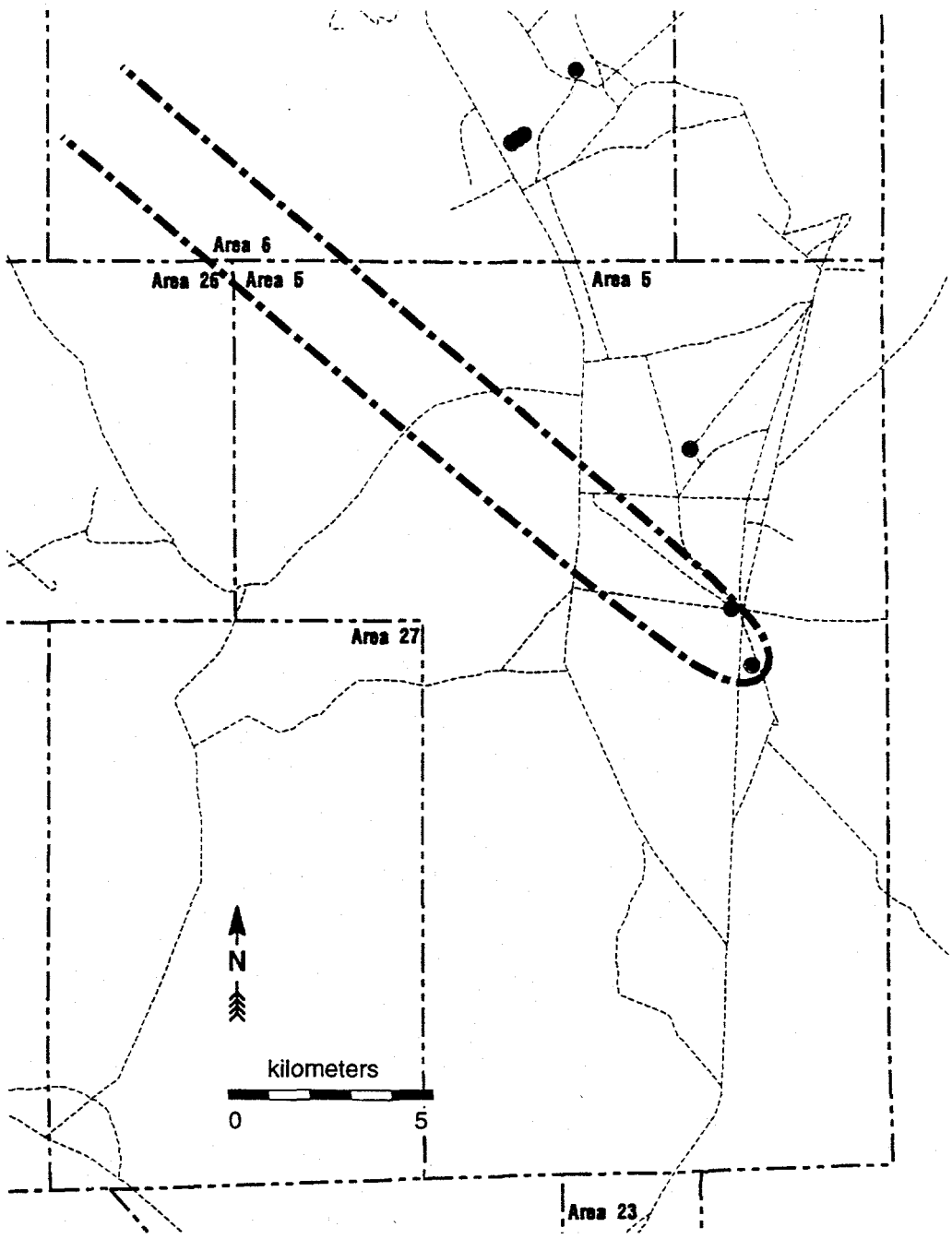

Figure 10a. Ultimate capture zone for the 50% reliability level for Well 5C. Filled circle indicates a well.

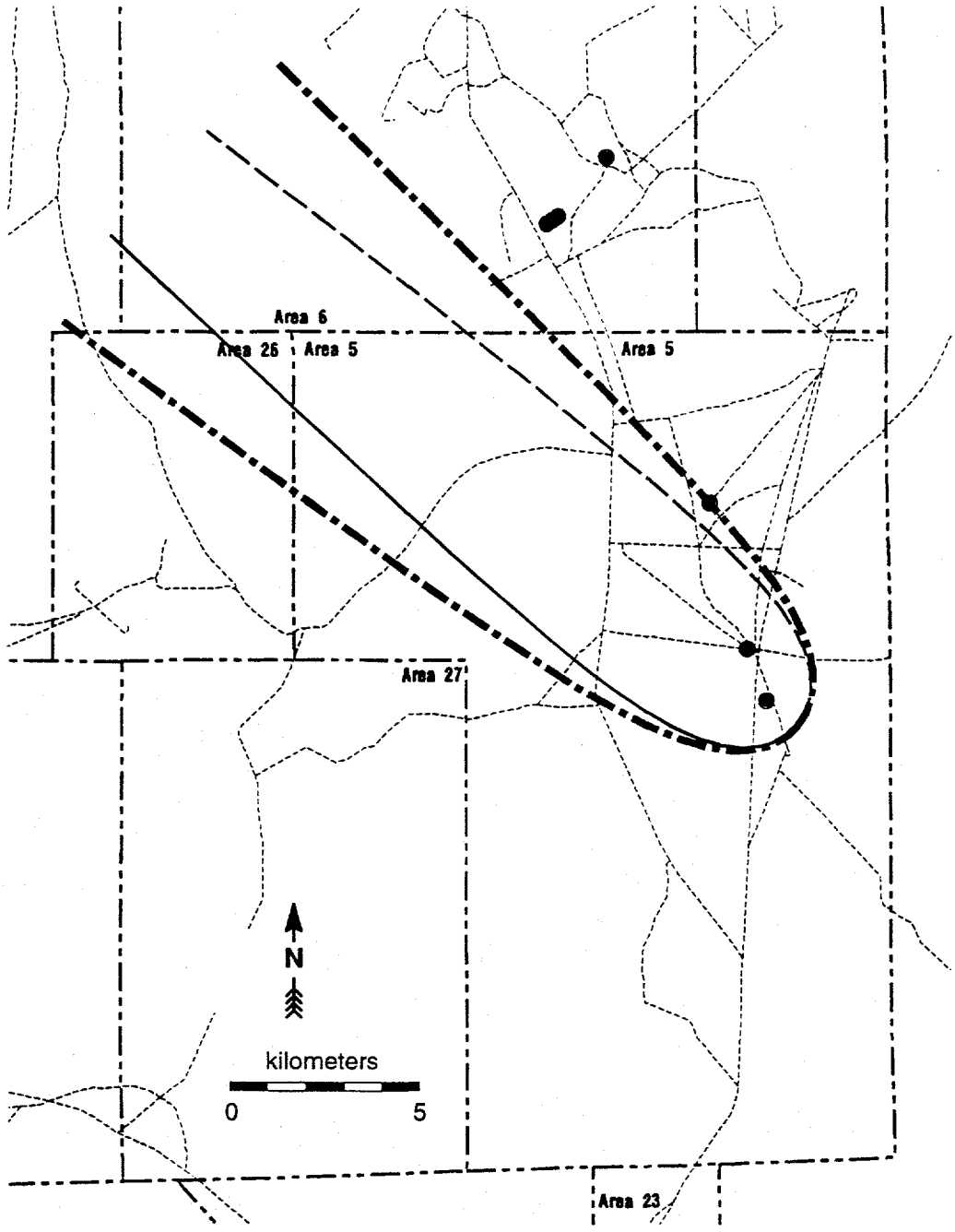

Figure 10b. Ultimate capture zones for the 95% reliability level for Well 5C. Heavy dashed line is outer envelope for the two curves. Filled circle indicates a well. Standard deviation on the angle is 1.8°.

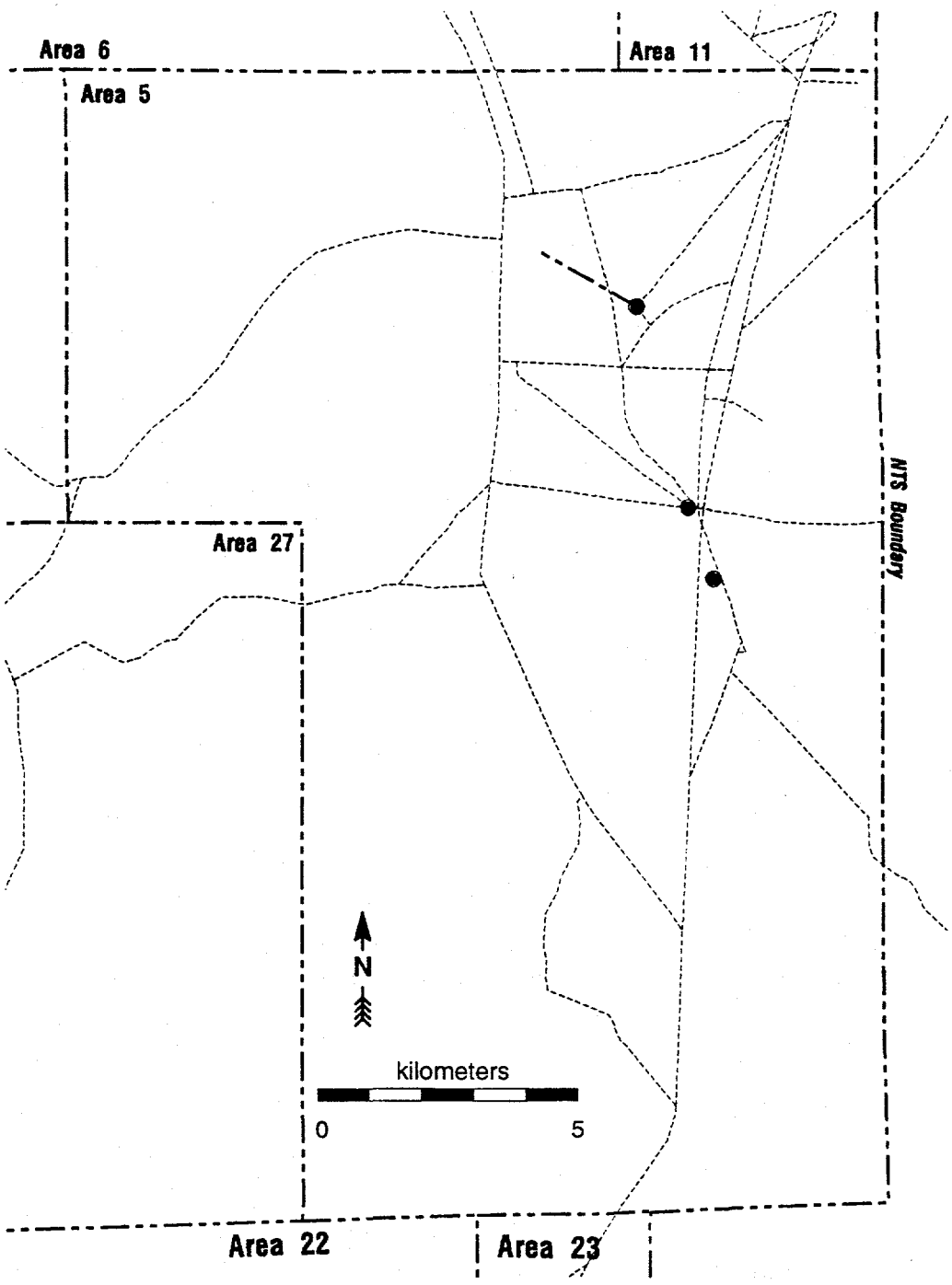

Figure 11a. Ultimate capture zone for the 50% reliability level for Well UE–5C. Filled circle indicates a well.

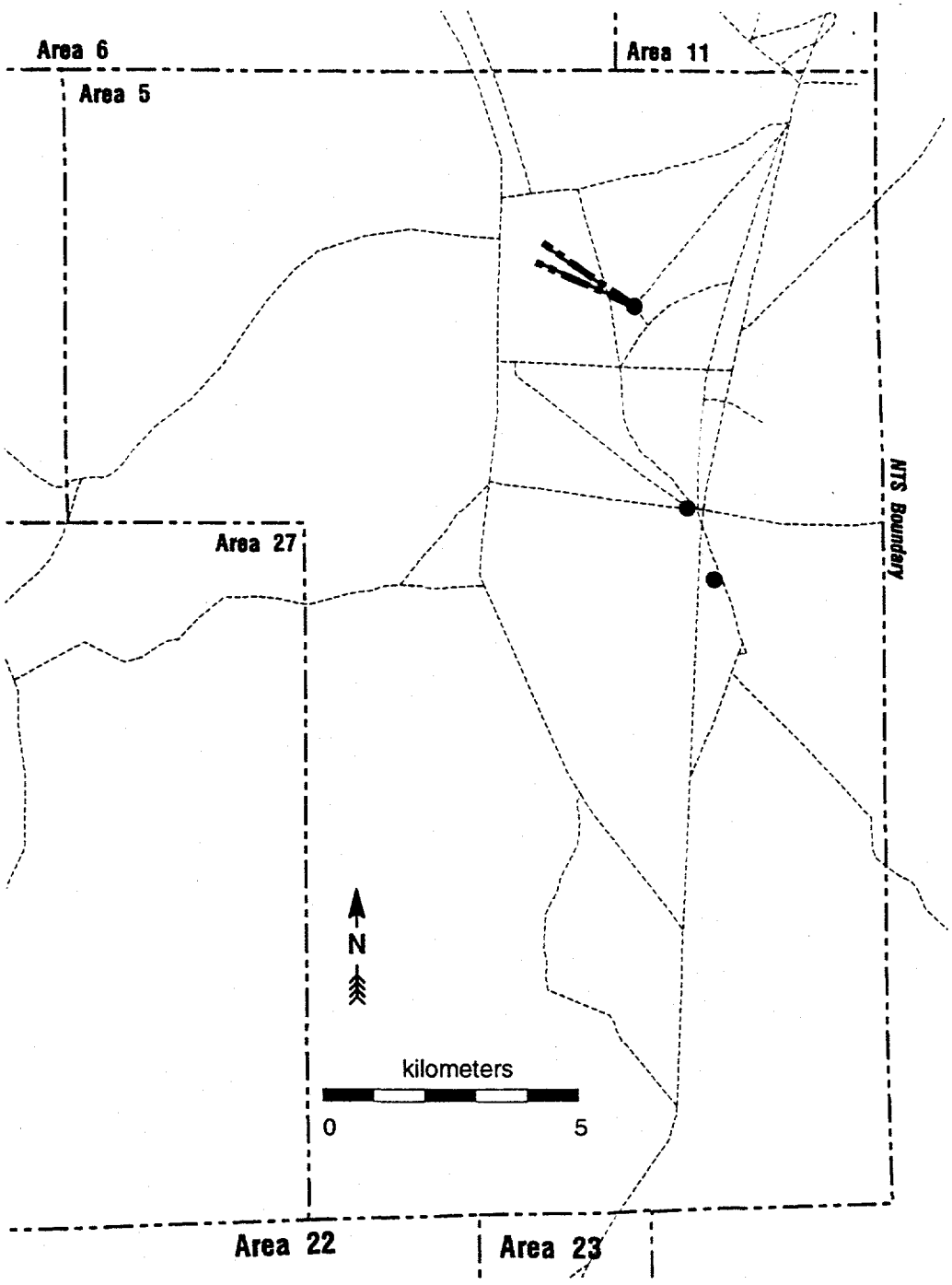

Figure 11b. Ultimate capture zones for the 95% reliability level for Well UE–5C. Heavy dashed line is outer envelope for the two curves. Filled circle indicates a well. Standard deviation on the angle is 2.5°.

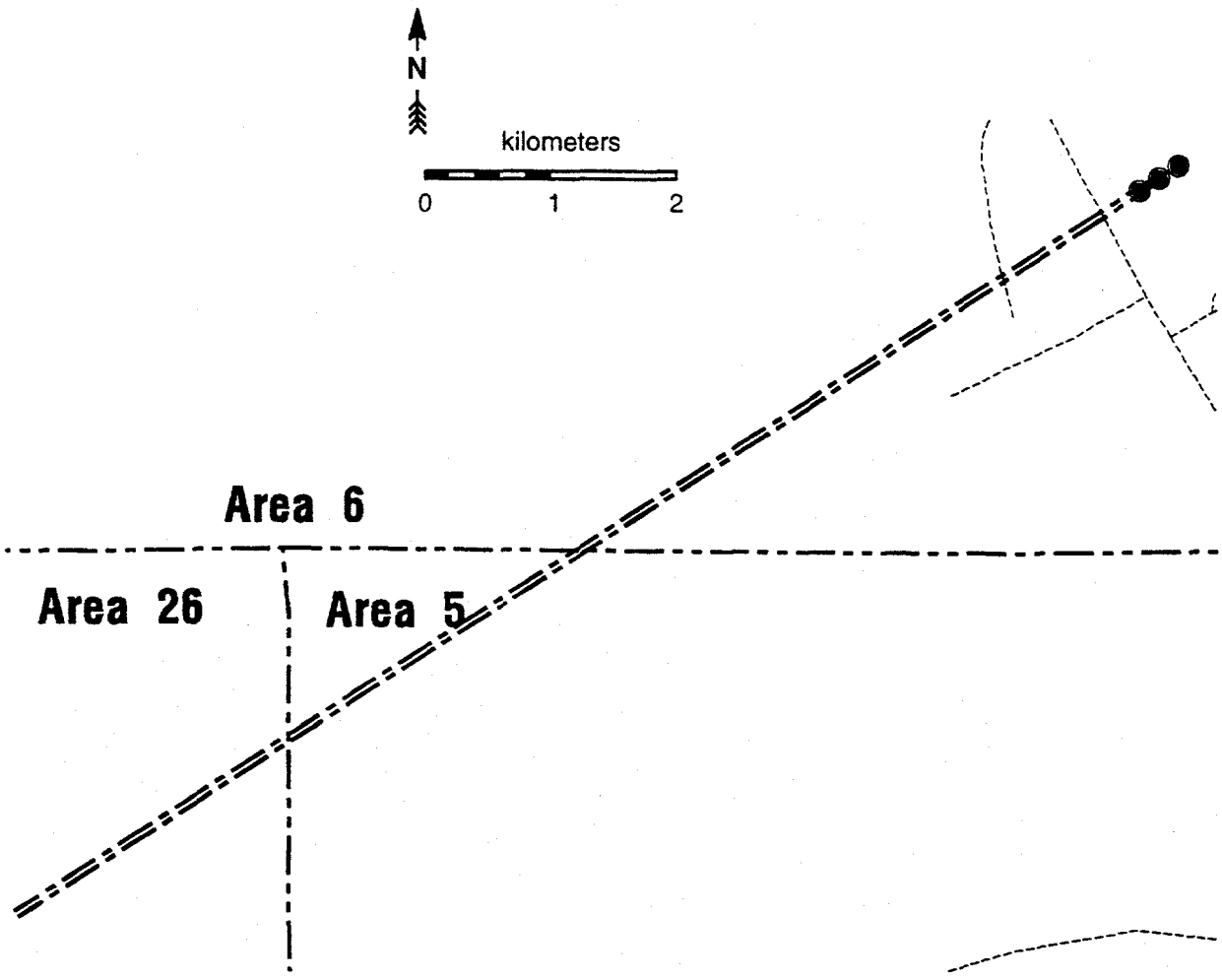

Figure 12a. Ultimate capture zone for the 50% reliability level for Wells 4 and 4A. Filled circle indicates a well.

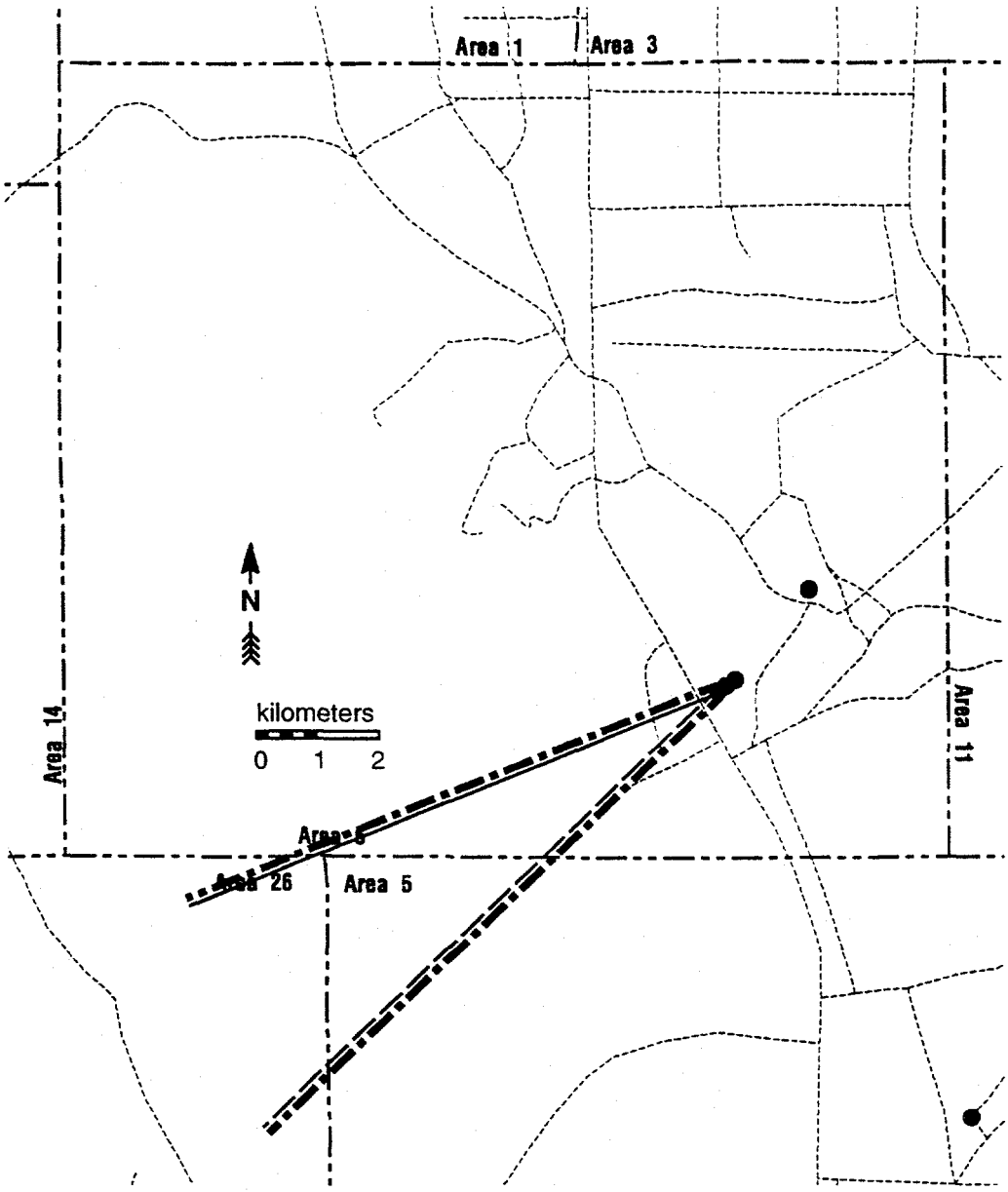

Figure 12b. Ultimate capture zones for the 95% reliability level for Wells 4 and 4A. Heavy dashed line is outer envelope for the two curves. Filled circle indicates a well. Standard deviation on the angle is 5.7°.

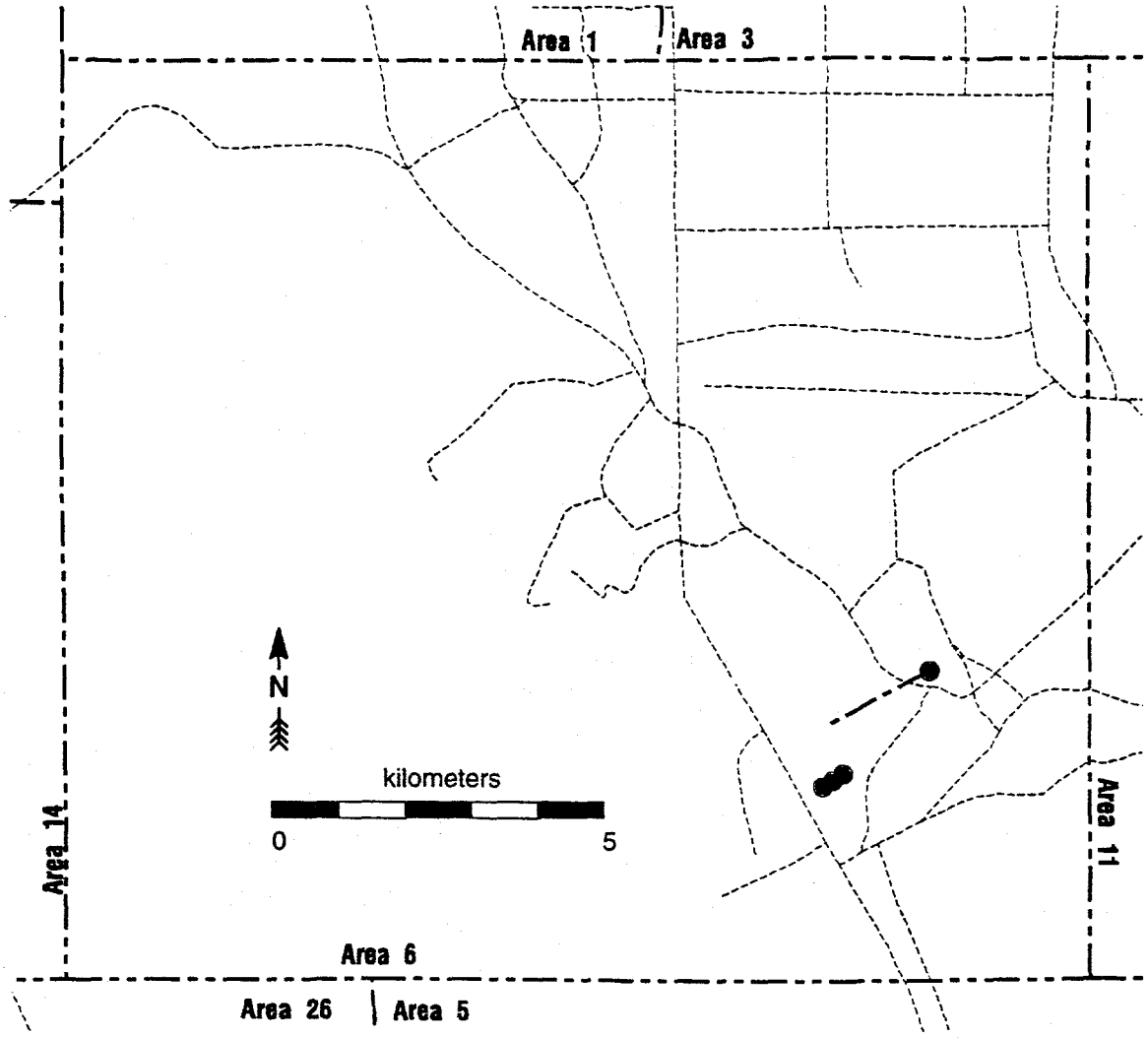

Figure 13a. Ultimate capture zone for the 50% reliability level for Wells C and C-1. Filled circle indicates a well.

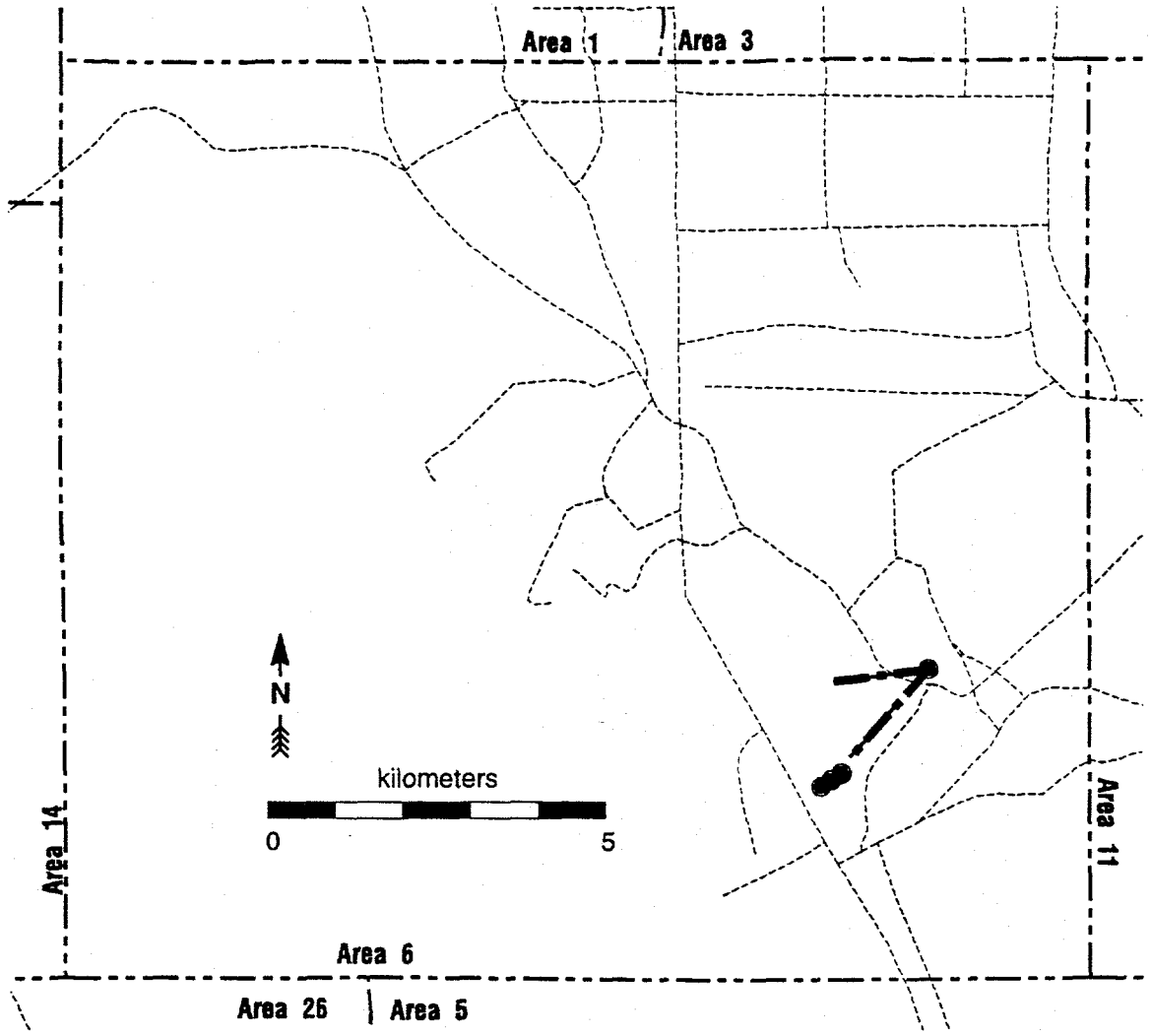

Figure 13b. Ultimate capture zones for the 95% reliability level for Wells C and C-1. Heavy dashed line is outer envelope for the two curves. Filled circle indicates a well. Standard deviation on the angle is 10.5°.

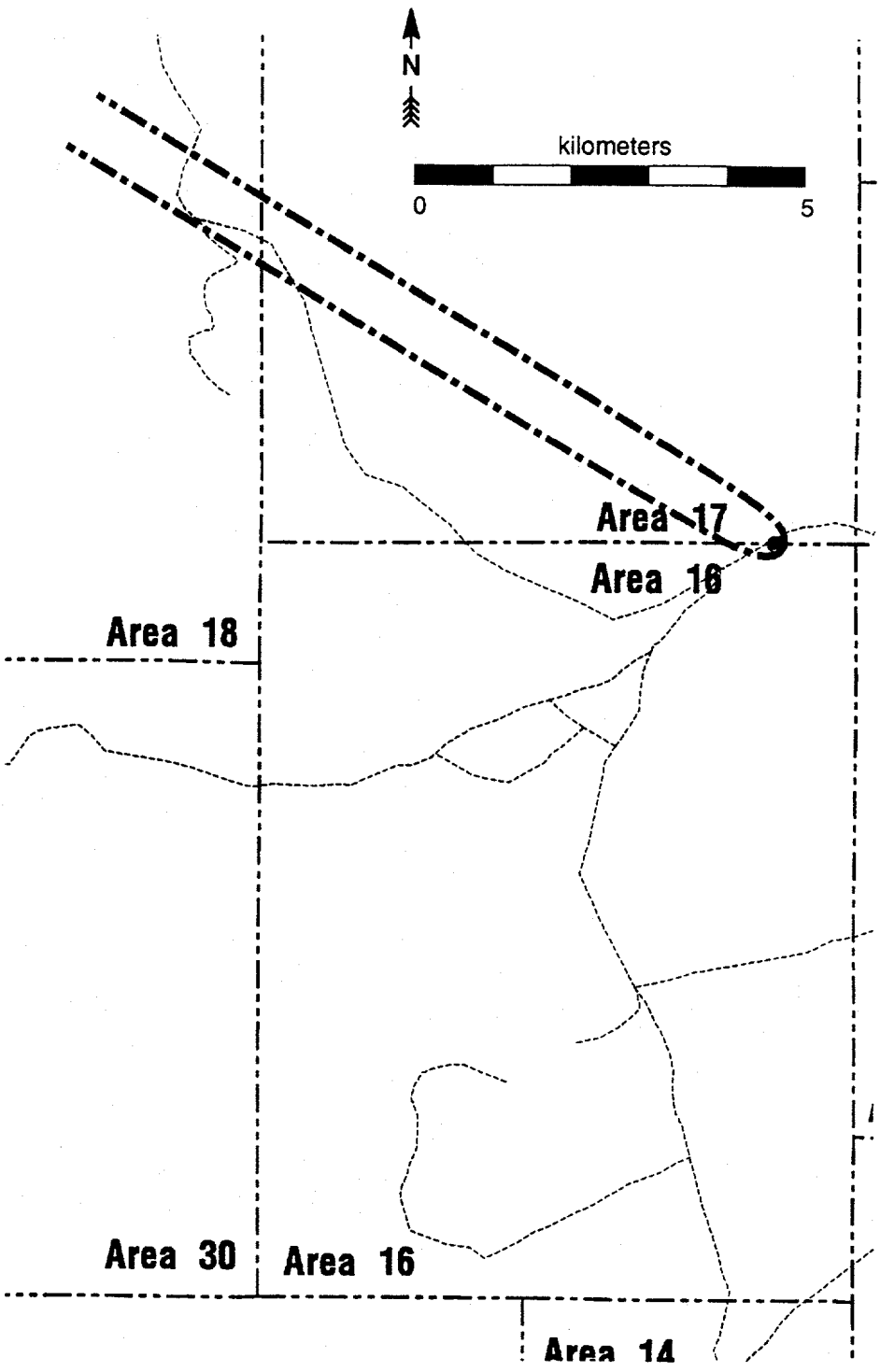

Figure 14a. Ultimate capture zone for the 50% reliability level for Well UE–16d. Filled circle indicates a well.

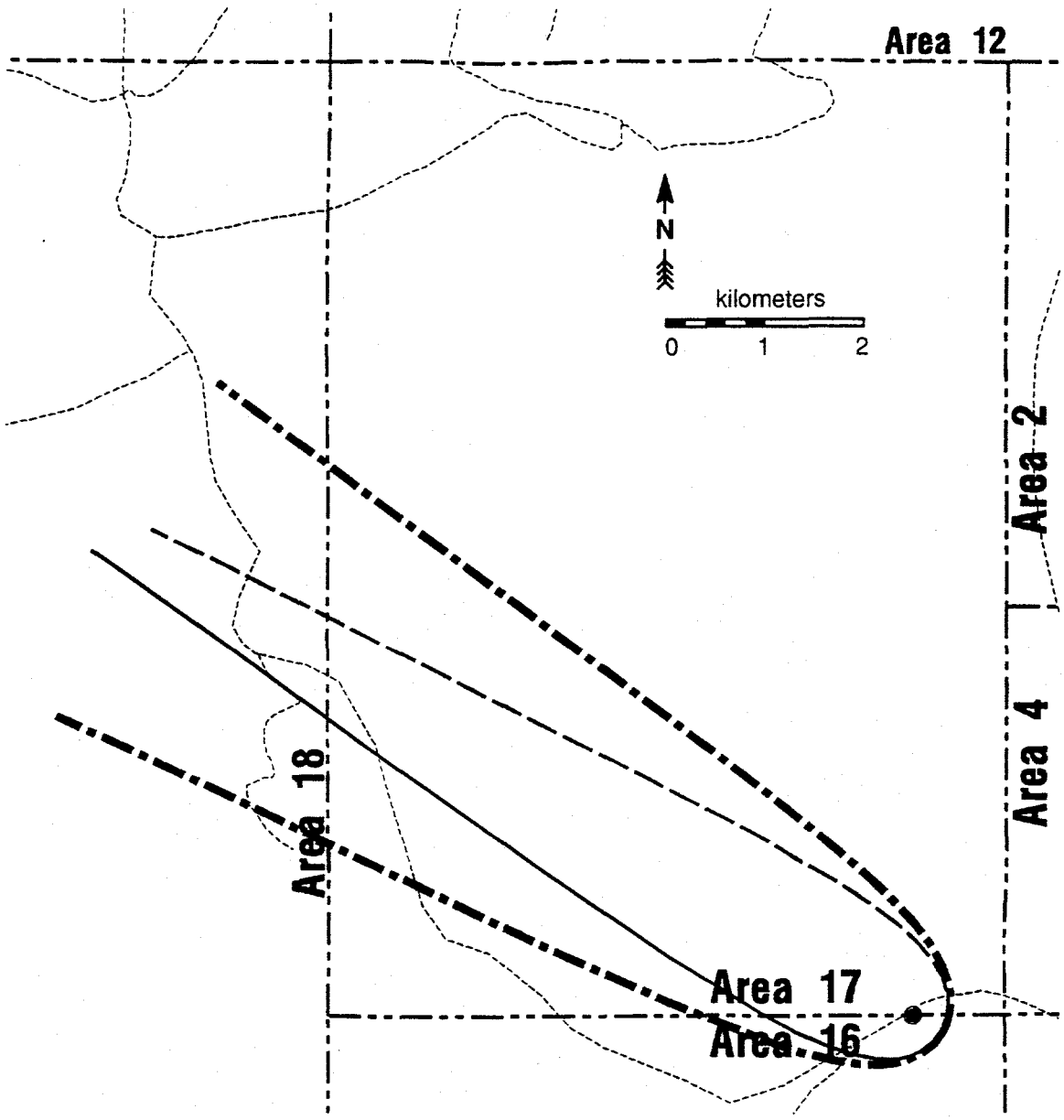

Figure 14b. Ultimate capture zones for the 95% reliability level for Well UE–16d. Heavy dashed line is outer envelope for the two curves. Filled circle indicates a well. Standard deviation on the angle is 2.7°.

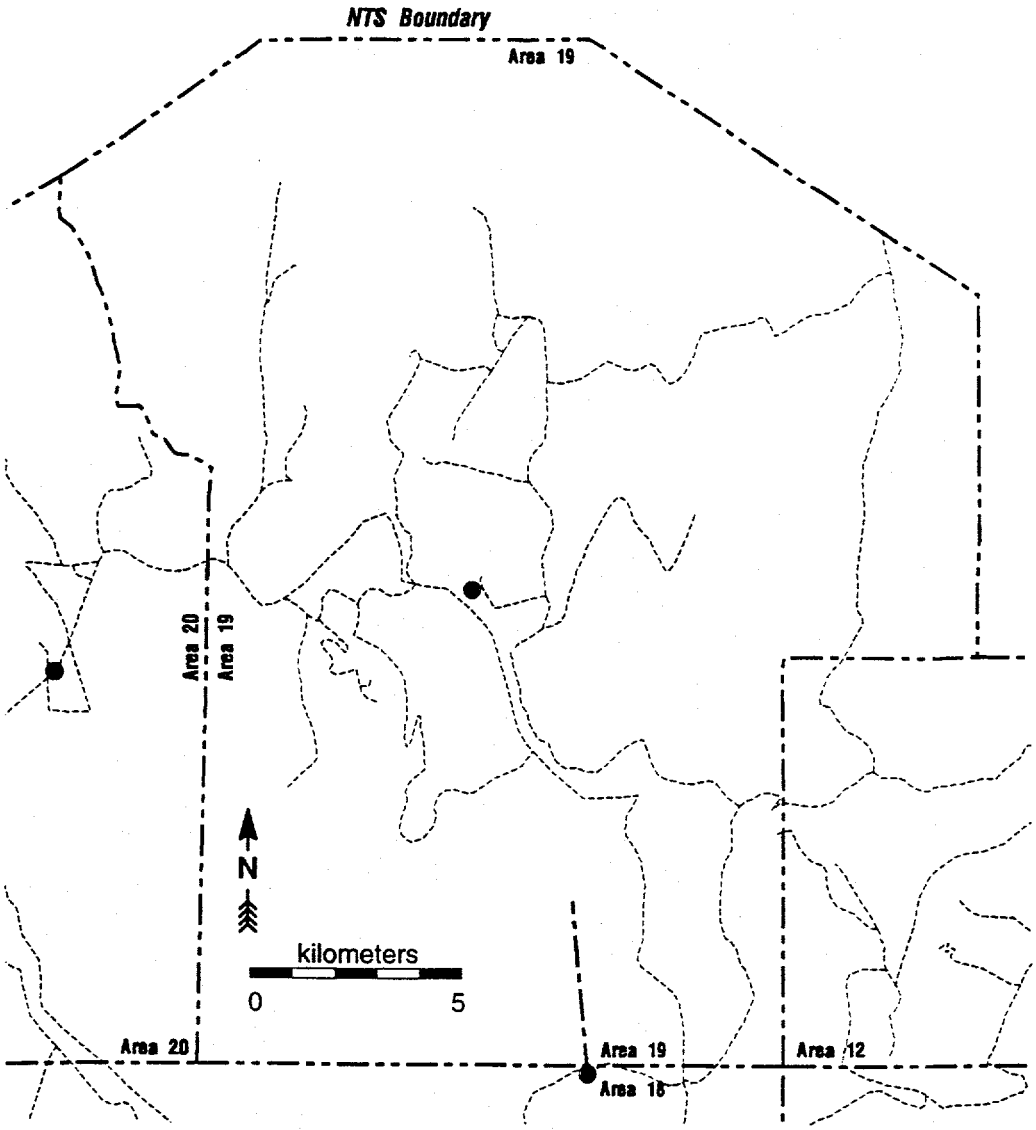

Figure 15a. Ultimate capture zone for the 50% reliability level for Well 8. Filled circle indicates a well.

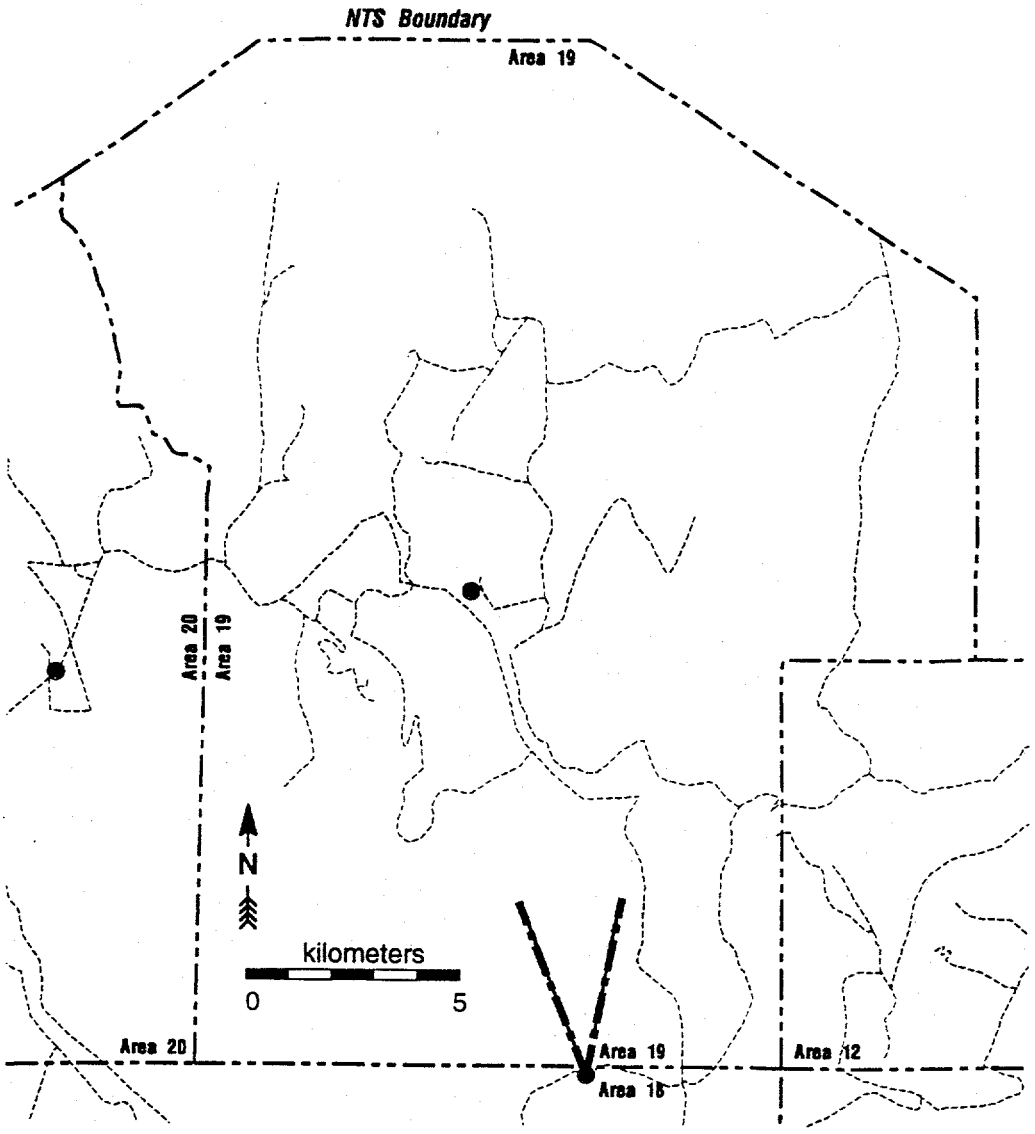

Figure 15b. Ultimate capture zones for the 95% reliability level for Well 8. Heavy dashed line is outer envelope for the two curves. Filled circle indicates a well. Standard deviation on the angle is 8.3°.

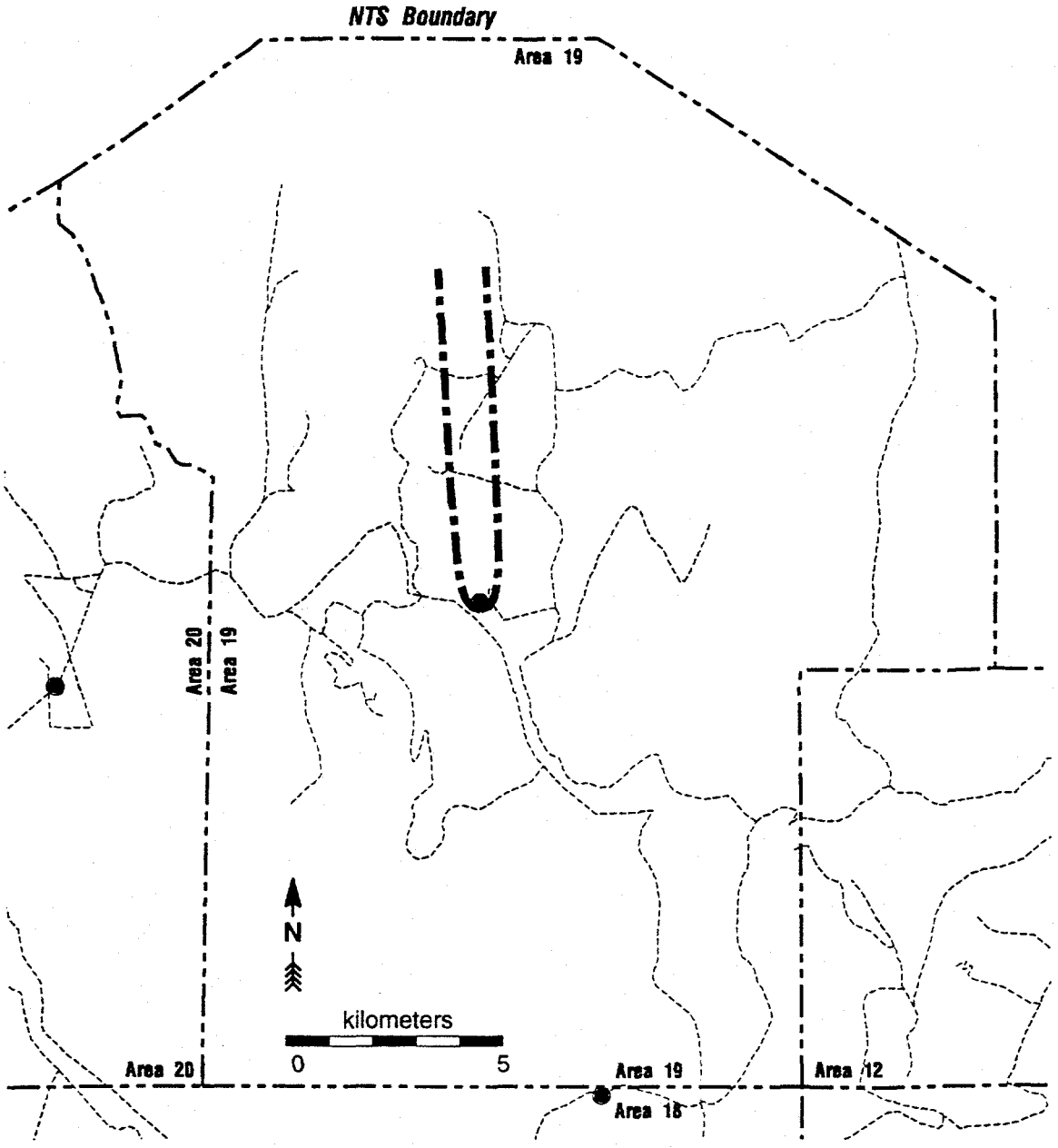

Figure 16a. Ultimate capture zone for the 50% reliability level for Well UE–19c. Filled circle indicates a well.

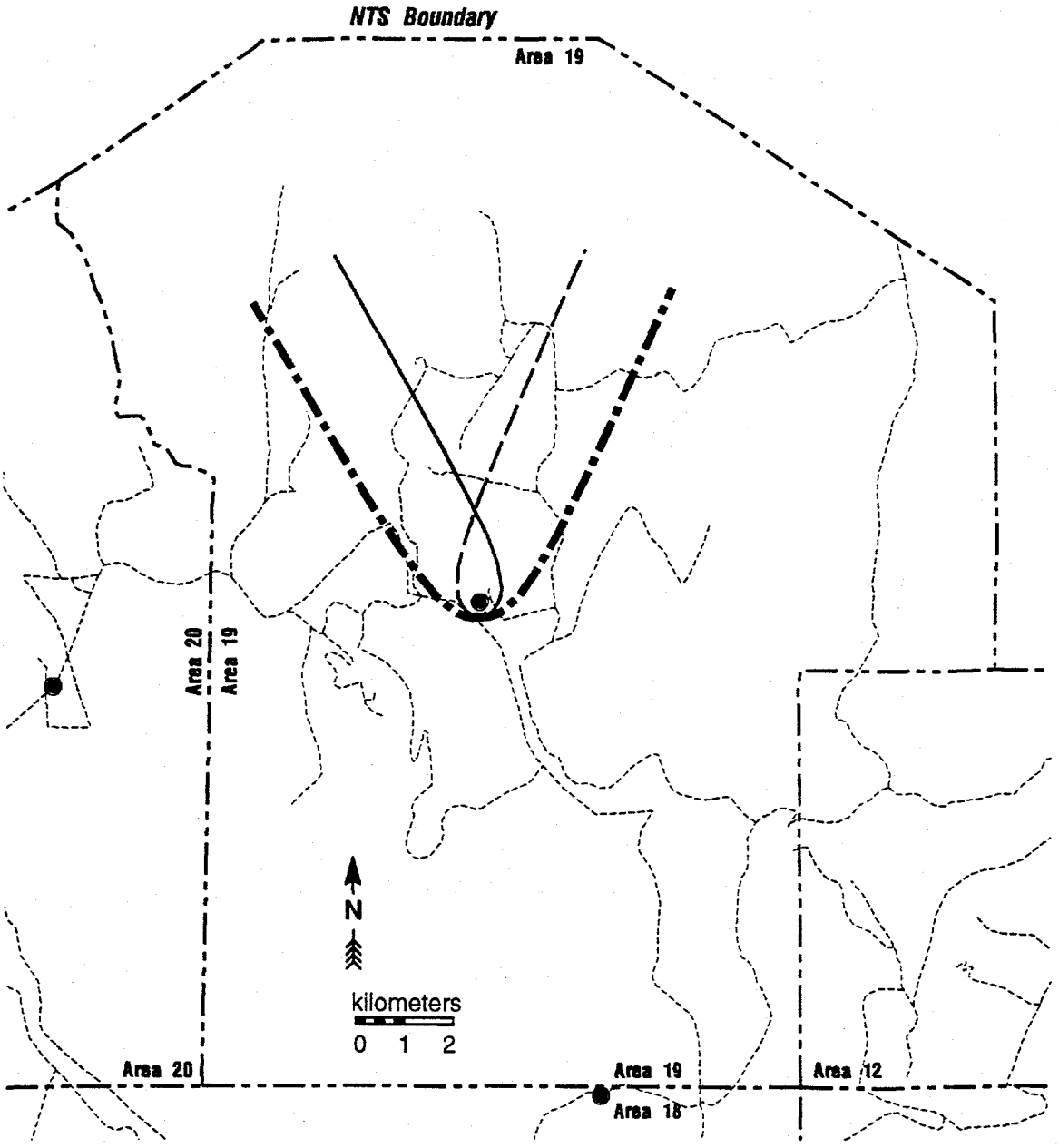

Figure 16b. Ultimate capture zones for the 95% reliability level for Well UE–19c. Heavy dashed line is outer envelope for the two curves. Filled circle indicates a well. Standard deviation on the angle is 14°.

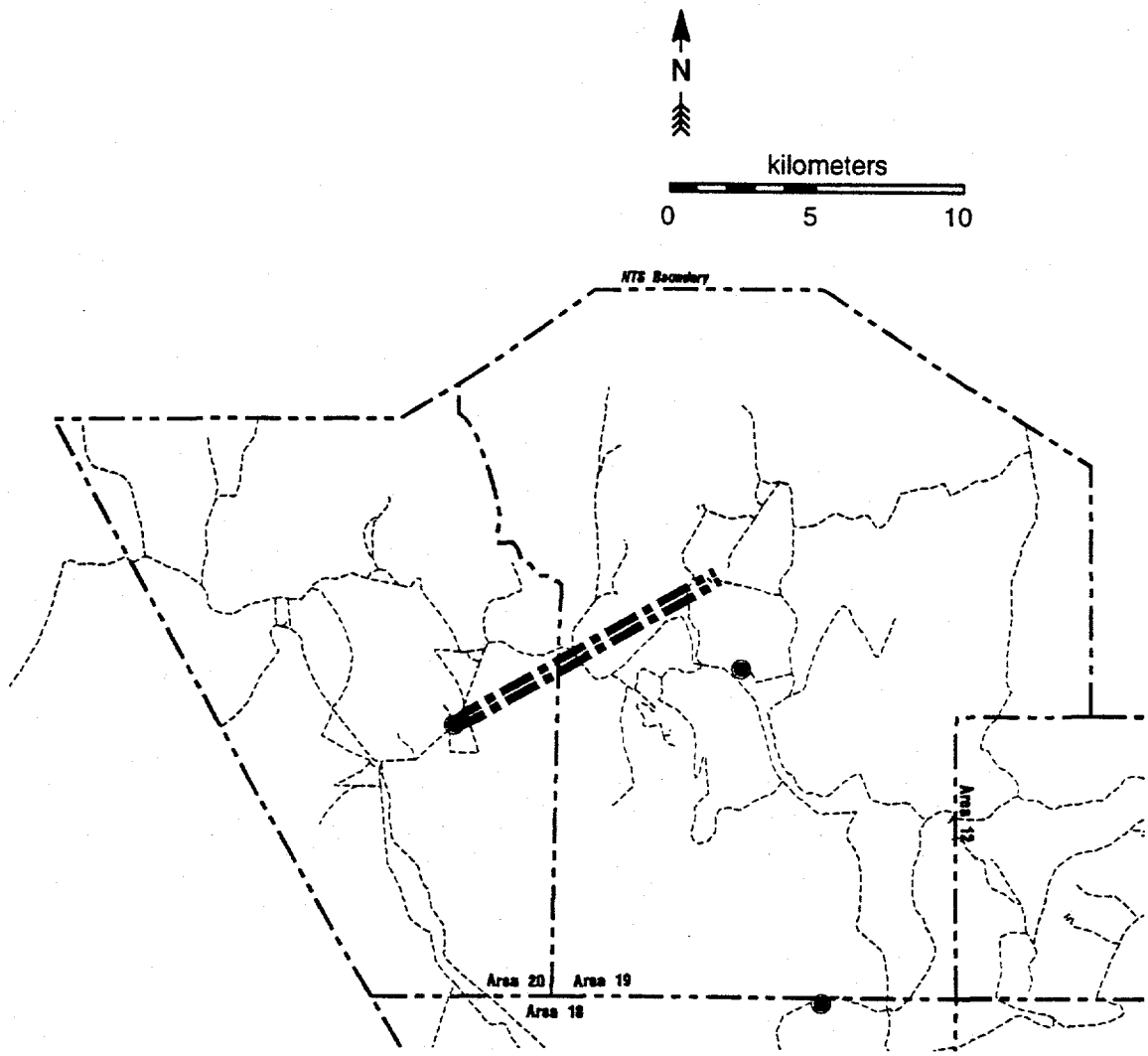

Figure 17a. Ultimate capture zone for the 50% reliability level for Well U–20. Filled circle indicates a well.

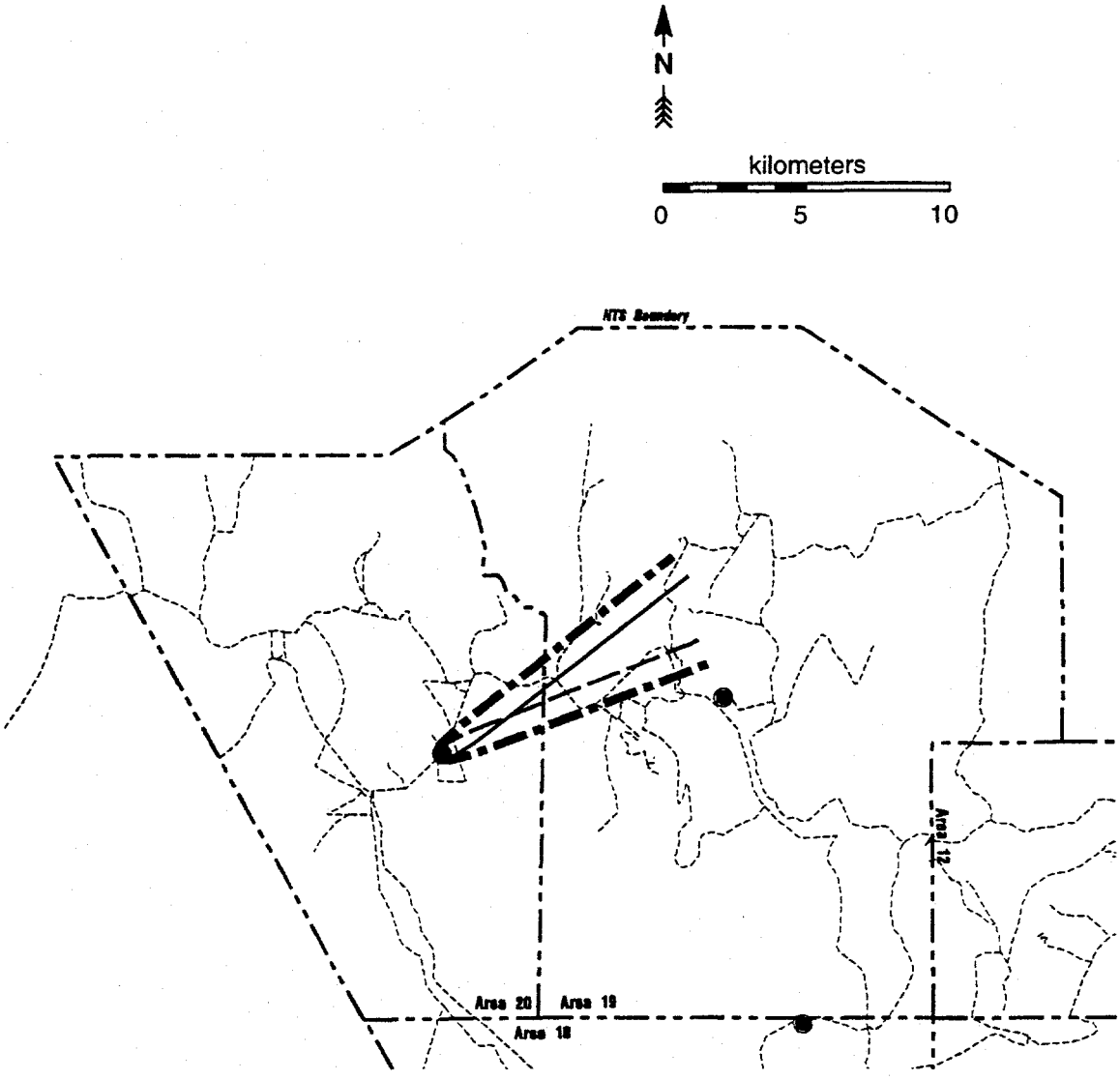

Figure 17b. Ultimate capture zones for the 95% reliability level for Well U–20. Heavy dashed line is outer envelope for the two curves. Filled circle indicates a well. Standard deviation on the angle is 4.3°.

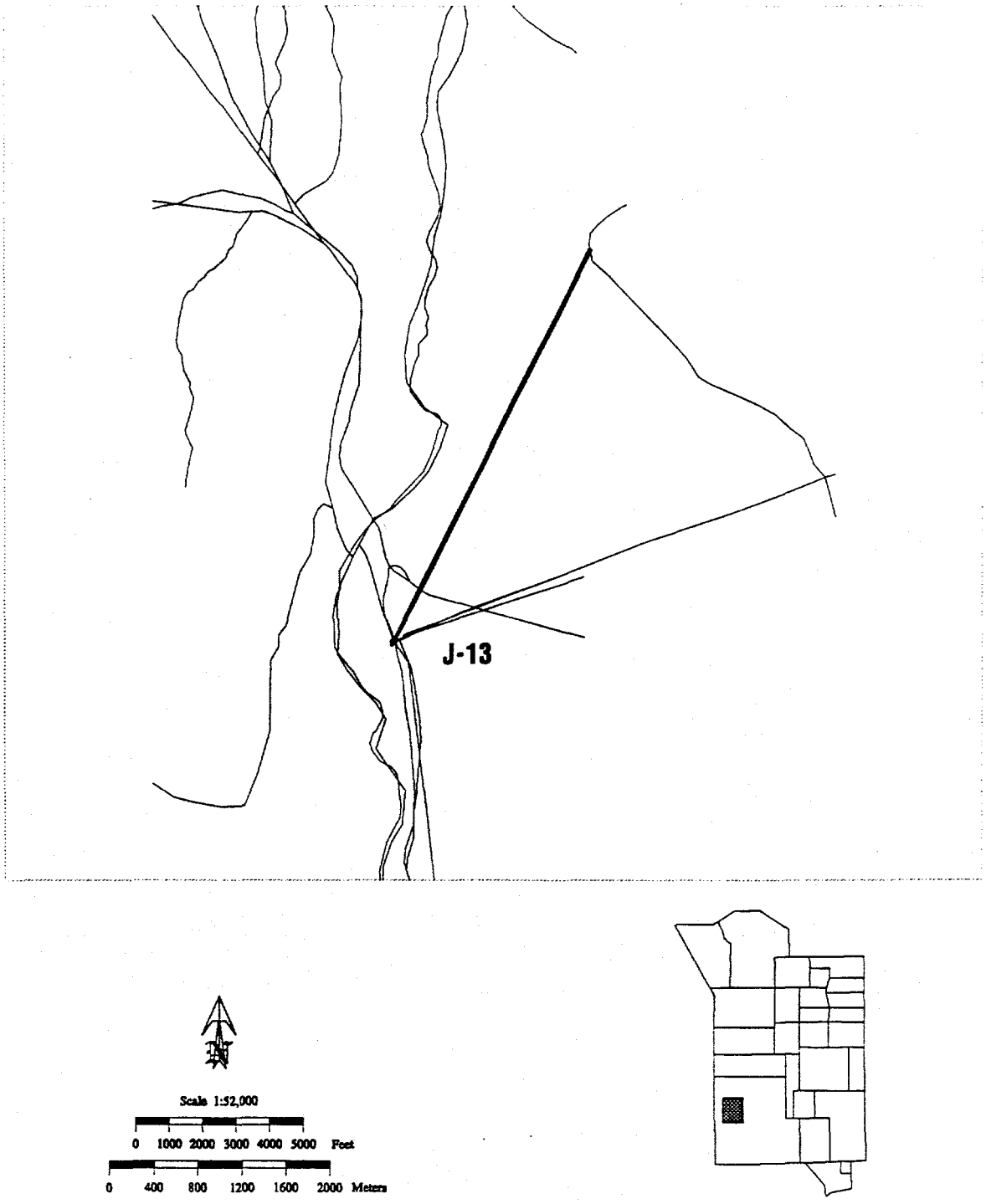

Figure 18a. Five–, 10– and 15–year time dependent capture zones for the 50% reliability level for Well J–13. Filled circle indicates a well.

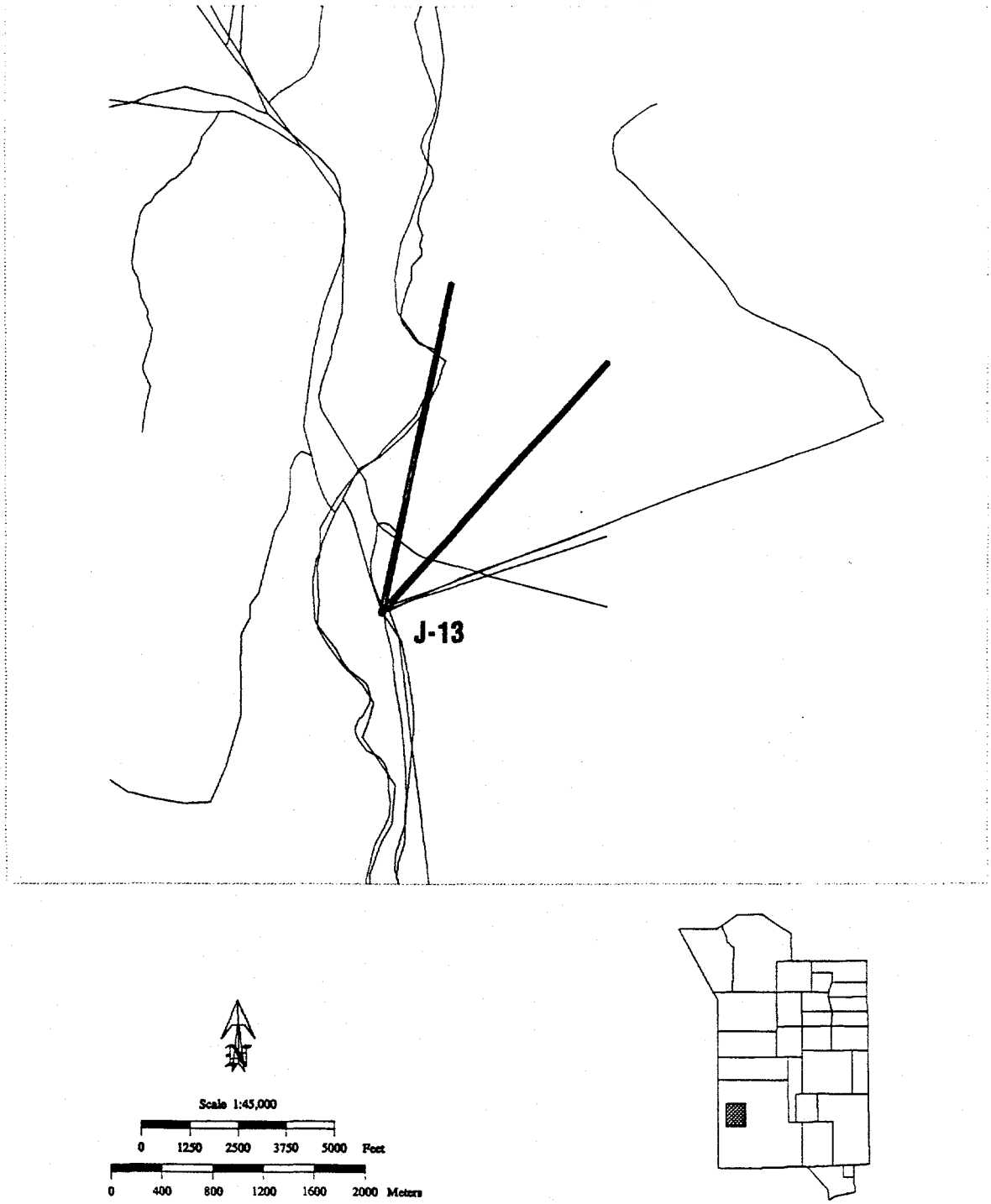

Figure 18b. Five–, 10– and 15–year time dependent capture zones for the 67% reliability level for Well J–13. Filled circle indicates a well.

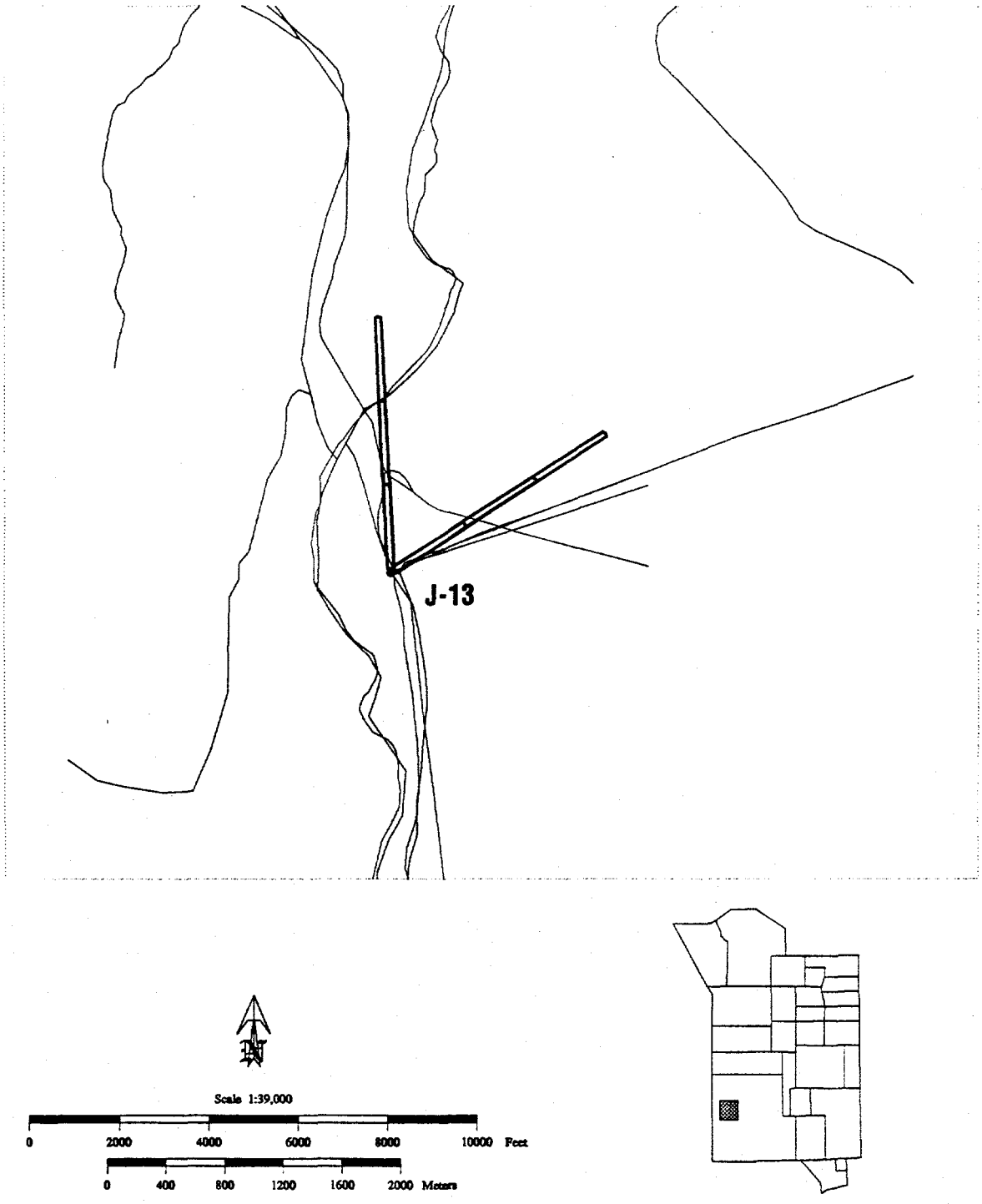

Figure 18c. Five–, 10– and 15–year time dependent capture zones for the 95% reliability level for Well J–13. Filled circle indicates a well.

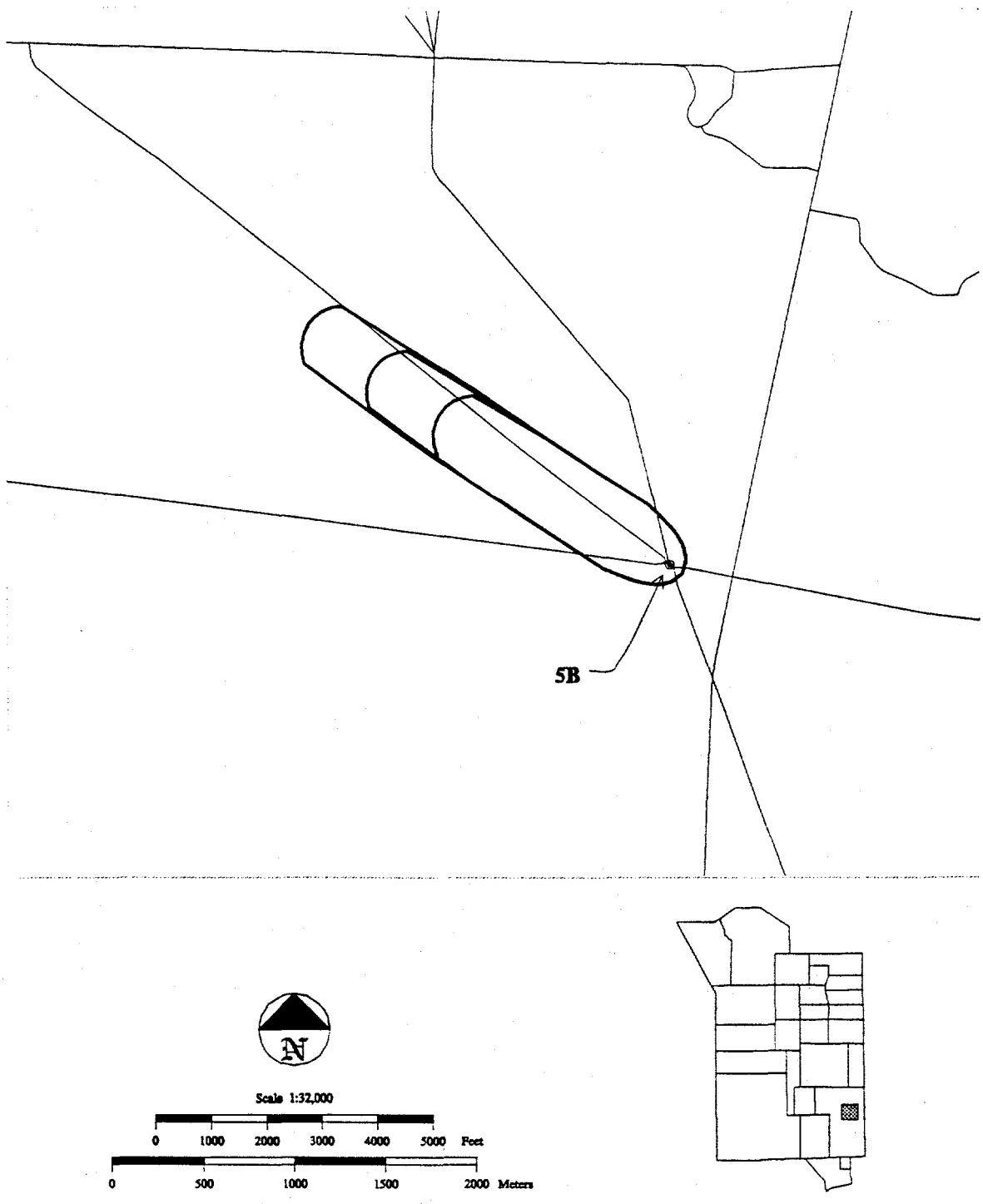

Figure 19a. Thirty–, 40– and 50–year time dependent capture zones for the 50% reliability level for Well 5B. Filled circle indicates a well.

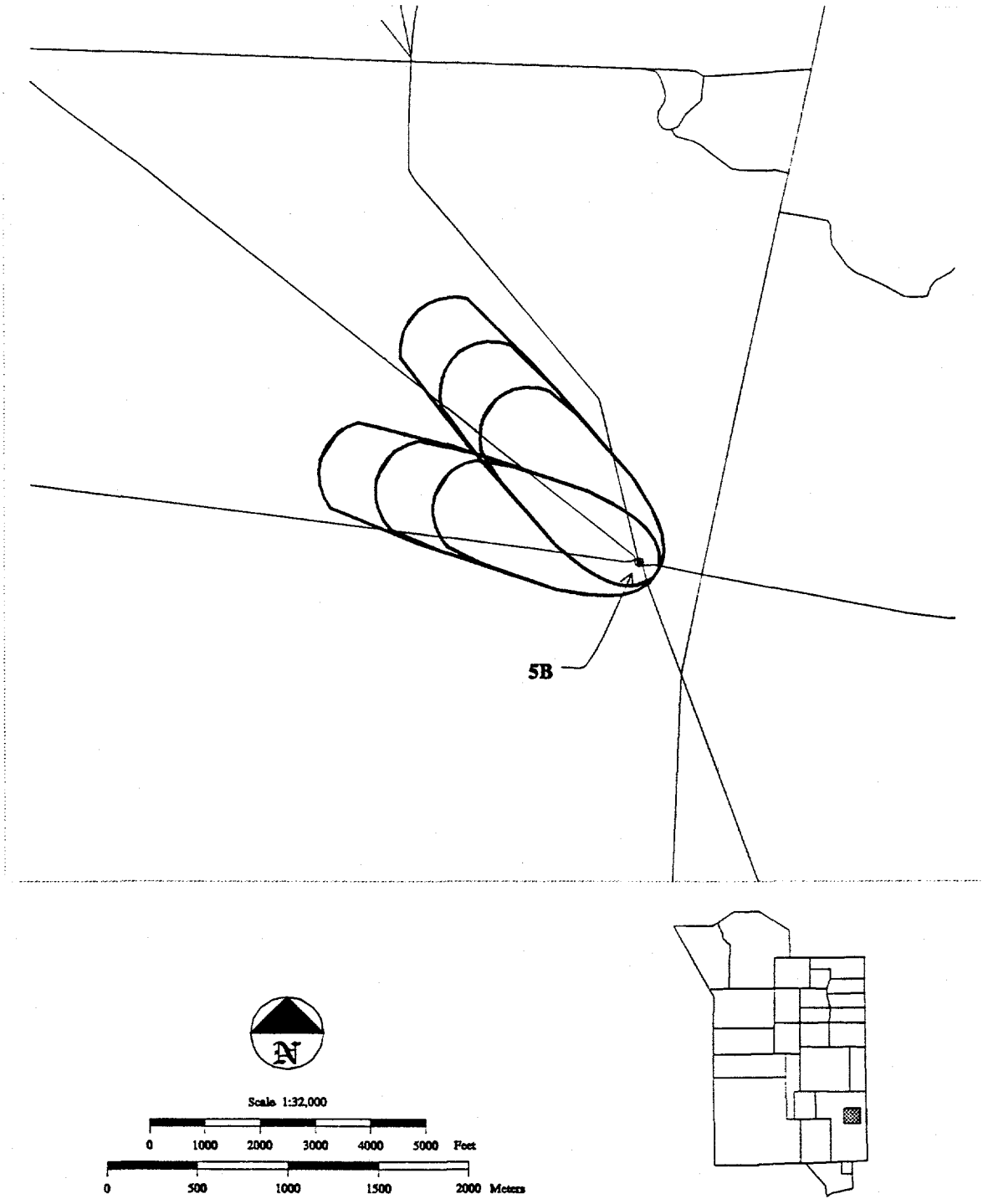

Figure 19b. Thirty–, 40– and 50–year time dependent capture zones for the 67% reliability level for Well 5B. Filled circle indicates a well.

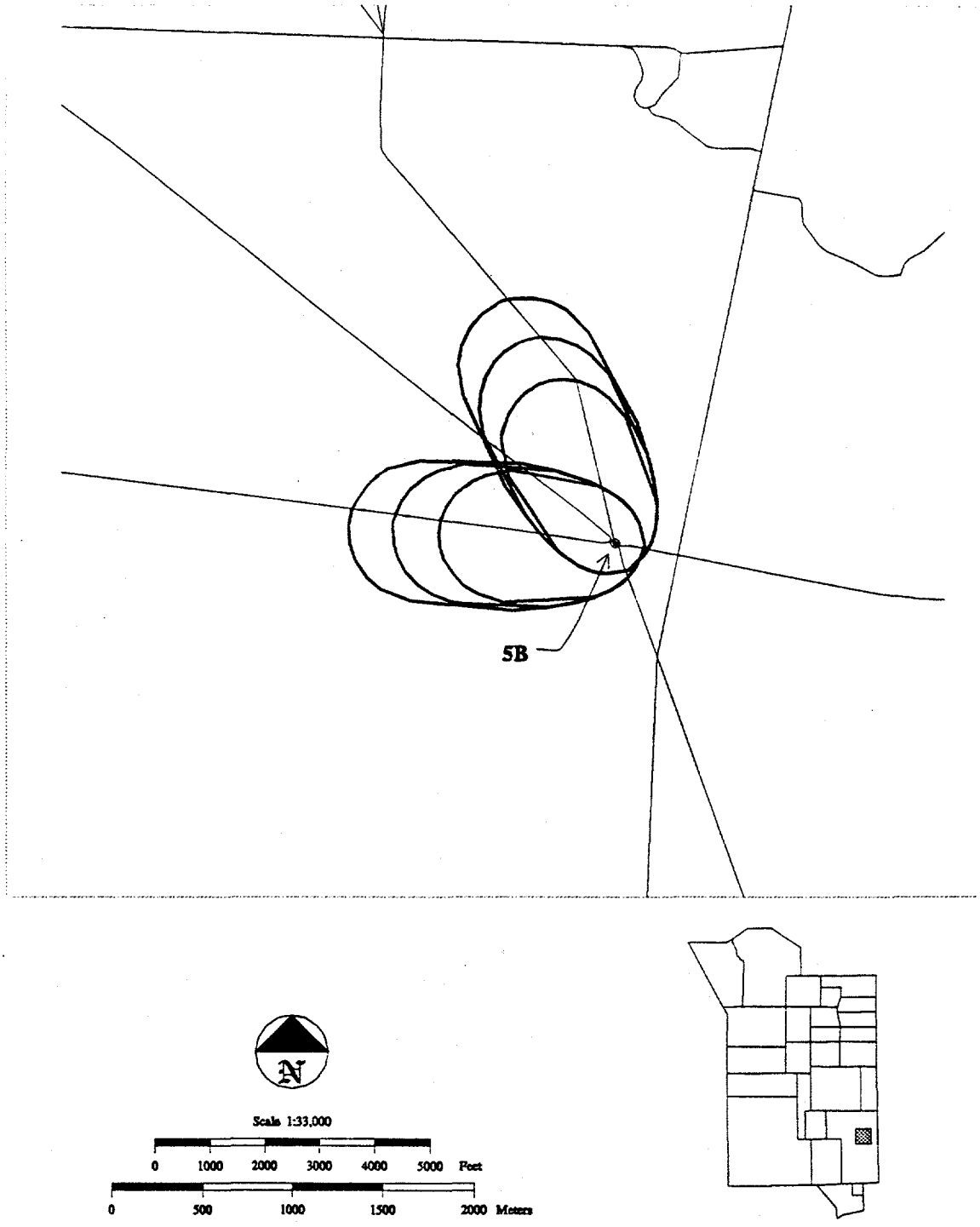

Figure 19c. Thirty–, 40– and 50–year time dependent capture zones for the 95% reliability level for Well 5B. Filled circle indicates a well.

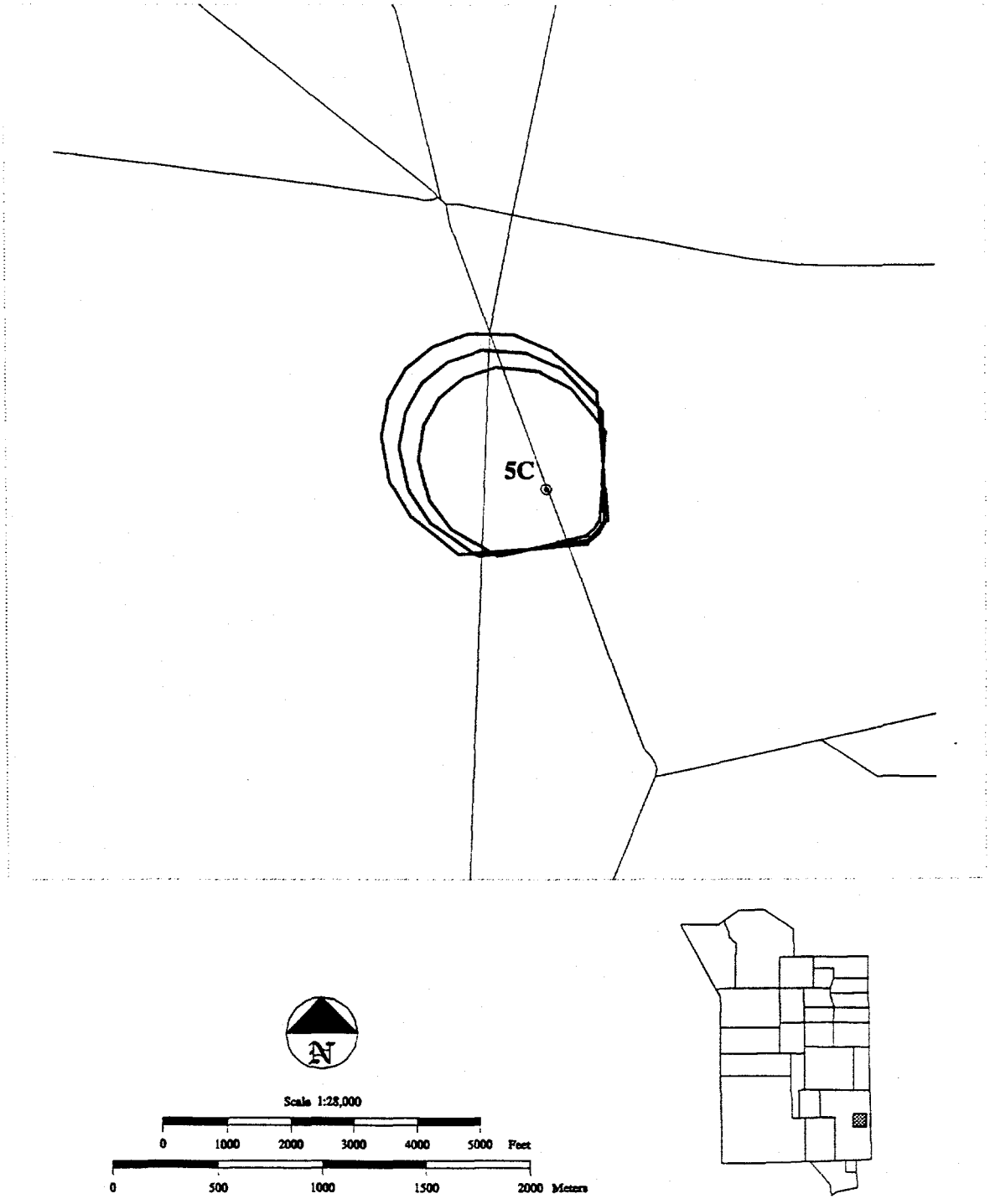

Figure 20a. Forty–, 50– and 60–year time dependent capture zones for the 50% reliability level for Well 5C. Filled circle indicates a well.

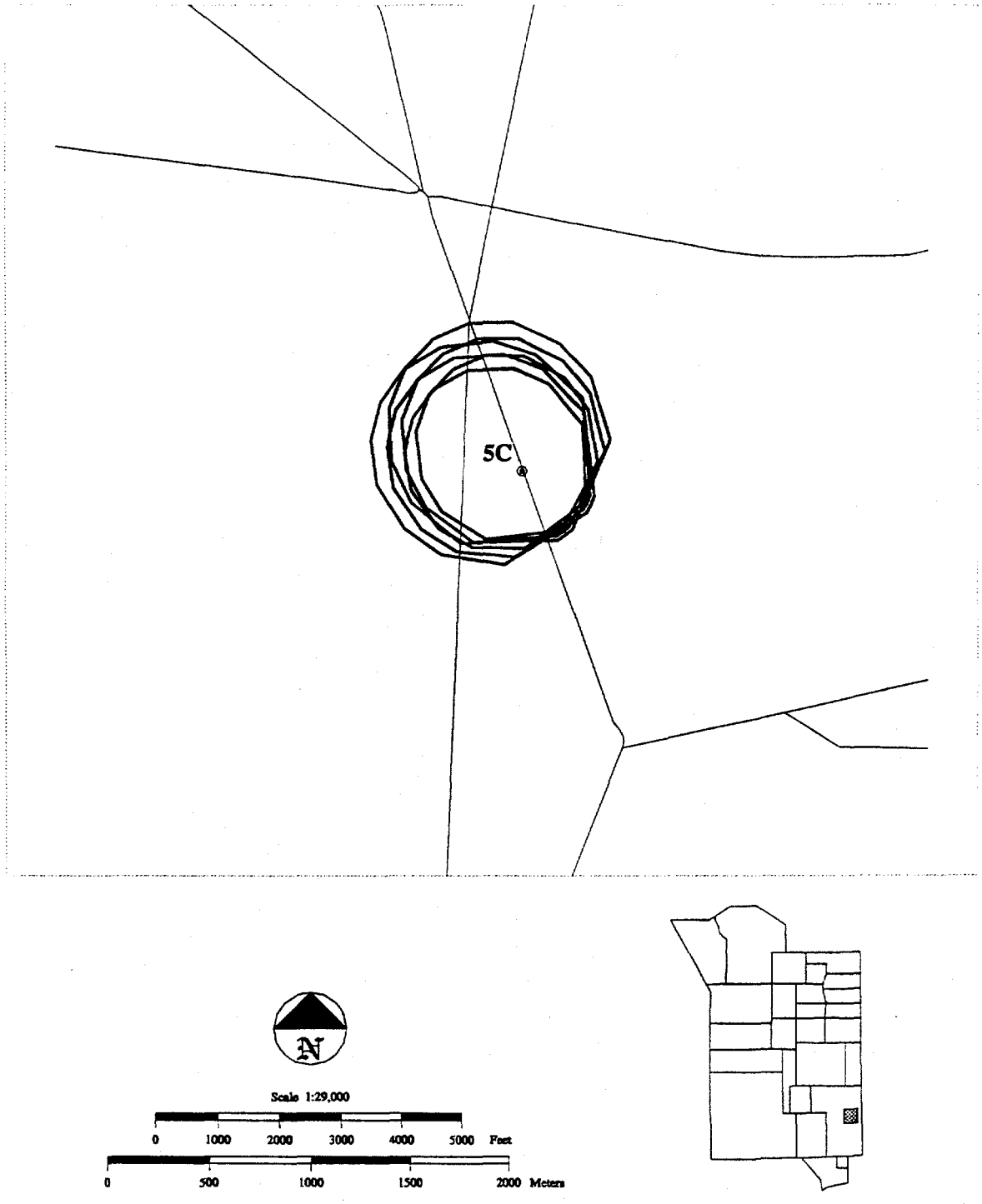

Figure 20b. Forty–, 50– and 60–year time dependent capture zones for the 67% reliability level for Well 5C. Filled circle indicates a well.

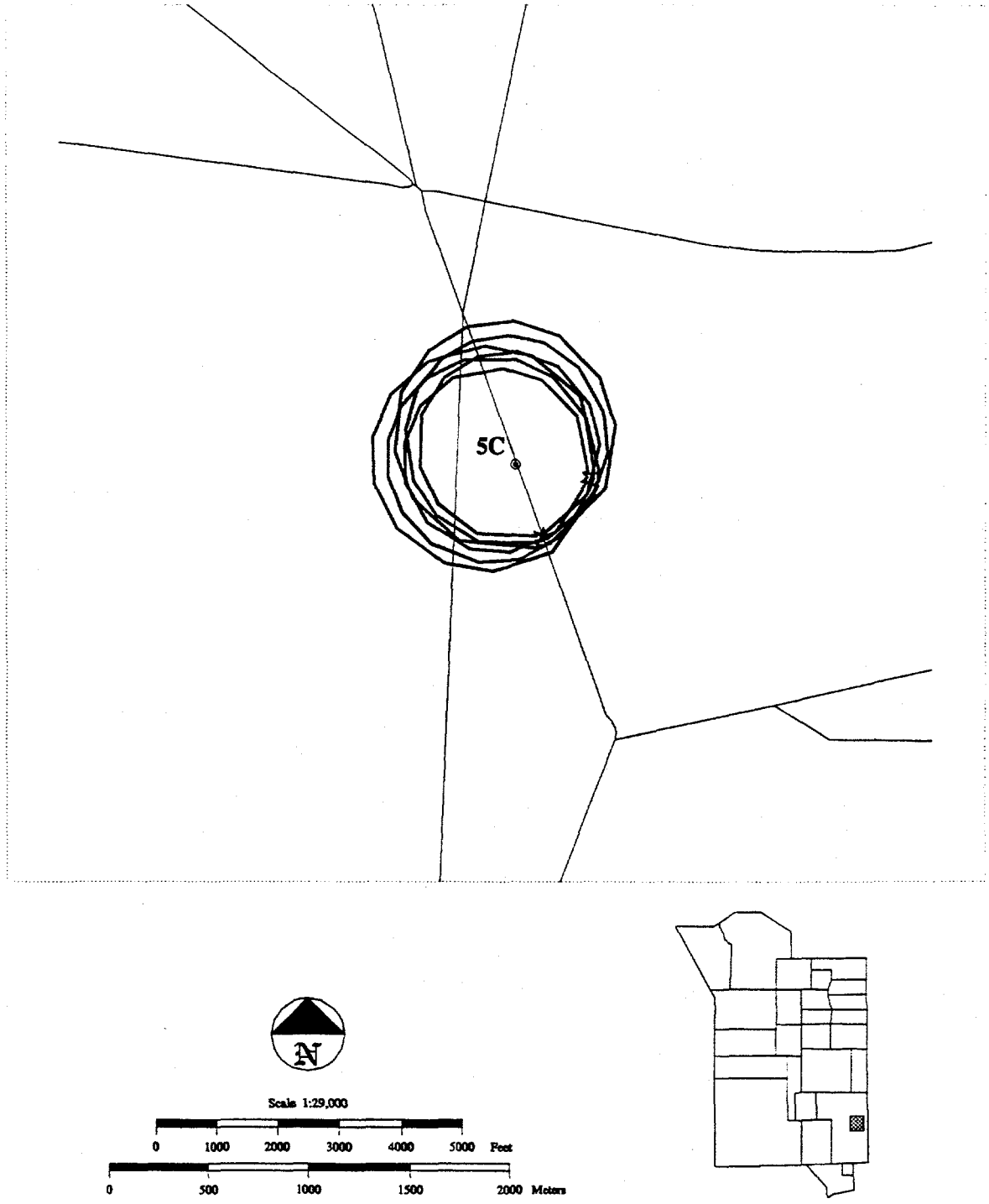

Figure 20c. Forty–, 50– and 60–year time dependent capture zones for the 95% reliability level for Well 5C. Filled circle indicates a well.

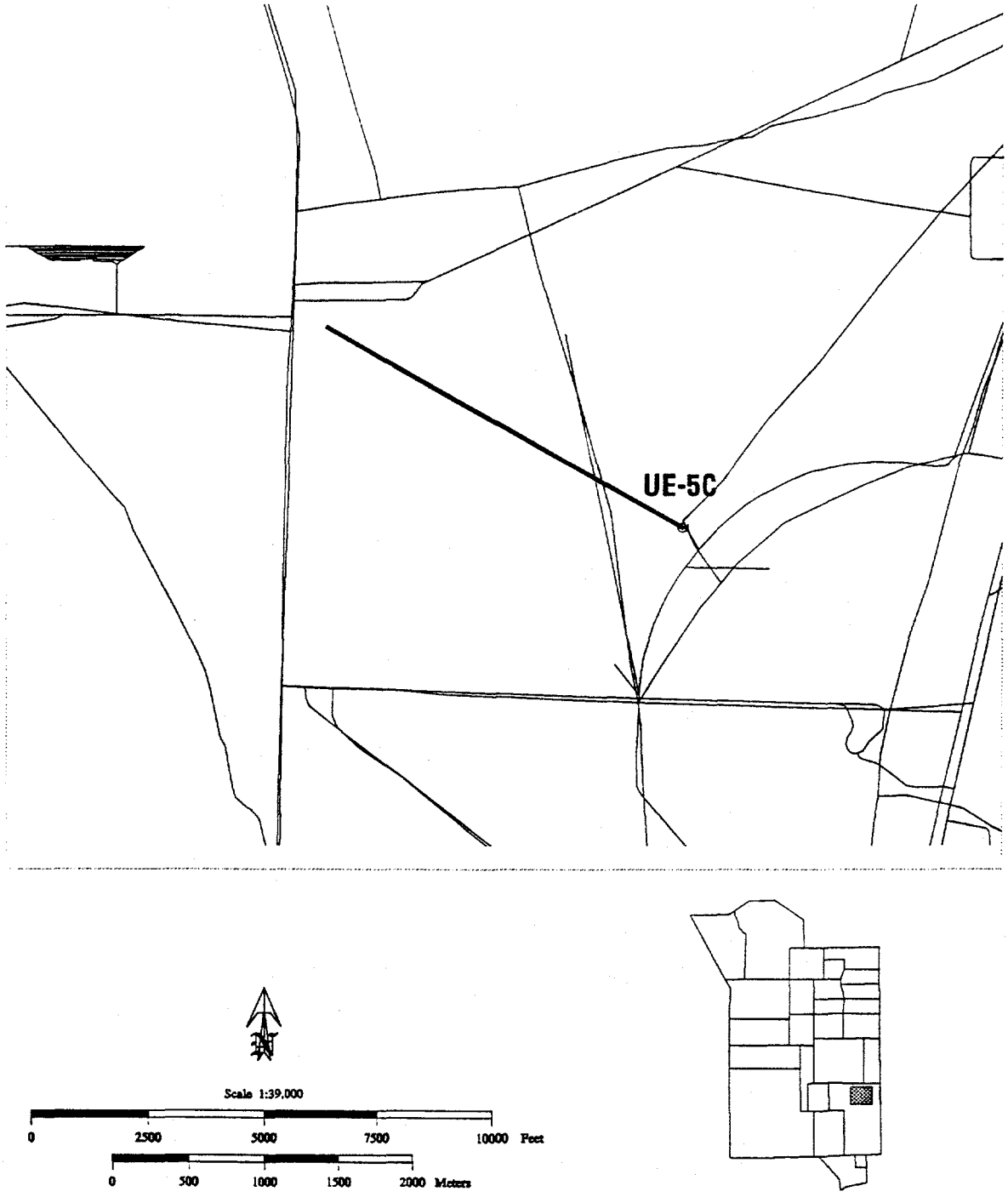

Figure 21a. Thirty–, 40– and 50–year time dependent capture zones for the 50% reliability level for Well UE–5C. Filled circle indicates a well.

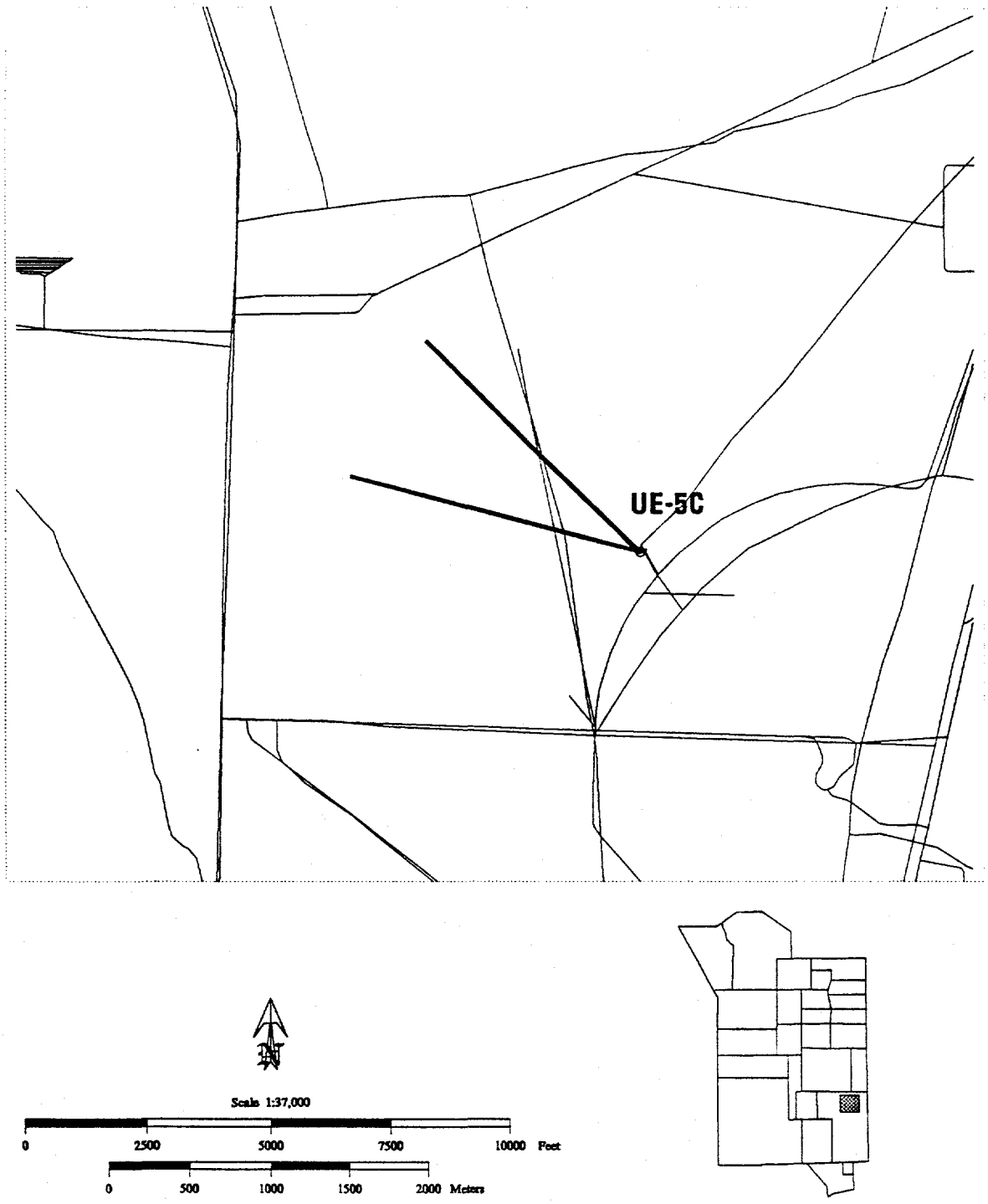

Figure 21b. Thirty–, 40– and 50–year time dependent capture zones for the 67% reliability level for Well UE–5C. Filled circle indicates a well.

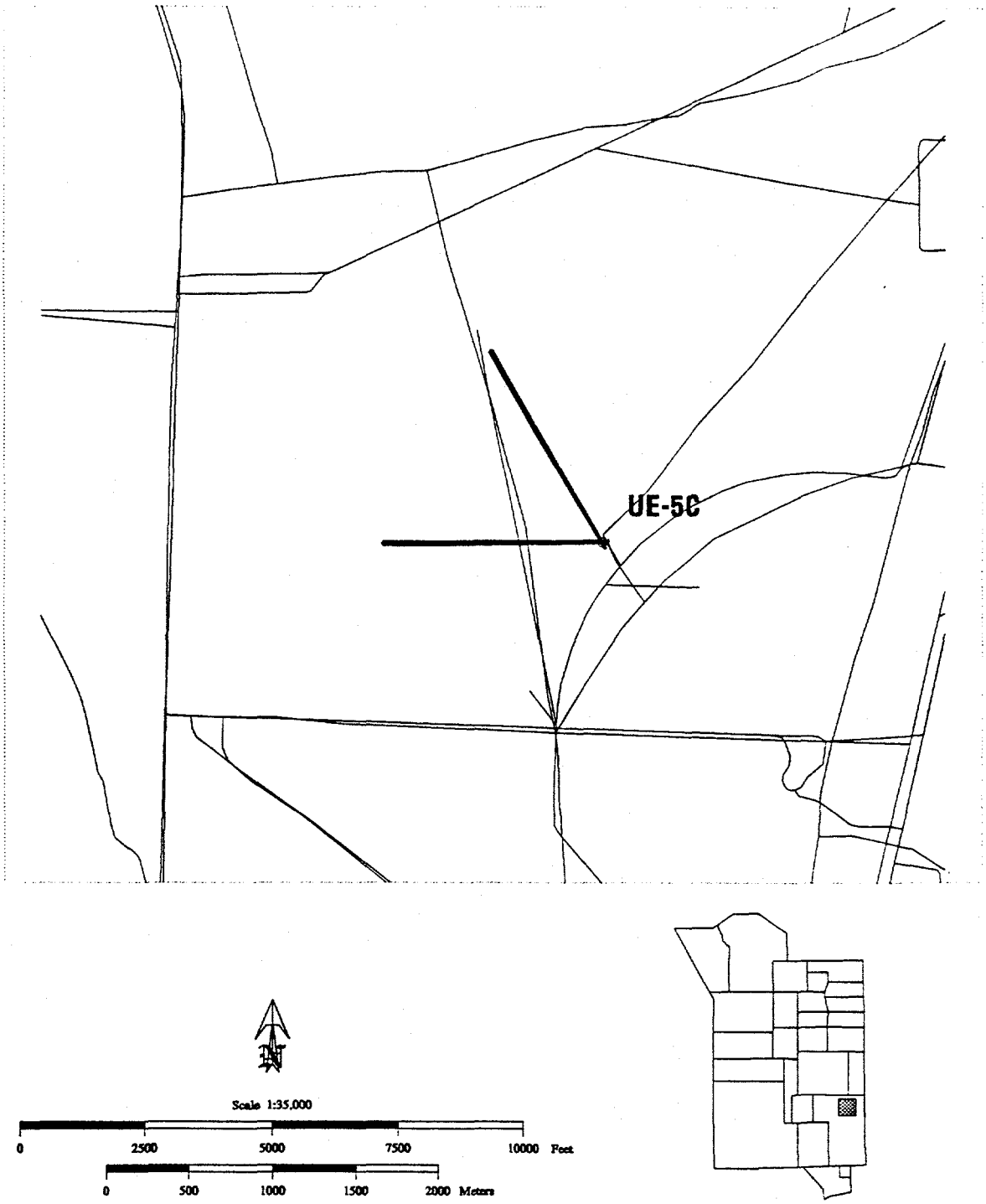

Figure 21c. Thirty–, 40– and 50–year time dependent capture zones for the 95% reliability level for Well UE–5C. Filled circle indicates a well.

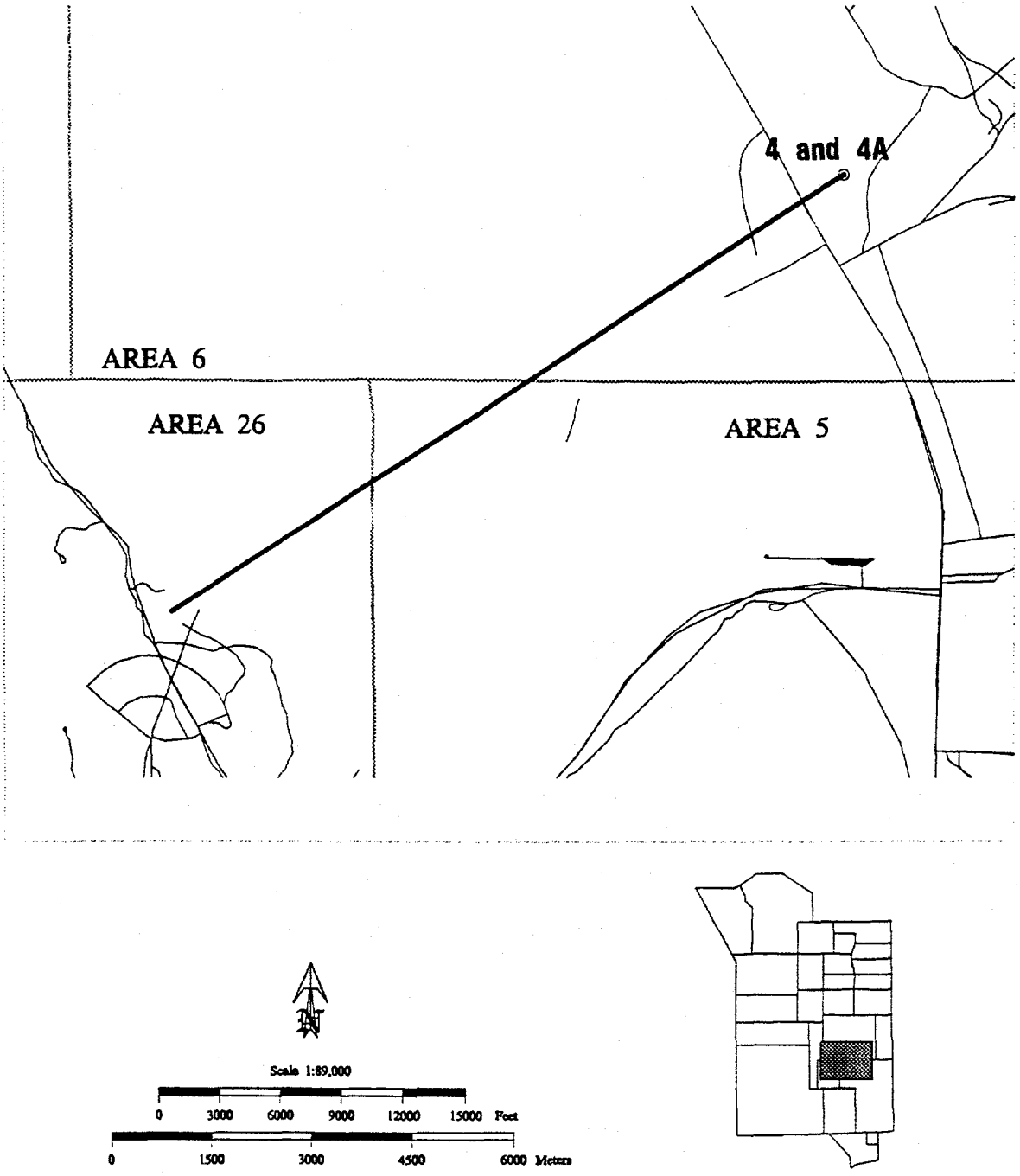

Figure 22a. Three–, four– and five–year time dependent capture zones for the 50% reliability level for Wells 4 and 4A. Filled circle indicates a well.

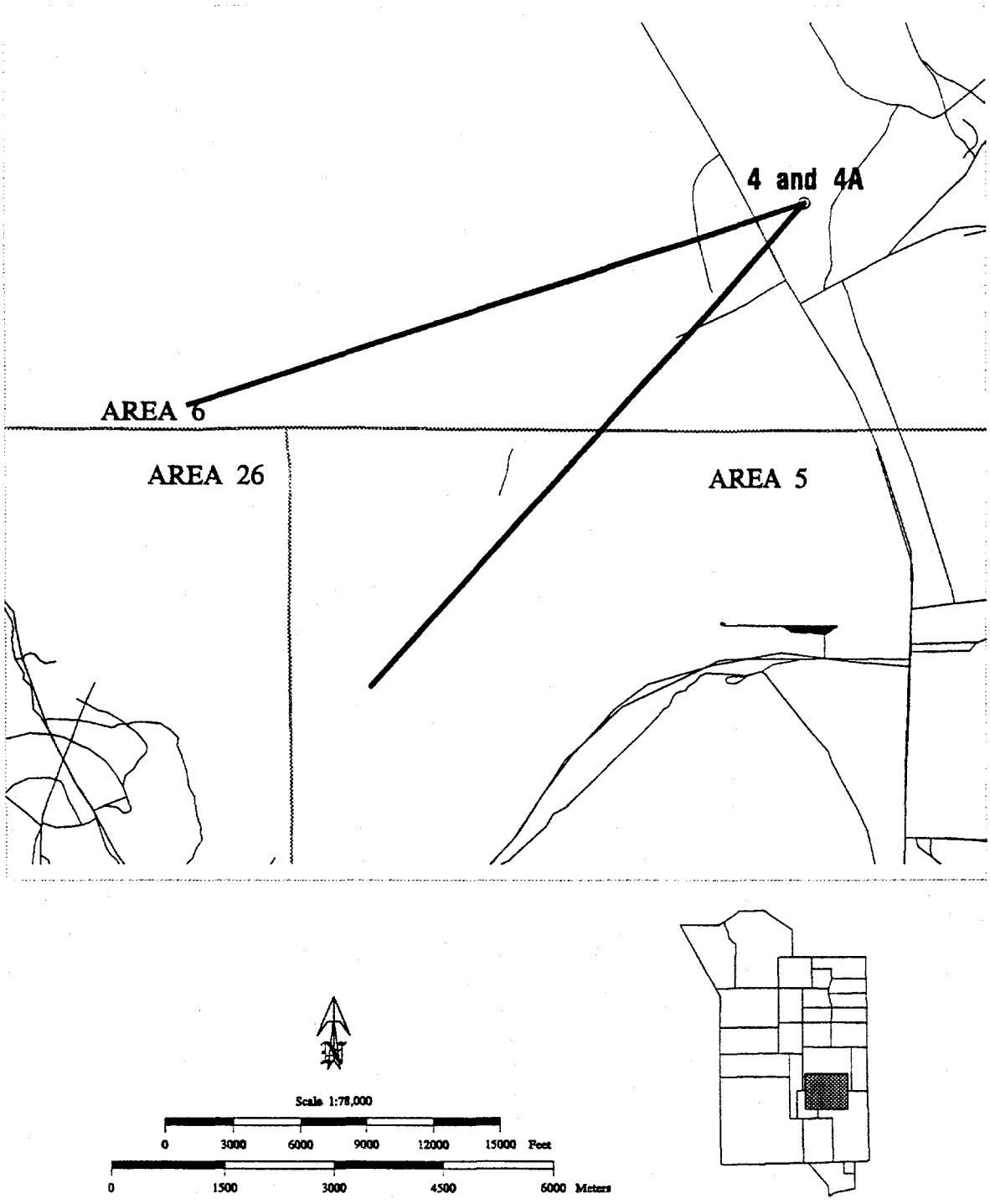

Figure 22b. Three–, four– and five–year time dependent capture zones for the 67% reliability level for Wells 4 and 4A. Filled circle indicates a well.

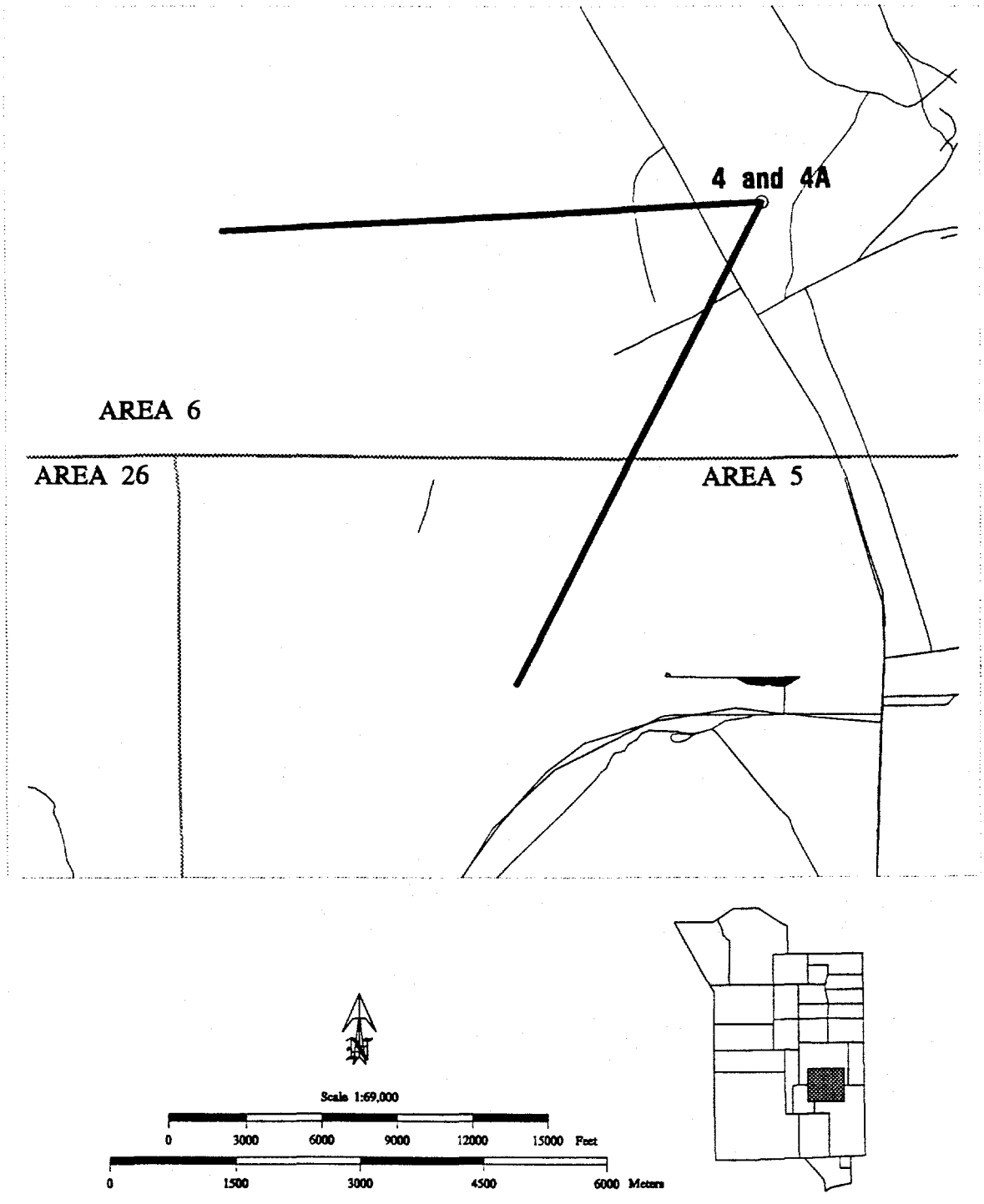

Figure 22c. Three–, four– and five–year time dependent capture zones for the 95% reliability level for Wells 4 and 4A. Filled circle indicates a well.

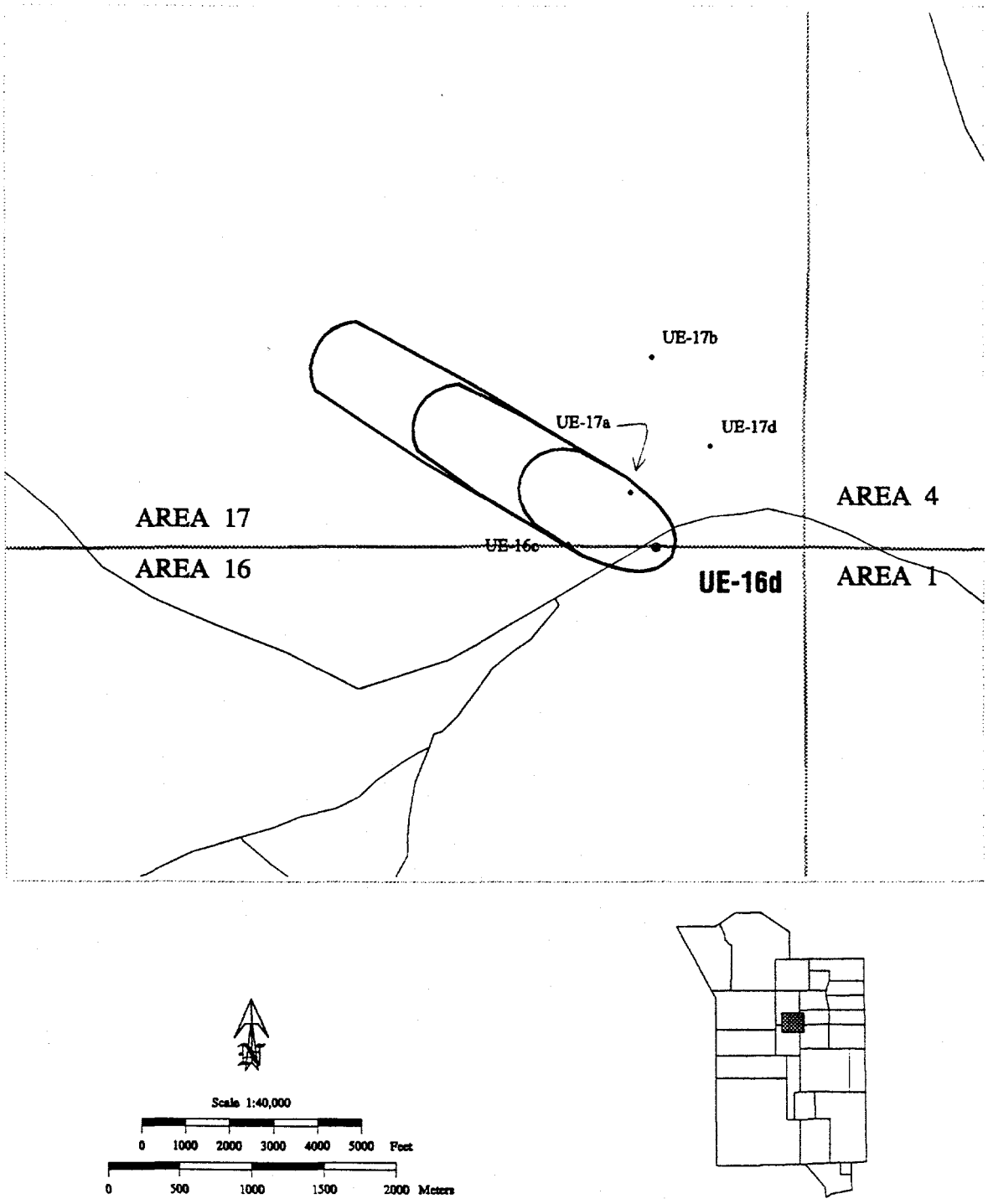

Figure 23a. Five–, 10– and 15–year time dependent capture zones for the 50% reliability level for Well UE–16d. Filled circle indicates a well.

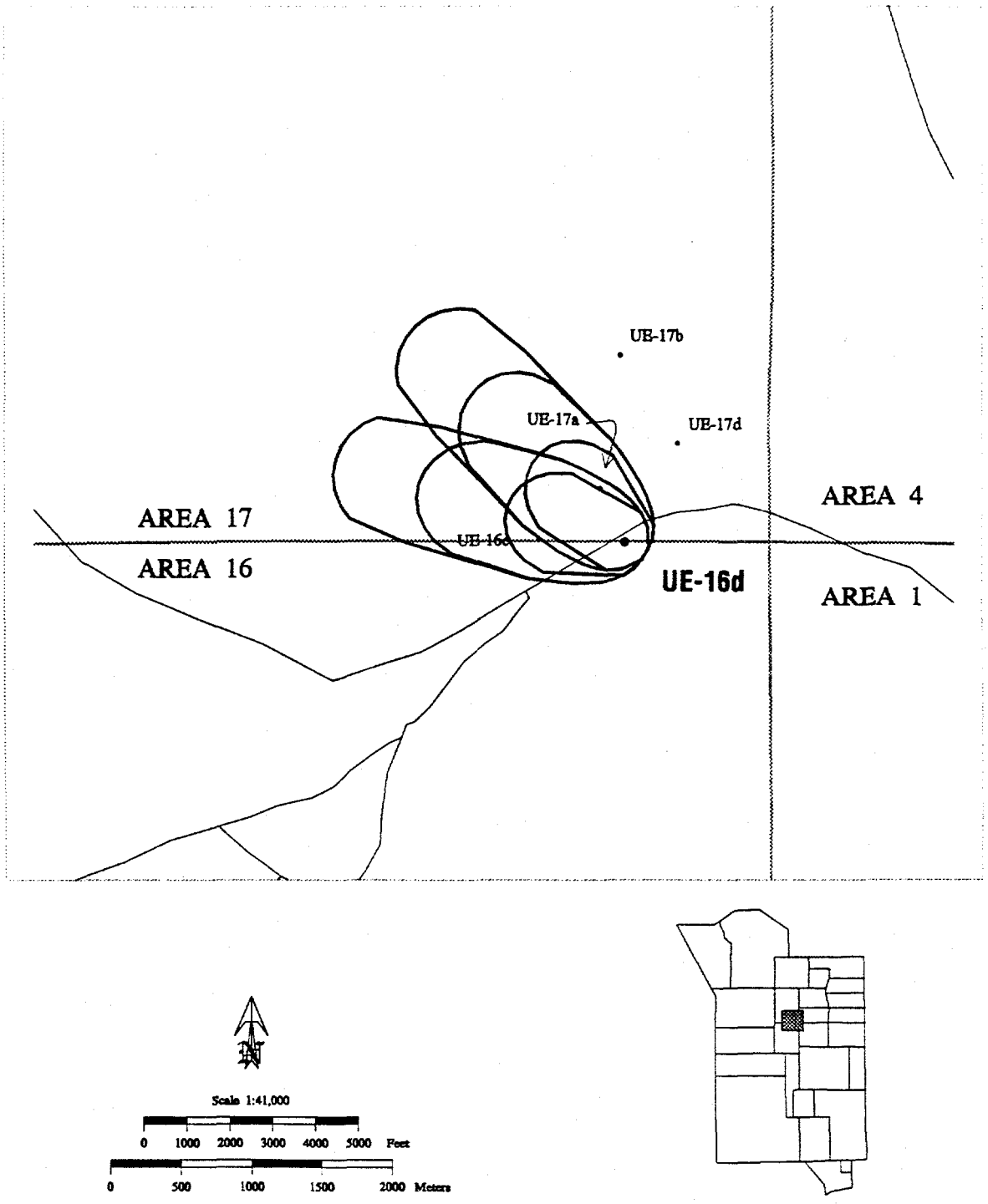

Figure 23b. Five–, 10–and 15–year time dependent capture zones for the 67% reliability level for Well UE–16d. Filled circle indicates a well.

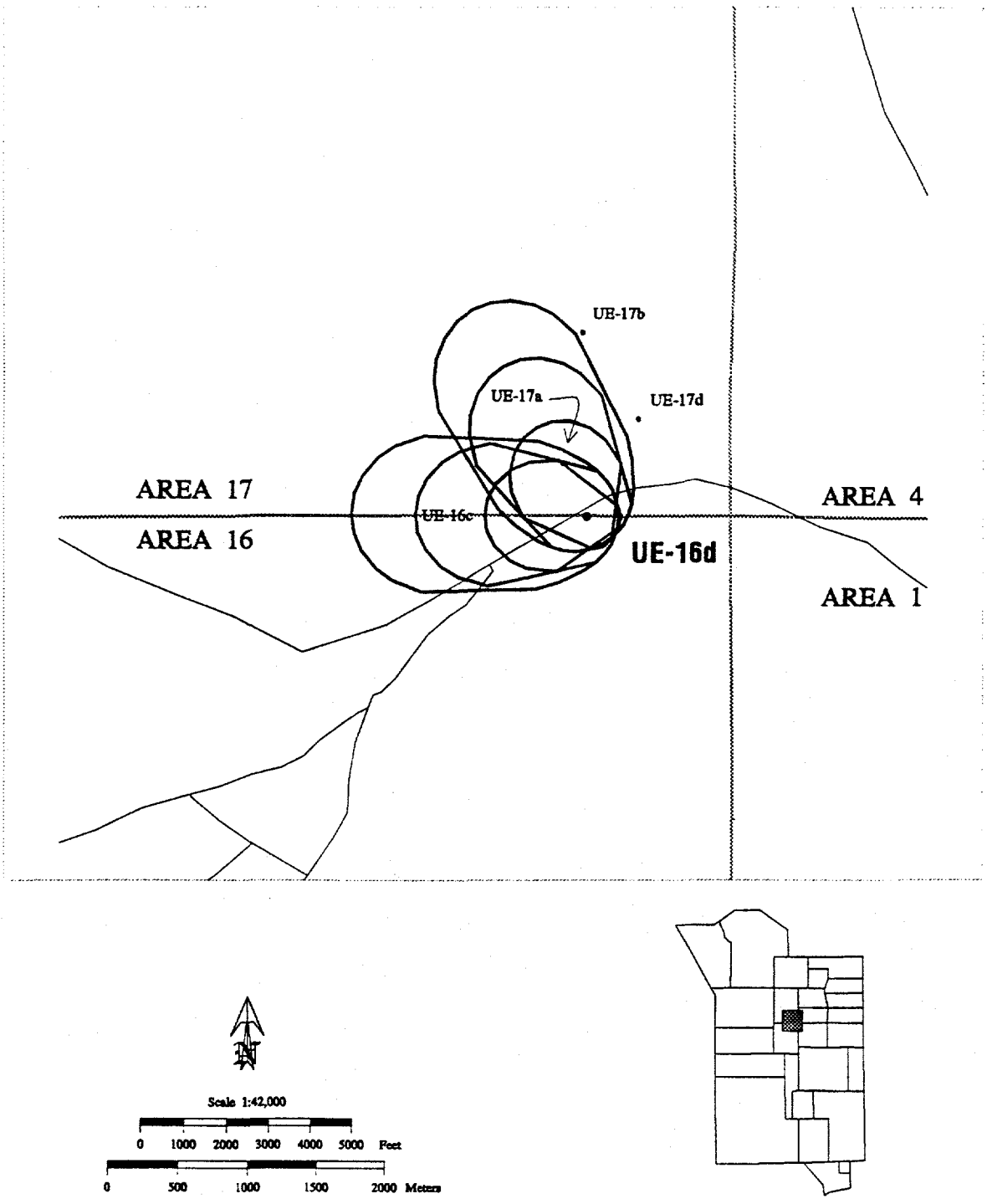

Figure 23c. Five–, 10– and 15–year time dependent capture zones for the 95% reliability level for Well UE–16d. Filled circle indicates a well.

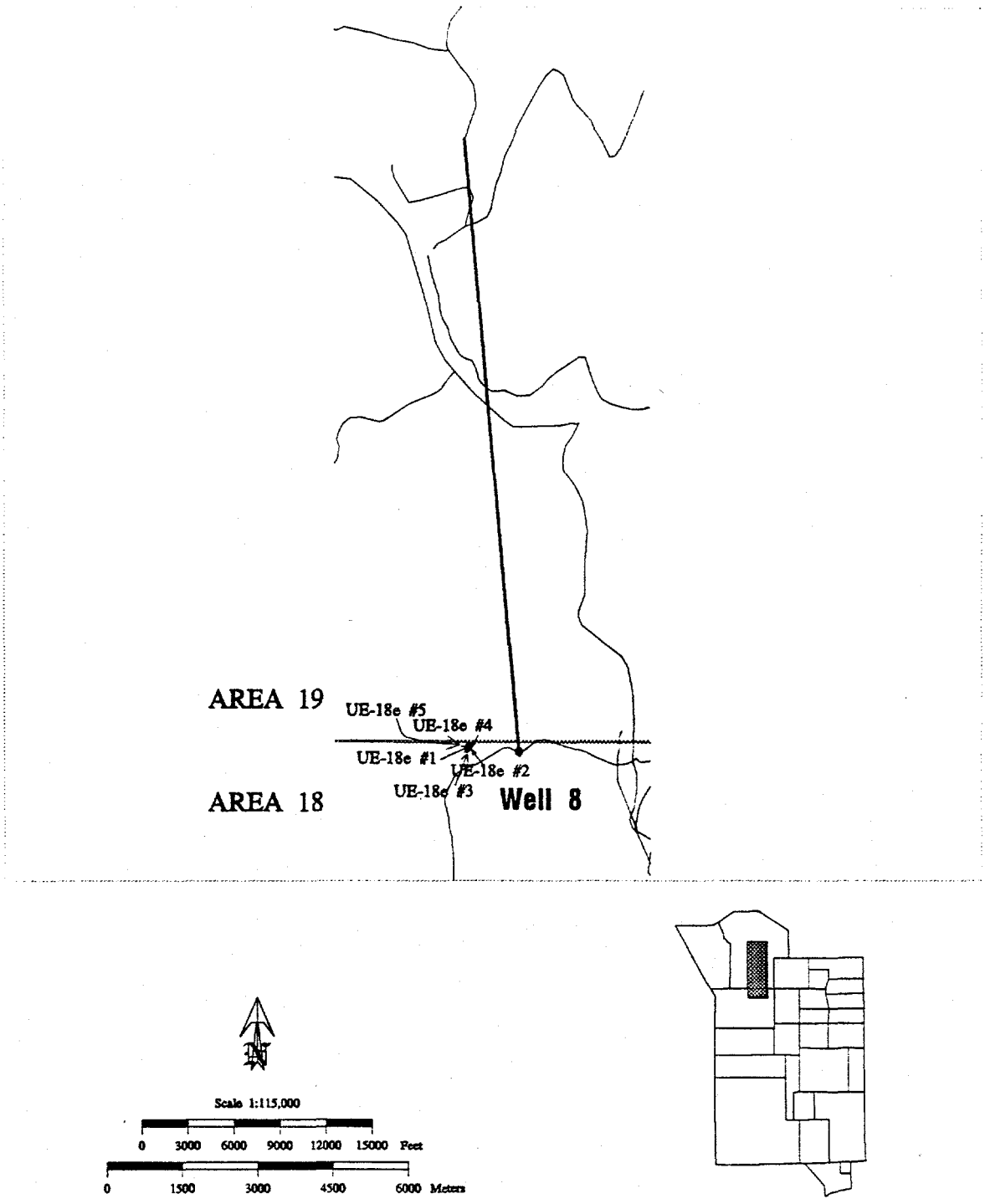

Figure 24a. Five–, 10– and 15–year time dependent capture zones for the 50% reliability level for Well 8. Filled circle indicates a well.

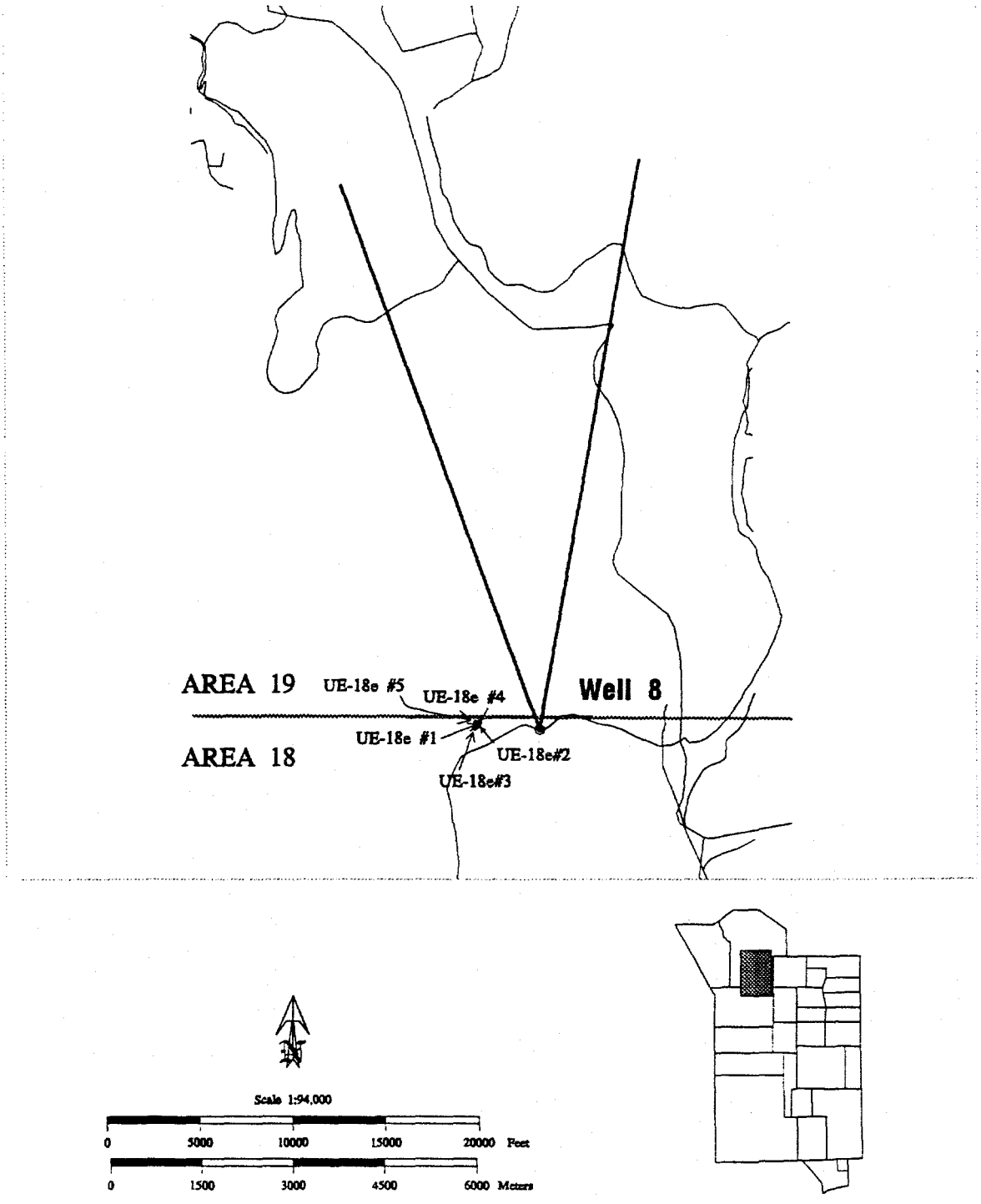

Figure 24b. Five–, 10–and 15–year time dependent capture zones for the 67% reliability level for Well 8. Filled circle indicates a well.

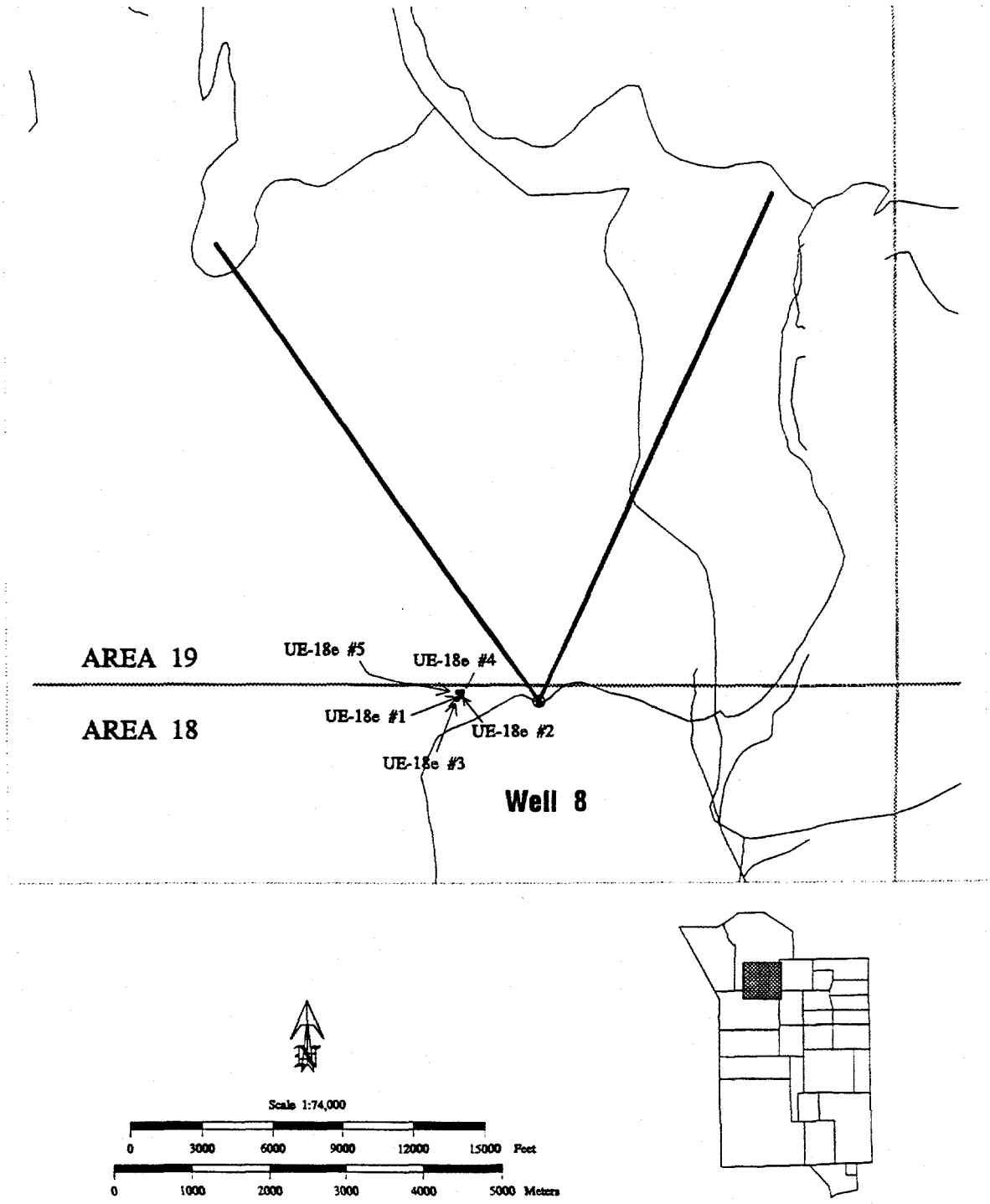

Figure 24c. Five–, 10– and 15–year time dependent capture zones for the 95% reliability level for Well 8. Filled circle indicates a well.

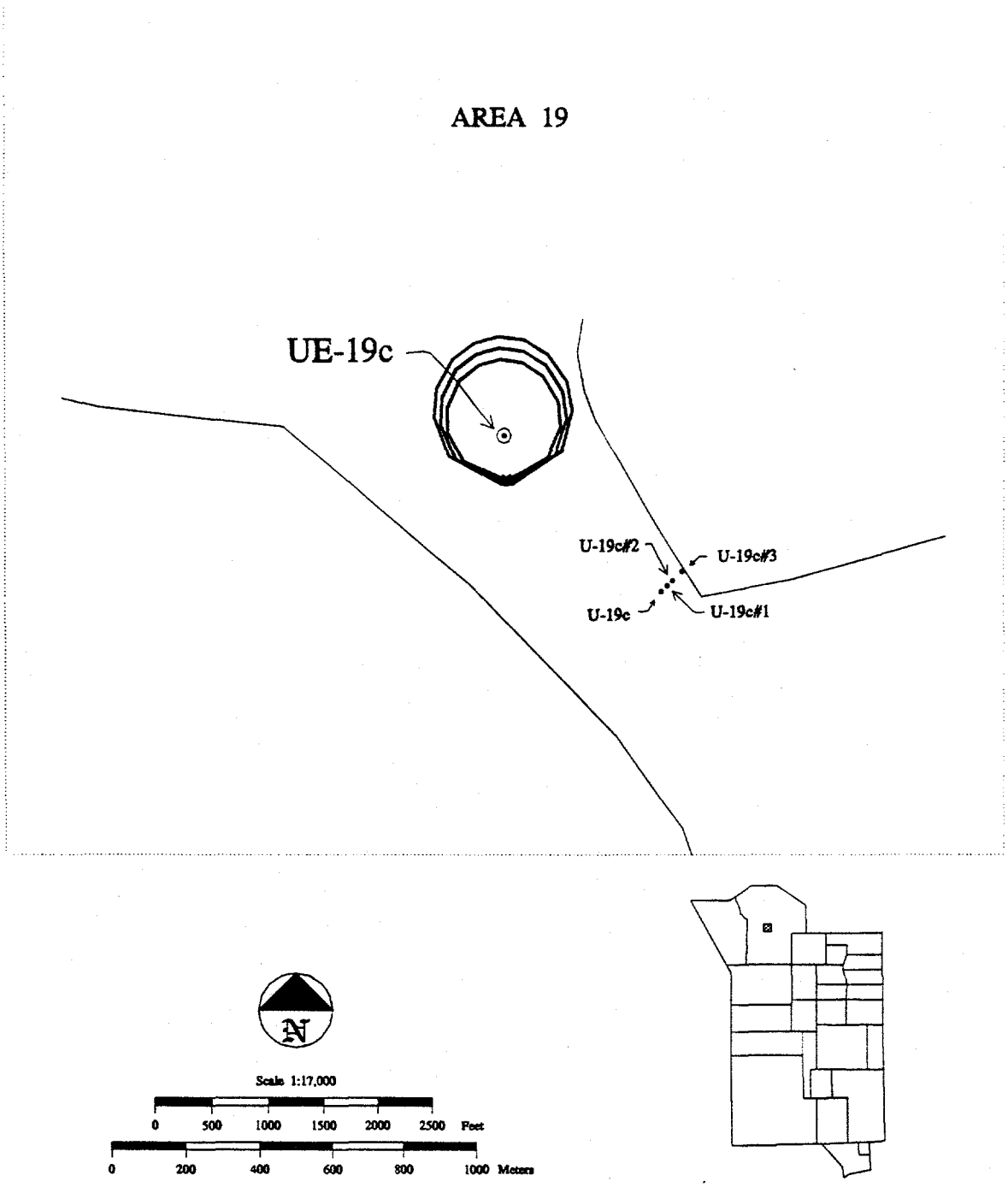

Figure 25a. Forty–, 50– and 60–year time dependent capture zones for the 50% reliability level for UE–19c. Filled circle indicates a well.

AREA 19

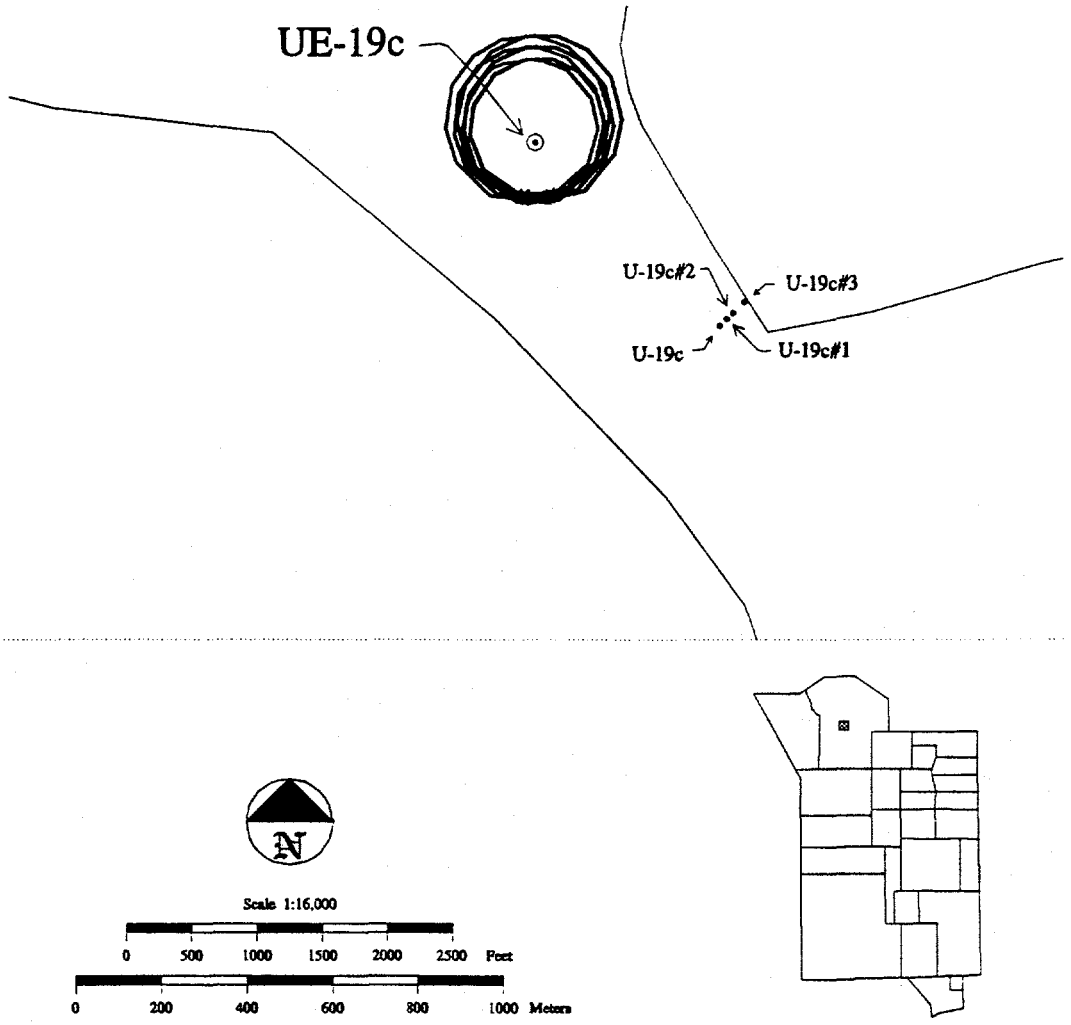

Figure 25b. Forty--, 50- and 60-year time dependent capture zones for the 67% reliability level for UE-19c. Filled circle indicates a well.

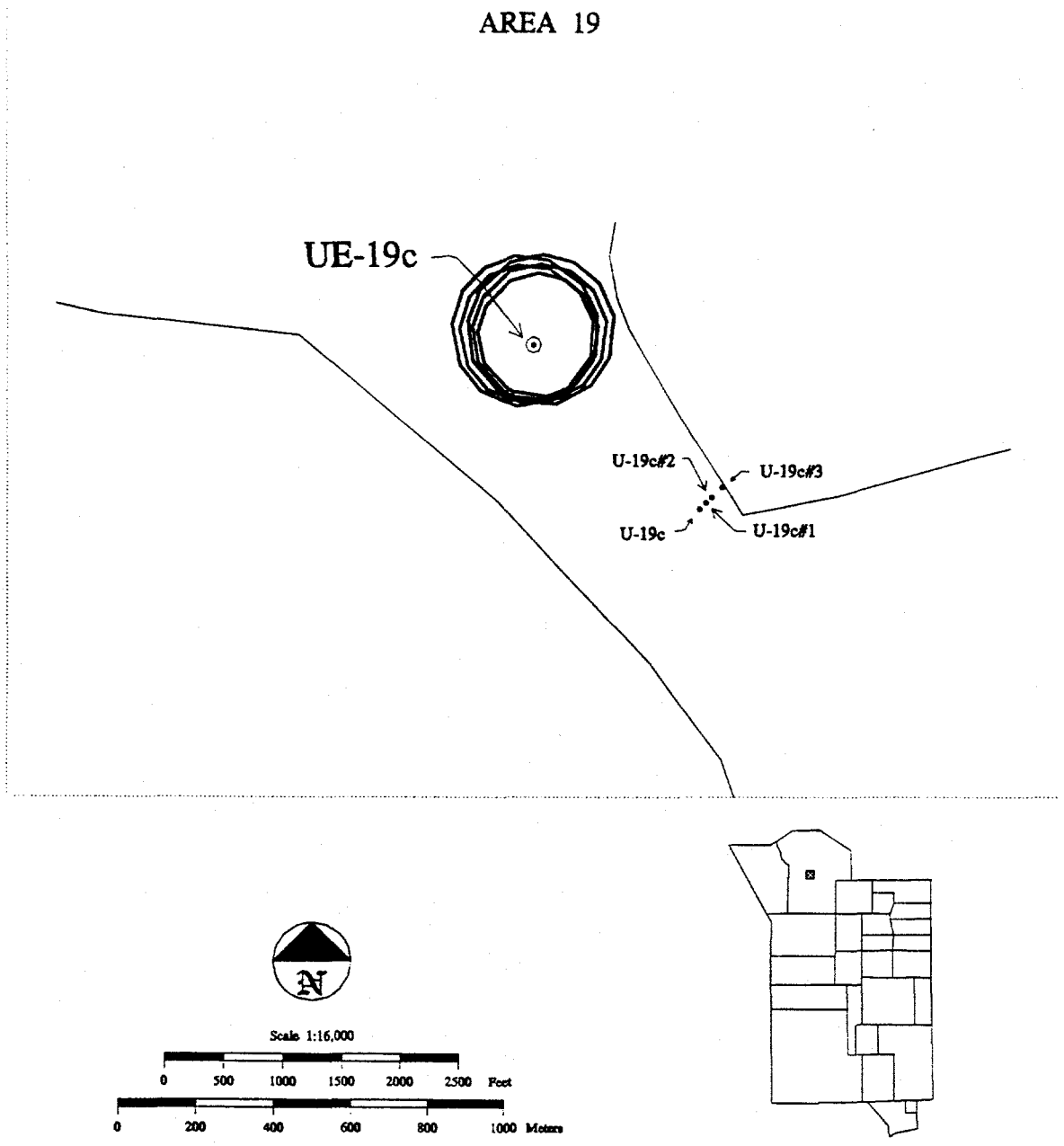

Figure 25c. Forty–, 50– and 60–year time dependent capture zones for the 95% reliability level for UE–19c. Filled circle indicates a well.

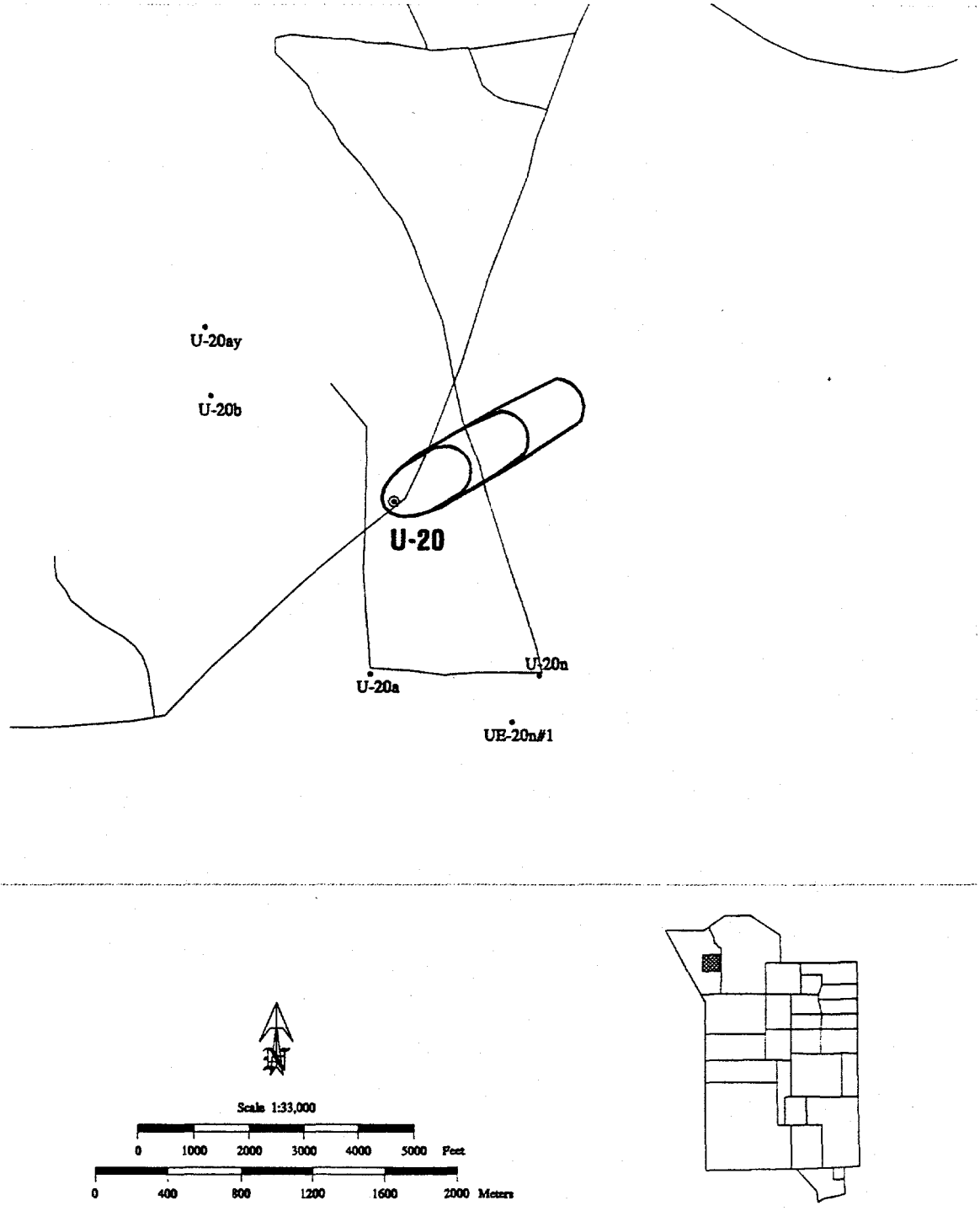

Figure 26a. Five–, 10– and 15–year time dependent capture zones for the 50% reliability level for U–20. Filled circle indicates a well.

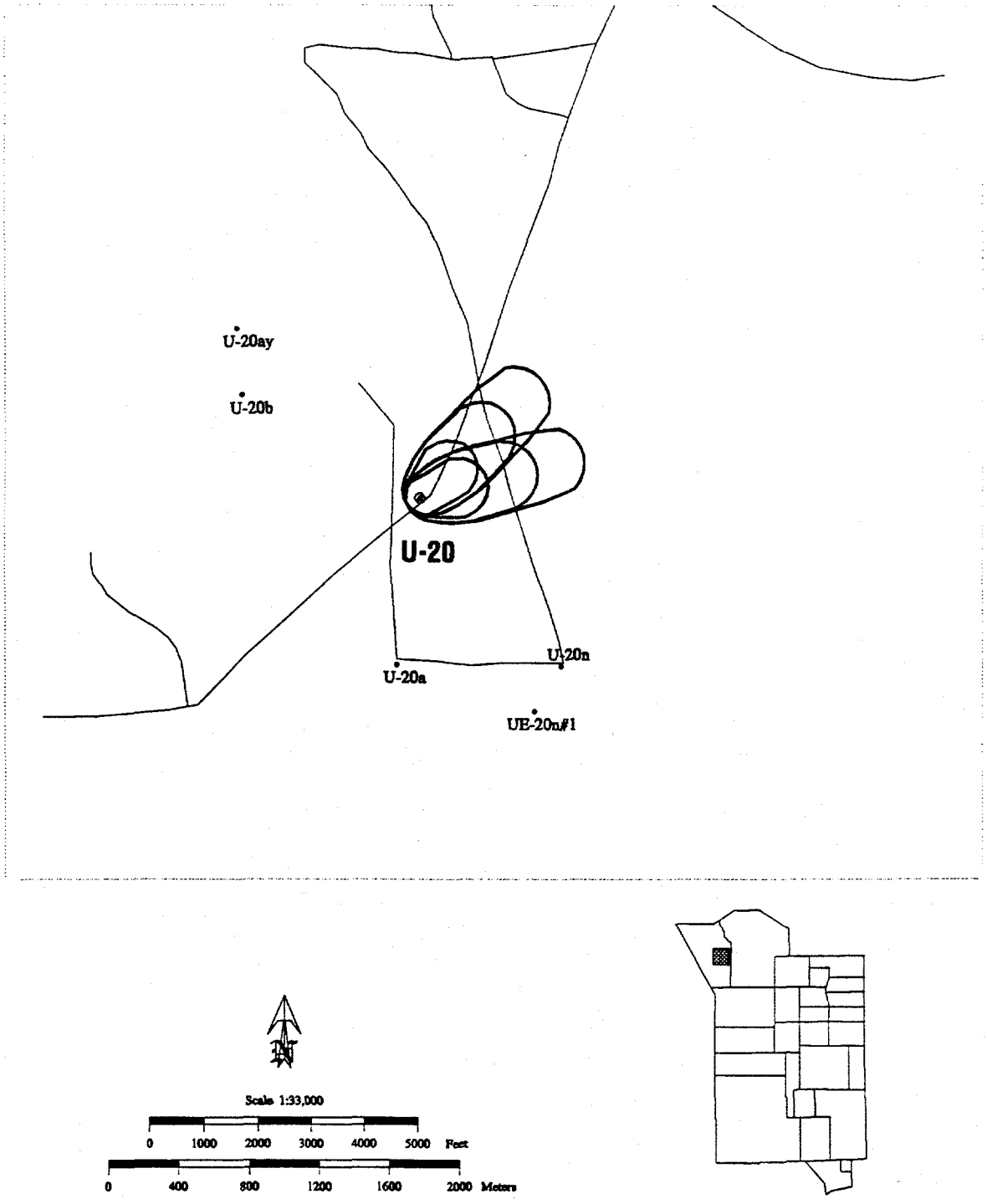

Figure 26b. Five–, 10– and 15–year time dependent capture zones for the 67% reliability level for U–20. Filled circle indicates a well.

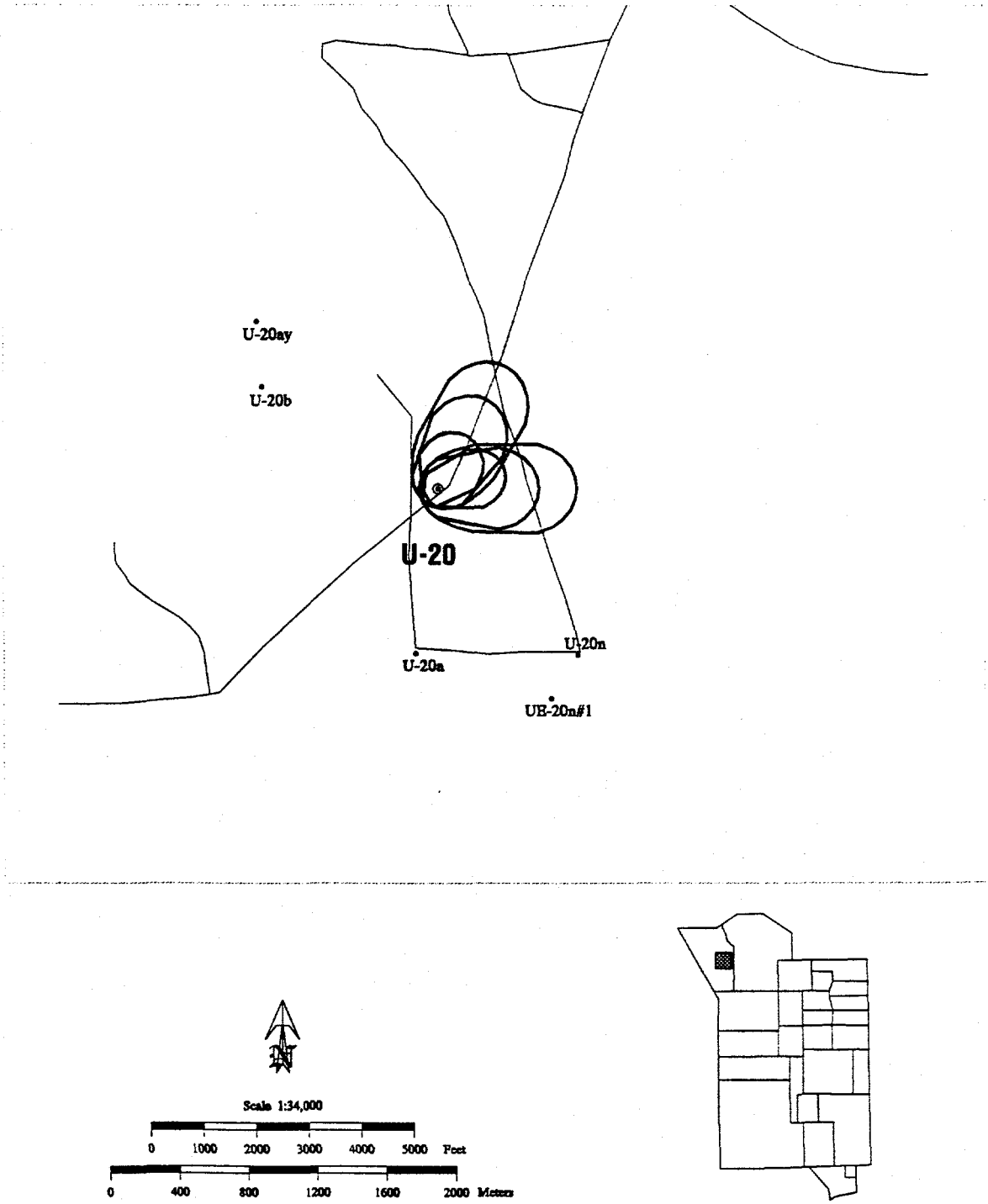

Figure 26c. Five–, 10– and 15–year time dependent capture zones for the 95% reliability level for U–20. Filled circle indicates a well.

REFERENCES

Arteaga, F.E., C.S. Savard, M.E. Johnson and J.C. Stone, 1991. Hydrogeologic Data from Selected Wells and Test Holes In and Adjacent to the Nevada Test Site, Nye County, Nevada, through 1986, U.S. Geol. Survey Open-File Report 87-536, 23 p.

Bear, J. and M. Jacobs, 1965. On the Movement of Water Bodies Injected into Aquifers, Journal of Hydrology, 3, p. 37-57.

Benjamin, J.R. and C.A. Cornell, 1970. Probability, Statistics, and Decision for Civil Engineers. McGraw-Hill, New York, 684 p.

Blandford, T.N., 1991. U.S. EPA WHPA Model, A Modular Semi-Analytical Model for the Delineation of Wellhead Protection Areas, Version 2.0, American Institute of Hydrology, Minneapolis, MN.

Blankennagel, R.K. and J.E. Weir, Jr., 1973. Geohydrology of the Eastern Part of Pahute Mesa, Nevada Test Site, Nye County, Nevada. U.S. Geol. Survey Prof. Paper 712-B, 35 p.

Boughon, C., 1986. Integrated Geochemical and Hydraulic Analyses of Nevada Test Site Ground Water Systems. Master's thesis, University of Nevada, Reno, 135 p.

McElwee, C.D., 1991. Capture Zones for Simple Aquifers, Ground Water, 29(4), p. 587-590.

Raytheon Services Nevada, 1990. Hole History Data, Water Well #4A. Draft, 9 p.

Raytheon Services Nevada, Technical Support Division, 1991. Nevada Test Site Drilling and Mining Summary "Red Book," Raytheon Services Nevada.

Sadler, W.R., 1990. A Deuterium-Calibrated, Discrete-State Compartment Model of Regional Groundwater Flow, Nevada Test Site and Vicinity. Master's thesis, University of Nevada, Reno, 249 p.

Todd, D.K., 1980. Groundwater Hydrology. John Wiley and Sons, New York, 535 p.

Winograd, I.J. and W. Thordarson, 1975. Hydrogeologic and Hydrochemical Framework, South-Central Great Basin, Nevada-California, with Special Reference to the Nevada Test Site. U.S. Geol. Survey Prof. Paper 712-C, 126 p.

Wood, D., 1993. U.S. Geological Survey, personal communication.

APPENDIX A

MATHEMATICAL DEVELOPMENT OF METHODOLOGY FOR WELLHEAD PROTECTION AREA DELINEATION UNDER UNCERTAINTY

CAPTURE ZONE DELINEATION

Consider a hypothetical flow system consisting of a single, fully penetrating pumping well in an infinite flow domain with a component of uniform regional flow, schematically shown on Figure 1 in the text.

The complex potential $f(z)$ for the combined flow in the horizontal (x,y) plane is obtained by superposition (Bear and Jacobs, 1965)

$$f(z) = -q(\cos\alpha - i\sin\alpha)z + \frac{Q}{2\pi}\ln z \quad ; \quad z = x + iy \tag{1}$$

having the velocity potential

$$\phi(x,y) = -q(x\cos\alpha + y\sin\alpha) + \frac{Q}{4\pi}\ln(x^2 + y^2) \tag{2}$$

and the stream function

$$\psi(x,y) = -q(-x\sin\alpha + y\cos\alpha) + \frac{Q}{2\pi}\tan^{-1}\left(\frac{y}{x}\right) \tag{3}$$

where $q[L^2/T]$ is the mean regional flow integrated over the aquifer thickness, $Q[L^3/T]$ is the well pumping rate, and α denotes the angle between x-axis and the direction of uniform regional flow. The velocity components in x and y direction are $v_x = -(bn)^{-1}\partial\phi/\partial x$, $v_y = -(bn)^{-1}\partial\phi/\partial y$, where n is the effective porosity and b is the aquifer thickness.

Assuming that all parameters are known with certainty, the single capture zone can be easily derived by setting the stream function ψ equal to zero and solving for

$$\left(\frac{y}{x}\right) = \tan\left[\frac{+2\pi q\theta}{Q}\right] \quad y > 0 \quad ; \quad \left(\frac{y}{x}\right) = -\tan\left[\frac{+2\pi q\theta}{Q}\right] \quad y < 0 \tag{4}$$

where $\theta = (-x\sin\alpha + y\cos\alpha)$. The above expression is the solution for the ultimate (steady state) capture zone which implies an unlimited pumping and infinite time. Equation (4) is widely used today (Blandford, 1991) to delineate the pumping well capture zone using the parameters estimated from the available field data. For the purpose of deriving the time-dependent capture zones, Bear and Jacobs (1965) followed the equation of pathlines (in the steady flow, pathlines coincide with streamlines) in the flow field given with $dx/v_x = dy/v_y = dt$. The solution of this equation defines at time t the position of a particle with respect to originating point. The solution is obtained in the dimensionless form as

$$\exp(\bar{x} - \bar{t}) = \cos\bar{y} + \frac{\bar{x}}{\bar{y}}\sin\bar{y} \tag{5}$$

where $\bar{x} = 2\pi qx/Q, \bar{y} = 2\pi qy/Q$, and $\bar{t} = 2\pi q^2 t/(nbQ)$. This transcendental equation for time-dependent capture zones is usually solved using some kind of iterative procedure (e.g.,

McElwee, 1991). Both solutions, (4) and (5), are conditioned on the set of parameters which are assumed to be perfectly known. A deterministic solution is based on these representative values for the various model parameters. They usually represent a mean or average value of the system. Since perfect knowledge in model parameters is seldom the case, the influence of the uncertainty becomes a major factor.

Modeling capture zones around pumping wells and understanding the physical nature of its development is fundamental for decision making. The associated risk involved and uncertainty in its evaluation represent an important component of the modeling effort. Risk analysis based on the deterministic solution, which results in single representations of the capture zone, may be insufficient for making decisions about protective areas, and particularly for monitoring measures to be taken to prevent contamination from reaching the water-supply wells.

In other words, the regional flow q is to be considered a random variable instead of a random field which requires the identification of the appropriate spatial structure.

METHODOLOGY TO INCLUDE UNCERTAINTY

The ability to obtain the capture zones conditioned on the uncertainty in the mean regional flow is a first step in delineating WHPA under uncertainty. In the following, the methodology for analyzing the ultimate capture zone under uncertainty is demonstrated.

Consider the steady state flow condition for the stream function given in (3). Under the uncertainty in the regional flow q and parameter θ, the stream function $\psi(x,y \mid q, \theta)$ is also an uncertain function that is conditioned on the values that q and θ may obtain. The corresponding unconditional stream function $\psi(x,y,q,\theta)$, i.e., the stream function for all possible values of q and θ, is obtained by using the basic relationship between the conditional and unconditional probabilities, i.e., $\psi(x,y \mid q, \theta) = \psi(x,y,q,\theta)/f(q,\theta)$, where $f(q,\theta)$ is the joint probability distribution function (pdf) of q and θ, obtained in the process of inference of parameter estimates from available field data. Assuming q and θ are independent, the joint probability distribution function of q and θ becomes $f(q,\theta) = f(q)f(\theta)$. Including the uncertainties in q and θ simultaneously to obtain an estimate of the uncertainty in the stream function would lead to an unmanageable solution, thus the uncertainties in q and θ will be treated separately. First, consider the uncertainty in q with θ fixed at its mean value $\langle\theta\rangle$. The first two moments of the stream function are now given by

$$\langle\psi(x,y,q,\theta)\rangle = -\int q\theta f(q)dq + \frac{Q}{2\pi}\tan^{-1}\left(\frac{y}{x}\right) = -\langle q\rangle\langle\theta\rangle + \frac{Q}{2\pi}\tan^{-1}\left(\frac{y}{x}\right) \tag{6}$$

$$\sigma_\psi^2 = \int [\psi(x,y,q,\theta)]^2 f(q)dq - \langle\psi(x,y,q,\theta)\rangle^2 = \sigma_q^2\langle\theta\rangle^2 \tag{7}$$

where $\langle q\rangle$ and $\langle\theta\rangle$ are means, respectively, of the regional flow q and parameter θ, and σ_q^2 is the variance of the flow.

In general, the mean flow is not measured, but rather estimated indirectly using a form of Darcy's law, $q = TJ$, where T is the aquifer transmissivity and J is the hydraulic head gradient. These parameters are estimated from the scarce field data, thus they are subject to an estimation error which produces the total uncertainty in the regional flow estimate. If both T and J are lognormally distributed, then so is q, such that the first two moments of the regional flow are $\langle ln\ q \rangle = \langle ln\ T \rangle + \langle ln\ J \rangle$ and $\sigma^2_{lnq} = \sigma^2_{lnT} + \sigma^2_{lnJ} + 2\varrho\sigma_{lnT}\sigma_{lnJ}$, respectively, where ϱ is the correlation coefficient between $ln\ T$ and $ln\ J$. The first two moments of q are then readily obtained by converting the moments into

$$\langle q \rangle = \exp(\langle \ln q \rangle + \sigma^2_{lnq}/2) \tag{8}$$

for the mean and

$$\sigma^2_q = \exp(2\langle \ln q \rangle + \sigma^2_{lnq})\left[\exp(\sigma^2_{lnq}) - 1\right] \tag{9}$$

for the variance of q. In the case of the parameter θ, which contains the regional flow direction angle α, the mean, $\langle \theta \rangle$, is calculated based on the mean $\langle \alpha \rangle$ by

$$\langle \theta \rangle = -x\sin\langle \alpha \rangle + y\cos\langle \alpha \rangle \tag{10}$$

The expected value capture zone is obtained by replacing all uncertain parameters with their mean values and in this case, the streamline function maintains the same form as the deterministic solution and is labeled with the probability of 0.5, as shown on Figure 2a in the text. The other probabilities are produced by evaluating the following expression of the stream function

$$\langle \psi(x, y, q, \theta) \rangle \pm m\sigma_\psi = -\langle q \rangle \langle \theta \rangle + \frac{Q}{2\pi}\tan^{-1}\left(\frac{y}{x}\right) \pm m\sigma_q\langle \theta \rangle \tag{11}$$

where m is a real valued number indicating the magnitude of departure from the mean streamline. Setting the left-hand side of (11) to zero, the probabilistic ultimate capture zone solution can be written in the following form

$$\left(\frac{y}{x}\right) = \pm \tan\left[\frac{-2\pi(\langle q \rangle \pm m\sigma_q)\langle \theta \rangle}{Q}\right] \tag{12}$$

An interpretation of the probabilistic ultimate capture zone solution given above can be made by looking at the reliability issue which corresponds to a level of confidence. For a normally distributed variable as seen in Figure 2b in the text, the 67 percent level of confidence corresponds to the values of ± 1. In equation (12), using $m = -1$ would yield a wider ultimate capture zone than using $m = +1$. Thus, the ultimate capture zone for the 67 percent reliability level would be generated using $m = -1$. For the 95 percent reliability level ultimate capture zone, m would be set equal to -2.

The uncertainty in the capture zone caused by the uncertainty in α can be estimated in the same manner based on the reliability level. Assuming α is normally distributed, the chosen reliability level will lead to an m value that is used in equation (12) to obtain the dimensions of the capture zone and is also used in the following equation

$$\langle \alpha \rangle \pm m\sigma_{\alpha} \tag{13}$$

to obtain the two angles corresponding to the same reliability level. The envelope of the capture zone is obtained by plotting the capture zone determined from equation (12) about the two angles obtained in equation (13), as shown in Figure 3 in the text. This envelope represents the area of the capture zone given the uncertainties in q and α at a certain reliability level.

DISTRIBUTION

Desert Research Institute

Roger Jacobson
Desert Research Institute
Water Resources Center
P.O. Box 19040
Las Vegas, NV 89132-0040

Marjory Jones
Desert Research Institute
Water Resources Center
P.O. Box 60220
Reno, NV 89506-0220

International Technology Corp.

Rick Waddell
Geotrans, c/o IT
4330 Valley View
Suite 112, MS-439
Las Vegas, NV 89103

Joe Yeasted
International Technology Corporation
4330 S. Valley View
Suite 114
Las Vegas, NV 89103

Lawrence Livermore National Laboratory

Lee Davisson
Nuclear Chemistry Division
Lawrence Livermore National Laboratory
P.O. Box 808
L-237
Livermore, CA 94550

Greg Nimz
Lawrence Livermore National Laboratory
P.O. Box 808
MS L233
Livermore, CA 94550

Los Alamos National Laboratory

Joe Thompson
Los Alamos National Laboratory
INC-11, MS J514
P.O. Box 1663
Los Alamos, NM 87545

Raytheon Services Nevada

Stuart E. Rawlinson
Raytheon Services Nevada
P.O. Box 95487, M/S 580
Las Vegas, NV 89193-5487

Reynolds Electrical & Engineering Co.

Martha DeMarre
Chief, Document Research Section
Health Protection Dept.
Reynolds Electrical & Engineering Co.
P.O. Box 98521
Las Vegas, NV 89193-8521

Brian Dozier
Reynolds Electrical & Engineering Co.
2501 Wyandotte
Mercury, NV 89102

State of Nevada

Larry Franks
Nevada State Health Department
Radiological Health Section
620 Belrose Avenue
Las Vegas, NV 89158

U.S. Department of Defense

David Bedsun
Defense Nuclear Agency
Field Command
Nevada Operations Office
P.O. Box 208
Mercury, NV 89023-0208

U.S. Department of Energy

Gylan Allen, Director
Test Operations Division
Nevada Operations Office
U.S. Department of Energy
P.O. Box 98518
Las Vegas, NV 89193-8518

Bob Bangerter
Environmental Restoration Division
Nevada Operations Office
U.S. Department of Energy
P.O. Box 98518
Las Vegas, NV 89193-8518

Joanne M. Bradbery, Director
Contracts Division
Nevada Operations Office
U.S. Department of Energy
P.O. Box 98518
Las Vegas, NV 89193-8518

Doug Duncan
Hydrology Program Manager
Office of Environmental Restoration
and Waste Management
Nevada Operations Office
U.S. Department of Energy
P.O. Box 98518
Las Vegas, NV 89193-8518

Donald Elle, Director
Environmental Protection Division
Nevada Operations Office
U.S. Department of Energy
P.O. Box 98518
Las Vegas, NV 89193-8518

Joseph N. Fiore, Acting Assistant Manager
Office of Environmental Restoration
and Waste Management
Nevada Operations Office
U.S. Department of Energy
P.O. Box 98518
Las Vegas, NV 89193-8518

Joseph M. Ginanni
Waste Management Division
Nevada Operations Office
U.S. Department of Energy
P.O. Box 98518
Las Vegas, NV 89193-8518

Joseph H. Kitchen
Project Control and Technology
Development Division
Nevada Operations Office
U.S. Department of Energy
P.O. Box 98518
Las Vegas, NV 89193-8518

Steve Lawrence
Environmental Restoration Division
Nevada Operations Office
U.S. Department of Energy
P.O. Box 98518
Las Vegas, NV 89193-8518

Steve Leedom
Test Operations Division
Nevada Operations Office
U.S. Department of Energy
P.O. Box 98518
Las Vegas, NV 89193-8518

Steve Mellington, Director
Environmental Restoration Division
Nevada Operations Office
U.S. Department of Energy
P.O. Box 98518
Las Vegas, NV 89193-8518

Richard Pearl
Environmental Protection Division
Nevada Operations Office
U.S. Department of Energy
P.O. Box 98518
Las Vegas, NV 89193-8518

U.S. Geological Survey

Virginia Glanzman
U.S. Geological Survey
Box 2506, MS 913
Denver Federal Center
Denver, CO 80225

Randy Laczniak
U.S. Geological Survey
Water Resources Division
6770 S. Paradise Rd.
Las Vegas, NV 89119

Paul Orkild
U.S. Geological Survey
Box 2506, MS 913
Denver Federal Center
Denver, CO 80225

Doug Trudeau
U.S. Geological Survey
Water Resources Division
6770 S. Paradise Rd.
Las Vegas, NV 89119

LIBRARIES

Annie Kelley
State Documents Department
Nevada State Library
Capitol Complex
Carson City, NV 89710

Archives
Getchell Library
University of Nevada, Reno

Beverly Carter
MacKay School of Mines Library
University of Nevada, Reno

Document Section, Library
University of Nevada, Las Vegas
4505 Maryland Parkway
Las Vegas, NV 89154

Library (Stead)
Desert Research Institute
P.O. Box 60220
Reno, Nevada 89506-0220

Library
IT Corporation
4330 S. Valley View
Suite 114
Las Vegas, NV 89103
ATTN: Toni Miller

Library
Southern Nevada Science Center
Desert Research Institute
P.O. Box 19040
Las Vegas, NV 89132-0040

Technical Information Resource Center
Nevada Operations Office
U.S. Department of Energy
P.O. Box 98518
Las Vegas, NV 89193-8518

Librarian
Water Resources Center Archives
410 O'Brien Hall
University of California
Berkeley, CA 94720-1718